To the Graduate Council:

We are submitting herewith a dissertation written by Robert Frank Mauldin entitled "Photochemical and Supercritical Fluid Extraction Studies of Polyclic Aromatic Hydrocarbons Adsorbed on Coal Stack Ash Fractions." We recommend that it be accepted in partial fulfillment of the requirements for the degree of Doctor of Philosophy, with a major in Chemistry.

E. L. Wehry, Major Professor

Gleb Mamantov, Major Professor

We have read this dissertation
and recommend its acceptance:

Accepted for the Council:

Vice Provost
and Dean of the Graduate School

PHOTOCHEMICAL AND SUPERCRITICAL FLUID EXTRACTION STUDIES OF POLYCYCLIC AROMATIC HYDROCARBONS ADSORBED ON COAL STACK ASH FRACTIONS

A Dissertation

Presented for the

Doctor of Philosophy

Degree

The University of Tennessee, Knoxville

Robert Frank Mauldin

May 1990

DEDICATION

The author wishes to dedicate this work to the memory of his late grandfather, Frank L. Mauldin. Frank L. Mauldin's work ethic and commitment to education greatly influenced the author's academic pursuits.

ACKNOWLEDGEMENT

The author expresses his sincerest appreciation to many people who have contributed to this work. His wife, Barbara, gave him loving support and encouragement during graduate study. The author's parents are extended gratitude for providing a healthy family atmosphere and promoting a high value for education. Appreciation is also extended to the author's sister, who played an integral role in the author's close-knit family. The parents-in-law of the writer are thanked for their confidence, and their love.

The author would like to thank the University of Tennessee Chemistry Department for assistance in the form of a teaching assistanship for the course of graduate study. The Department of Energy (and, hence, the taxpayers of America) is (are) also thanked for the funding of this research and a research assistantship for three years.

Dr. Earl Wehry and Dr. Gleb Mamantov, co-advisors of this research, are appreciated for their participation in this vital area of research.

John Sanders, a fellow graduate student of the author, is extended appreciation for design and construction of the elutriator, drawing the figure of the elutriator, performing surface area measurements, and extensive computer advice. Gary Woody, also a graduate student, is appreciated for his help with the SFE-GC-MS studies, the modified diffusion cell, and the revised method for "baking out" the vapor deposition apparatus. Gratitude is extended to Don

Dunstan, a postdoc, for help with the fractionation of Kaneb coal stack ash. The author thanks Zhong Jinxian, a research associate, for data on the photolysis of pyrene adsorbed on the ferromagnetic fraction F3 of coal stack ash. Priscilla Gannicott, yet another graduate student, is thanked for her patience in teaching the IBM software, termed Lotus, to the author. Jonathan Krueger, fellow graduate student for one year (1985-86), is extended appreciation for familiarizing the author with experimental procedures of the fly ash research group. Rod Cole, instrument operator of the GC-MS, is thanked for his cooperation.

Elaine Hall, the author's high school chemistry teacher for 2 years, is appreciated for her enthusiasm. The chemistry faculty at the University of Tennessee at Martin (UTM) are extended gratitude for preparation of the author for graduate school in chemistry. The author's father, Dr. Louis Mauldin, is thanked for his excellent philosophy courses at UTM that helped prepare the author for graduate school in numerous ways.

The writer also thanks the host of support personnel that fixed his messes and made research run smoothly (as smoothly as possible!). Such support personnel include: glassblowers Arthur Pratt, L.H. Norman, and Elder Mellon; storeroom personnel Daryll Lay, Bobby Lay, Roy Hodges, Glen Johnson, and Eric Ripple; electronic shop personnel Arlene Garrison, Joel Alley, and Bill Gurley; machine shop personnel John Nelson, Tim Free, and Paul Beal.

ABSTRACT

Coal stack ash was separated into carbonaceous, ferromagnetic, and two nonmagnetic mineral fractions by the use of solvent density separation, magnetic separation, and elutriation. The efficiency of photolysis of adsorbed pyrene and benz(a)anthracene (BaA) was monitored on the surface of each fraction, with the carbonaceous fraction being primarily responsible for stabilization of adsorbed pyrene and BaA.

Supercritical fluid extraction was applied in an effort to improve the recovery of adsorbed pyrene from the carbonaceous coal ash fraction. Supercritical fluid extraction was shown to yield recoveries (approximately 2/3) of adsorbed pyrene, similar to those obtained using traditional extraction methods (Soxhlet and ultrasonic extraction with methanol or toluene).

Supercritical fluid extraction, directly coupled to gas chromatography, was utilized for the identification of a photochemically-produced product (benz(a)anthracene-7,12-dione (BaAD)) of BaA adsorbed on surface of a coal stack ash. The primary advantage of this methodology compared to traditional extraction-concentration techniques is the absence of solvent in the extract (giving rise to a lower limit of detection), because the supercritical fluid is converted to a gas upon collection of the extracted compounds. A yield of ca. 20% of BaAD was calculated from the photochemical consumption of adsorbed BaA on silica gel and a mineral fraction of coal stack ash.

TABLE OF CONTENTS

CHAPTER PAGE

I. INTRODUCTION....1

A. Environmental Effects of Fossil Fuel Combustion.... 1

B. Problems and Objectives....2

1. Fly Ash Particle Types....2

2. "Solution" vs. "Vapor" Deposition of PAH on Adsorbent Surfaces....4

3. Chemical Analysis of Adsorbed PAH....4

4. Phototransformation of PAH Adsorbed on Coal Fly Ash..5

II. FRACTIONATION OF KANEB COAL STACK ASH....6

A. Introduction....6

B. Experimental....8

1. Materials....8

2. Methods....8

a. Separation of Coal Ash by Particle Diameters....8

b. Removal of Ferromagnetic Particles....9

c. Separations by Particle Density....9

d. Elutriation....12

e. Bulk and Surface Chemical Analyses....14

C. Results and Discussion....15

1. Fractionation of Kaneb Ash....15

2. Characterization....19

a. Bulk Elemental Compositions....19

b. Surface Analyses....22

c. Specific Surface Areas.....28

D. Conclusions.....34

III. SUPERCRITICAL FLUID EXTRACTION OF VAPOR-DEPOSITED PYRENE FROM CARBONACEOUS STACK ASH.....35

A. Introduction.....35

B. Experimental.....39

1. Materials.....39

2. Sample Preparation.....40

3. SFE Apparatus.....46

4. SFE Methods.....49

5. Traditional Extraction Methods.....50

C. Results and Discussion.....50

1. Performance of the Modified Calibration Coil.....50

2. Performance of the Modified Diffusion Cell.....51

3. SFE Extract Collection Study.....52

4. Efficiency of Supercritical Fluid Extraction of Pyrene.....54

5. Efficiency of Extraction of Pyrene by Traditional Liquid Extraction Methods.....56

D. Conclusions.....57

IV. PHOTOCHEMISTRY STUDY OF PAH ADSORBED ON COAL STACK ASH.....61

A. Introduction.....61

B. Experimental Goals.....66

1. Photochemical Depletion of Vapor-Deposited BaA and Pyrene on Four Stack Ash Fractions.....66

2. Photoproduct Identification by SFE-GC-MS.....66

3. SFE Extraction Efficiency Study of BaAD.....66

4. SFE-GC-FID Photochemical Kinetic Study.....67

5. Study of the Relative Photoreactivities of BaA and BaAD.....67

6. Collection Efficiency and Precision Experiments.....68

C. Experimental Materials and Apparatus.....68

D. Experimental Methods.....69

1. Deposition and Photochemical Techniques.....69

2. Techniques used in Supercritical Fluid Extraction Studies.....71

E. Results and Discussion.....74

1. Disappearance Studies of Pyrene and BaA on Kaneb Coal Stack Fractions.....74

2. Confirmation of BaAD as a Photoproduct of BaA.....77

3. BaAD Extraction Efficiency Study.....82

4. Study of the Rate of Photodecomposition of Adsorbed BaA and Yield for Production of BaAD....82

5. Relative Photoreactivities of BaAD and BaA.....92

6. SFE-GC-FID Collection Efficiency and Precision Study.....101

F. Conclusions.....102

V. SUMMARY.....104

LIST OF REFERENCES.....107

APPENDIX.....112

VITA.....119

LIST OF TABLES

TABLE PAGE

I. BULK CARBON COMPOSITION OF SIZE FRACTIONS AND FERROMAGNETIC FRACTIONS....18

II. ELEMENTAL COMPOSITION OF COAL FLY ASH STANDARD REFERENCE MATERIAL 1633A BY ICP-AES....20

III. ELEMENTAL COMPOSITION, AS OXIDE EQUIVALENTS, OF KANEB COAL STACK ASH FRACTIONS....21

IV. EXPERIMENTAL PARAMETERS FOR ESCA ANALYSIS OF KANEB COAL STACK ASH FRACTIONS....23

V. ESCA SURFACE ANALYSES OF KANEB COAL STACK ASH FRACTIONS....24

VI. BET SPECIFIC SURFACE AREAS OF KANEB STACK ASH FRACTIONS....31

VII. MUNSELL SOIL COLOR DESIGNATIONS OF KANEB COAL STACK ASH FRACTIONS....33

VIII. PROPERTIES OF GASES, LIQUIDS, AND SUPERCRITICAL FLUIDS....37

IX. RECOVERIES OF ADSORBED PYRENE FROM FRACTION C3E OBSERVED WITH SFE AND TRADITIONAL EXTRACTION METHODS....58

X. APPARENT PHOTOCHEMICAL CONSUMPTION OF BaA ADSORBED ON KANEB COAL STACK ASH FRACTIONS....75

XI. APPARENT PHOTOCHEMICAL CONSUMPTION OF PYRENE ADSORBED ON KANEB COAL STACK ASH FRACTIONS....76

XII. EXTRACTION EFFICIENCY OF BaAD FROM COAL STACK ASH FRACTIONS AND SILICA GEL....85

PAGE

XIII. YIELD OF BaAD FROM PHOTOLYSIS OF BaA ADSORBED ON SILICA GEL.....89

XIV. YIELD OF BaAD FROM PHOTOLYSIS OF BaA ADSORBED ON TX M3BH.....90

XV. KINETIC DATA FOR PHOTOLYSIS OF BaA AND BaAD ON SILICA GEL AND TX M3BH.....100

LIST OF FIGURES

FIGURE PAGE

1. Schematic Representation of Production of Atmospheric PAH, their Chemical Transformation, and the Ingestion of Particulate Polycyclic Organic Matter by Humans.....3
2. Fractionation Scheme for Kaneb Coal Ash, Showing Separation of "Size Fraction 3" Particles into Composition Fractions...10
3. Schematic Diagram of Elutriator.....13
4. Fractionation Scheme Including Weight Percentages of Each Fraction Relative to the Preceding Ash in the Scheme.....16
5. ESCA Analyses for Carbon in Sputtered Fractions of C3E, M3AL, and M3BH.....27
6. ESCA Analyses for Sulfur in Sputtered and Unsputtered Fraction C3E.....29
7. ESCA Analyses for Oxygen in Sputtered and Unsputtered Fraction M3AL.....30
8. Phase Diagram of a Pure Compound.....36
9. Schematic Diagram of Vapor Deposition Apparatus.....41
10. Schematic Diagram of Adsorption and Diffusion Cell.....43
11. Schematic Diagram of Calibration Coil.....45
12. Schematic Diagram of Supercritical Fluid Extraction Apparatus.....47
13. Efficiency of Extraction of Pyrene from Fraction C3E by Various Supercritical Fluids.....55

PAGE

14. Photochemical Reactions of Anthracene and BaA on Coal Stack Ash....64

15. Photoreactivity Comparison of BaA and Pyrene on Kaneb Coal Stack Ash Fractions....78

16. GC-MS Total Ion Chromatogram of Illuminated BaA Adsorbed on TX M3BH....79

17. Mass Spectrum of Photochemically-Produced BaAD on TX M3BH....80

18. Mass Spectrum of Authentic Sample of BaAD....81

19. UV Absorption Calibration Curve for BaA....83

20. UV Absorption Calibration Curve for BaAD....84

21. Formation of BaAD from Photolysis of BaA Adsorbed on Silica Gel....87

22. Formation of BaAD from Photolysis of BaA Adsorbed on TX M3BH....88

23. First-Order Photochemical Decay of BaA Adsorbed on Silica Gel....94

24. First-Order Photochemical Decay of BaAD Adsorbed on Silica Gel....95

25. First-Order Photochemical Decay of Photochemically-Produced BaAD on Adsorbed Silica Gel....97

26. First-Order Photochemical Decay of BaA Adsorbed on TX M3BH....98

27. First-Order Photochemical Decay of BaAD Adsorbed on TX M3BH....99

CHAPTER I

Introduction

A. Environmental Effects of Fossil Fuel Combustion

Coal is a complex material consisting primarily of carbon, hydrogen, and smaller amounts of oxygen, sulfur, and nitrogen.[1] Noncombustible inorganic compounds are also present in coal.[1] The projected increase in the use of coal as an energy source merits the study of pollution brought about by the combustion of coal.[2] Coal fly ash is a particulate by-product of coal combustion that is capable of escaping a coal-fired power plant stack and being subsequently dispersed into the atmosphere. The composition of the coal fly ash depends on the composition of the coal that is burned, and on the conditions of combustion. Coal fly ash is generally an inhomogeneous material containing carbonaceous, ferromagnetic, and mineral (primarily aluminosilicate) particles.[3]

A by-product of the incomplete combustion of carbonaceous materials (e.g., coal, petroleum, wood) is a class of chemical compounds known as polycyclic aromatic hydrocarbons (PAH).[4] PAH are produced in the vapor phase during the combustion process, and, upon release into the atmosphere, can exist in the gas phase or as adsorbates on the surface of atmospheric particulate matter (including coal fly ash).[5] PAH in the atmosphere may undergo chemical transormations induced by solar radiation or by non-photochemical reactions with other atmospheric species (e.g. O_3).[6] Human exposure to PAH, and their chemical transformation products, is of concern, since PAH and PAH derivatives

have been noted to be carcinogenic and/or mutagenic.[2] This entire process is summarized in Figure 1.[7]

The main objective of this dissertation is to determine the photochemical fate of PAH adsorbed on the surface of coal fly ash. The effect of distinct particulate types on PAH phototransformation processes is also an important process under investigation in this dissertation. Knowledge of the ultimate fate of PAH, present as adsorbates on each type of coal fly ash particle, is imperative in the assessment of the environmental impact of pollution caused by the combustion of coal.

B. Problems and Objectives

1. Fly Ash Particle Types

Coal fly ash is an inhomogeneous mixture containing large numbers of aluminosilicate particles, with smaller numbers of ferromagnetic and carbonaceous particles.[3] A study of the photochemistry of PAH adsorbed on the surface of coal fly ash is actually a study of the interaction of light with PAH adsorbed on a variety of distinctly different surfaces. Thus, it is often difficult to determine which surface is responsible for the observed photochemical behavior of adsorbed PAH. A primary goal of this research is to separate coal fly ash into three main particle types: carbonaceous, ferromagnetic, and mineral, as is discussed in Chapter II (p. 6). When this is achieved, it should be possible to correlate observed photochemical behavior of adsorbed PAH with the type of coal fly ash particle.

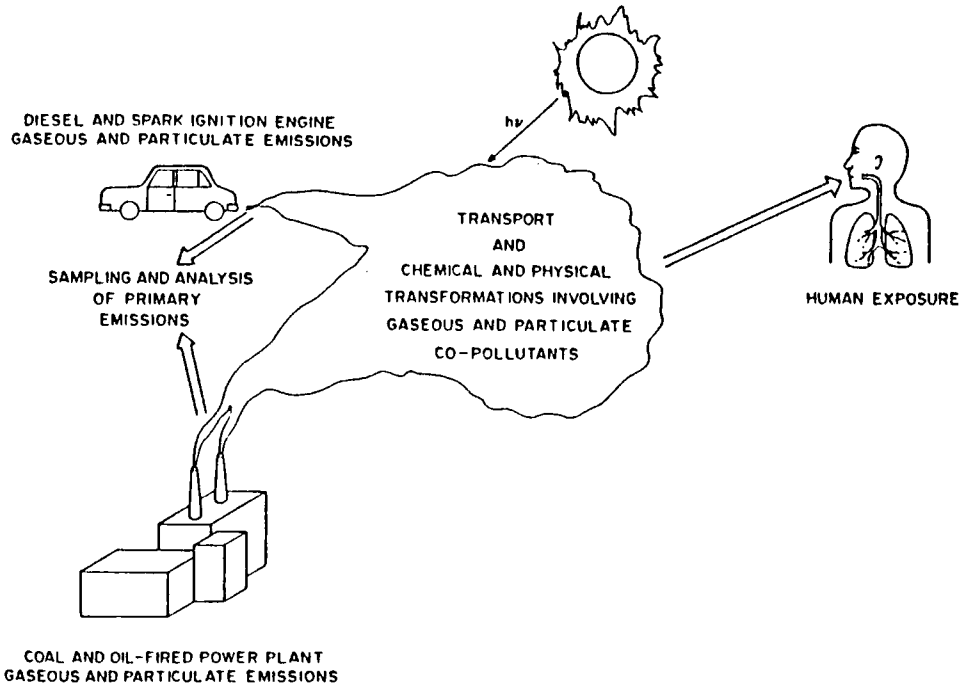

Figure 1. Schematic Representation of Production of Atmospheric PAH, their Chemical Transformation, and the Ingestion of Particulate Polycyclic Organic Matter by Humans.[7]

2. "Solution" vs. "Vapor" Deposition of PAH on Adsorbent Surfaces

In this work, it is desired to perform studies of the chemical transformation of PAH adsorbed, in known quantity in the laboratory, on well-characterized coal ash particles. For this purpose, it is necessary to deposit the PAH of interest on the adsorbent to be studied. The adsorption process of PAH on coal fly ash (or other atmospheric particulate matter) in the atmosphere is best mimicked in the laboratory by the deposition of PAH onto the surface of the adsorbent from the vapor phase.[8]

A more experimentally convenient method of deposition is performed by preparing a solution of the PAH(s) in a volatile organic solvent, placing the solution in contact with the adsorbent, and allowing the solvent to evaporate, thus leaving behind the PAH as an adsorbate on the surface of the coal fly ash. This procedure is commonly termed "solution deposition". With "solution deposition", PAH might compete with solvent molecules for strong adsorption "sites", possibly leading to adsorption of the PAH on weaker adsorption "sites". Thus, the strength of PAH-adsorbent interactions could be less with solution deposition than observed with vapor deposition.

3. Chemical Analysis of Adsorbed PAH

To discern whether a PAH has undergone chemical transformation subsequent to adsorption on a particulate surface, it is necessary to measure the quantity of adsorbed PAH present as a function of time following deposition. When transformation occurs, the quantity of PAH present on the adsorbent decreases with time, and tranformation products are produced.

Since the opaque and inhomogeneous nature of coal fly ash surfaces decreases the likelihood of the study of PAH while adsorbed on the surface, an extraction step is necessary. Regardless of the method of deposition of the PAH, a typical problem in the study of PAH adsorbed on coal fly ash is the incomplete recoveries of adsorbed PAH that are observed, i.e., one often cannot recover the same amount of PAH that was deposited on the surface.[9] Chapter III (p. 35) will detail efforts to recover quantitatively adsorbed PAH from coal fly ash by use of Soxhlet, ultrasonic, and supercritical fluid extraction.

4. Phototransformation of PAH Adsorbed on Coal Fly Ash

The influence of each particle type on the efficiency of photolysis of adsorbed PAH must be discerned. Once the particle type that contributes to the highest efficiency of photodecomposition of adsorbed PAH is found, identification of photoproduct(s) of photochemical reaction(s) should follow. The relative rates of photolysis of the parent PAH and the PAH photoproduct need to be studied. Measurement of the depletion of the parent PAH and subsequent formation of the PAH photoproduct with increasing illumination time also confirm identification of suspected photoproduct. Finally, the extractability of the PAH photoproduct is a vital piece of information for the calculation of a yield of the photoproduct. Chapter IV (p. 61) describes these experiments.

CHAPTER II

Fractionation of Kaneb Coal Stack Ash

A. Introduction

Coal fly ash has been noted to contain "mineral", "ferromagnetic", and "carbonaceous" particles.[10] Mineral particles, which constitute the majority of the weight of coal fly ash, are present primarily as aluminosilicate glass and crystalline materials.[11] Ferromagnetic particles are derived from the naturally occurring mineral found in coal, pyrite (FeS_2).[12] Carbonaceous particles, ranging from uncombusted coal particles to fully coked particles, are found in coal fly ash as a result of a variety of degrees of coking.[13] The classification of coal fly ash into these three particle "types" is a possibly oversimplified attempt to categorize the extremely complex material termed coal stack ash. Such a classification can allow one to identify the general particle types, and, as is the purpose of the work described in this chapter, to fractionate a stack ash (collected prior to release into the atmosphere) into the three particle types and subsequently characterize each fraction for total elemental concentrations and for surface elemental concentrations. Ideally, the carbonaceous fraction will contain only carbonaceous particles, the ferromagnetic fraction will contain only ferromagnetic particles, and the mineral fraction will contain only mineral particles. In practice, such "complete" separations of particle types are not expected to be achieved.

A variety of methods can be used for separation of the particle types by taking advantage of distinct physical characteristics of each particle type. The sizes of the particles can be used to separate stack ash into different size fractions. The ferromagnetic particles can be removed by magnetic action. Further separation of fractions previously separated by size and magnetic action can be achieved by discriminating between densities of the particle types by solvent density separation. Carbonaceous particles can be removed from nonmagnetic, size-separated ash by a process termed "elutriation." The term "elutriation" describes the separation of a mixture of particles on the basis of aerodynamic density. The passage of N_2 through the ash particles causes porous particles, e.g. carbonaceous particles, with low aerodynamic density to be separated from nonporous particles, e.g. mineral particles, with high aerodynamic density.

As noted previously, one reason for carrying out the fractionation of coal stack ash is so that the photochemistry of adsorbed PAH can be studied on each distinct particle type surface, rather than on a mixture of particle types and thus a mixture of types of surfaces. Another reason for fractionation and subsequent characterization of coal stack ash is that some particles can be more hazardous than others; thus, the determination of weight percentages of particle types in different coal ashes, as well as surface and bulk concentrations of constituent elements within each particle type, may be of considerable importance in assessing the possible health hazards associated with respiratory ingestion of coal fly ash particles.[14]

B. Experimental

1. Materials

"Kaneb" coal stack ash was obtained from a coal power plant in Lakeland, Florida, that was having operating difficulties at the time of collection, resulting in an unusually large amount of carbon in the ash (5.5% carbon in the bulk ash). National Bureau of Standards Standard Reference Material 1633a ("coal fly ash") was used as a standard for estimation of the accuracy of elemental analysis of the coal stack ash fractions.

Reagent grade ethyl iodide, chloroform, 1,2-dibromoethane, and hexane were obtained from Aldrich and were used as received for solvent density separations.

2. Methods

a. Separation of Coal Ash by Particle Diameters. Size separation was achieved with sieves of 45, 75, 125, and 150 μm mesh size. Ash was placed in the 150 μm sieve and sieved, using a mechanical sieve shaker, until no more ash passed through the sieve. This process was repeated in sequence with each of the other sieves in decreasing order of size in order to assure exhaustive size separation of each size fraction. The five fractions that were obtained in this manner were labelled "U" for unseparated (unseparated by means other than by size), with the numbers 1-5 being used to indicate the size fraction, and with 1 denoting the smallest size fraction and 5 denoting the size fraction containing the largest diameter particles. Thus, the <45 μm size fraction was termed U1, 45-74 μm size fraction was termed U2, 75-124 μm size fraction was termed U3, 125-149 μm size fraction was termed U4, and

the >150 μm size fraction was termed U5. Figure 2 illustrates the size separation process as the first step in the fractionation scheme.

b. Removal of Ferromagnetic Particles. A large horseshoe magnet, placed inside a 250 ml beaker, was passed over each of the size-separated fractions (U1-U5) before the actual magnetic separation procedure as a sort of "preconcentration step." Removal of the magnet from the beaker enabled ash that was magnetic in character to be collected. Ferromagnetic particles were then removed from each of the "preconcentrated" magnetic fractions via use of a stirring bar magnet housed in a 6" test tube.[15] With the magnetic stirring bar housed in the test tube, the magnetic stirring bar could be passed over the ash while avoiding direct contact of the magnetic stirring bar with the ash. Gentle tapping of the magnetic stirring bar-test tube apparatus allowed for nonmagnetic particles, that were trapped between magnetic particles and the magnet, to be eliminated from the ferromagnetic fraction. Collection of the magnetic particles was performed by lifting the magnetic stirring bar out of the test tube with a screwdriver, allowing the magnetic particles to fall from the test tube. As can be noted in Figure 2, the third size fraction (75-125 μm) was separated into N3 and F3, which symbolize nonmagnetic (N) and ferromagnetic (F) fractions of size fraction three.

c. Separations by Particle Density. Since the majority of coal stack ash is usually comprised of mineral particles,[11] the choice of which size fraction to utilize for further separation depended on the possibility that usable quantities of the carbonaceous and ferromagnetic fractions could be produced. Size fraction three was chosen for further

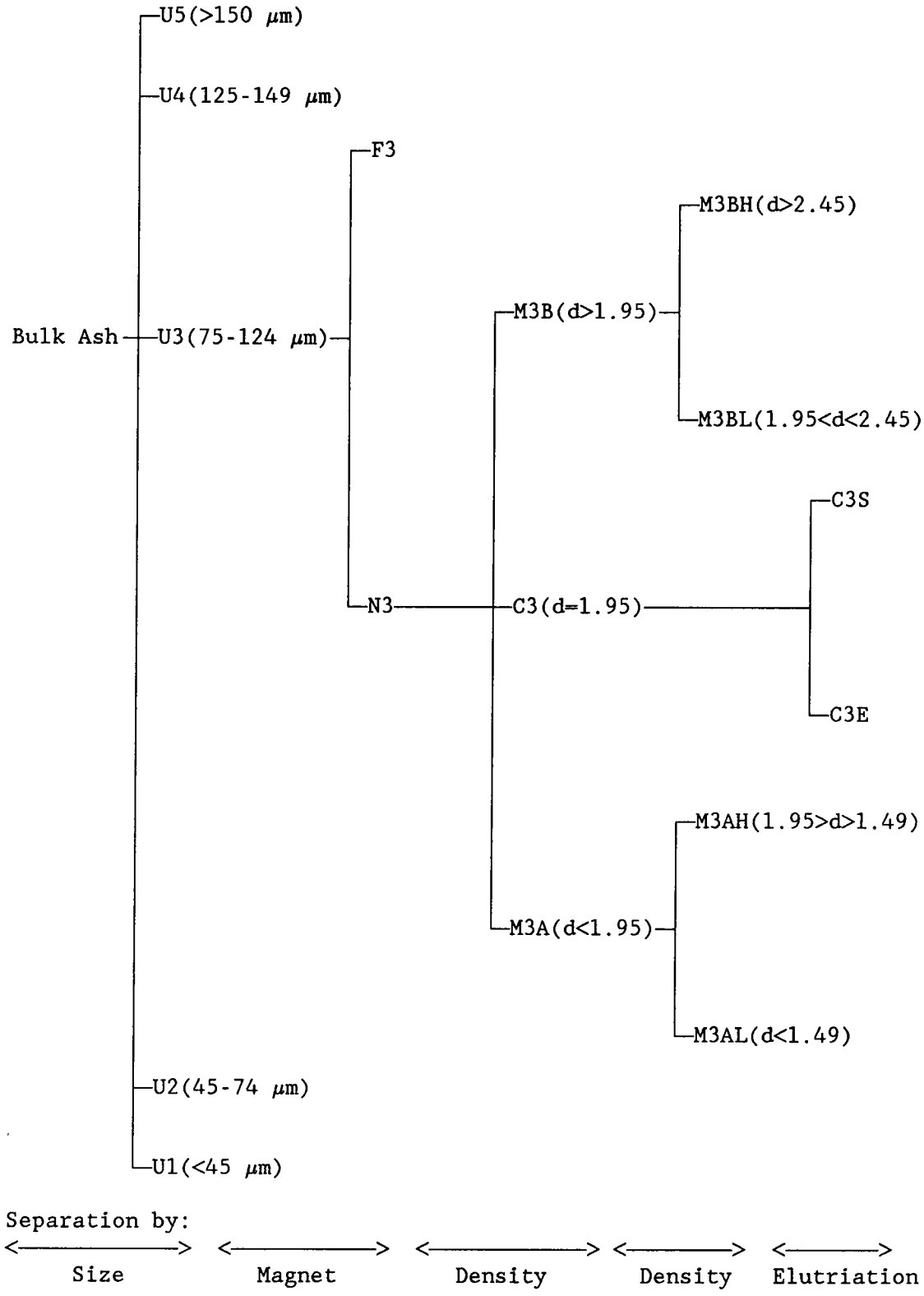

Figure 2. Fractionation Scheme for Kaneb Coal Ash, showing separation of "Size Fraction 3" (75-124 μm) Particles into Composition Fractions.

separation since a significant amount of carbon (7.42 %C, see p. 14) is contained in size fraction U3, and a significant portion of the ferromagnetic fraction F3 (5% by weight), which contains a relatively small amount of carbon (0.64 %C), is present in size fraction U3.

Solvent density separation, also known as the "float-sink" technique,[16] was used to further fractionate the nonmagnetic ash fraction (N3). This method discriminates between particles of different density (d). Approximately 30 g of nonmagnetic ash was placed in a 1000 ml separatory funnel along with 300 ml of solvent, and shaken. A preliminary separation was carried out with ethyl iodide (d = 1.95 g/ml) as the solvent. The particles that floated had a density less than 1.95 g/ml, the particles that sunk had density greater than 1.95 g/ml, and, if present, the particles that remained suspended had a density equal to 1.95 g/ml. Fractions were then removed from the 1000 ml separatory funnel by opening the stopcock and collecting each fraction in a beaker. Each fraction was rinsed in hexane in order to rid any residual solvent left from the solvent density separation. The fractions were allowed to dry overnight at room temperature in a hood. The portions of the ash that floated in ethyl iodide, and the portions that sank in ethyl iodide, appeared to be enriched in mineral particles (carbonaceous particles are dark in color, mineral particles are light in color) and thus were labelled "M" for mineral. The designation "M3A" was used for the mineral fraction of the third size fraction that had a density less than 1.95 g/ml. The abbreviation of "M3B" was assigned to the mineral fraction with a density greater than 1.95 g/ml. A fraction that appeared to be enriched in carbonaceous particles (due to its dark

color) was observed to be suspended in the ethyl iodide, and thus contained particles of approximately 1.95 g/mL density. This fraction was labelled C3, meaning carbonaceous particles from size fraction three. See Figure 2 (p. 10) for an illustration of this solvent density separation.

At this point, fractions M3A and M3B contained 4.54 %C and 5.61 %C, respectively. In an effort to decrease the carbon content of these "mineral" fractions, further solvent density separation of the mineral fractions M3A and M3B was carried out by using the solvents chloroform (d = 1.49) and 1,2-dibromoethane (d = 2.45), respectively. For these further solvent density separations, the letters H (for heavy) and L (for light) were attached to the end of the name, e.g., M3AL is the "light" fraction (d < 1.49) obtained when M3A was placed in chloroform. The light fraction of M3A (M3AL) and the heavy fraction of M3B (M3BH) appeared to contain less carbon than the original mineral fractions M3A and M3B. This process is also illustrated in Figure 2 (p. 10).

d. Elutriation. A process termed elutriation was used in an effort to separate carbonaceous particles from an ash sample. The elutriation apparatus used in this study was designed and constructed by John Sanders.[17] About 30 g of ash was placed on a glass frit (Figure 3). A stream of N_2 flowed through the ash bed at 2 L/min, and then through a 1 mm orifice into a separate chamber. Generally, the carbonaceous particles of a fraction were swept into the upper chamber with the appropriate flow rate of N_2, since carbonaceous particles have the highest specific surface area and the lowest aerodynamic density.

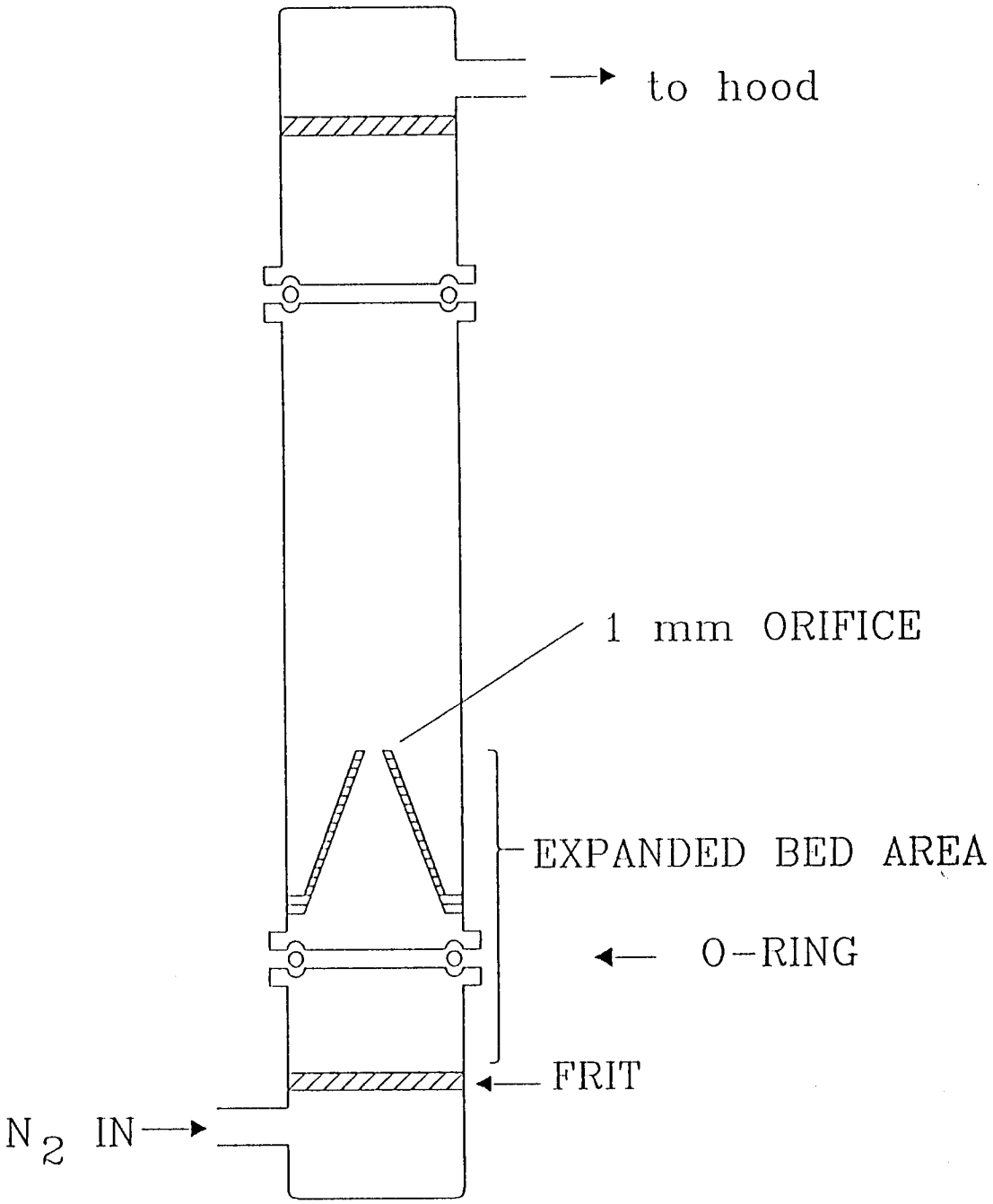

Figure 3. Schematic Diagram of Elutriator.[17]

e. Bulk and Surface Chemical Analyses. Characterization of the total (surface and bulk) elemental composition of ash fractions of the third size fraction (75-124 μm) of Kaneb coal stack ash was performed. Total carbon analyses were performed by Galbraith Laboratories, Knoxville, Tennessee by a combustion/gravimetric analysis method. For the determination of bulk elemental concentrations of fractions F3, M3AL, M3BH, and C3E, inductively-coupled plasma-atomic emission spectroscopy (ICP-AES) was carried out with a Thermo Jarrell Ash Model 61 ICP-AES spectrometer, by Vincent B. Conrad (Consolidated Coal Company, Library, PA). Prior to ICP-AES analysis, each fraction was dissolved in a mixture of HF, HCl, and HNO_3. The dissolution process of Farrell et al.[18] was followed, except that samples were heated in a water bath to promote dissolution rather than heated in a microwave oven.

To estimate the surface concentrations of ash fractions F3, M3AL, M3BH, and C3E, electron spectroscopy for chemical analysis (ESCA) was performed by irradiation of ash surfaces with Mg Kα 1253.9 eV X-rays. A PHI 5100 ESCA system (Perkin-Elmer) was used for these surface analyses. The sample chamber was maintained at 1 x 10^{-9} torr pressure during the analyses. Sputtering of the surface was carried out for one minute with a 4 keV argon ion source before and after analysis in order to obtain information concerning elements below the surface and to "clean" the surface by eliminating contaminants. Sensitivity factors, associated with the instrument, relate the number of photoelectrons detected to the response of a known concentration of standard material. Sensitivity factors were used for quantitative analysis of elements

present of the surface. Ash samples were mounted on a 1 cm^2 piece of indium foil for analysis by pressing the ash into indium foil with a mortar and pestle (used for fractions F3 and M3BH). Alternatively, an ash sample was placed on a piece of indium foil, followed by pressing another piece of indium foil on top of the ash. One piece of the indium foil, with embedded ash particles, was used for analysis. This alternative method was used for analysis in instances in which the ash sample was destroyed by the above sample preparation method (fractions C3E and M3AL).

Surface area determinations were performed by John Sanders[17] of the University of Tennessee with a Quantasorb instrument, using the Brunauer, Emmett, and Teller method.[19] The ash was degassed at 250 °C in a flowing stream of N_2 for 2 days before surface area analysis. The amount of sample ranged from 0.5 to 2.0 g. In this method, N_2 is adsorbed on the surface of each ash fraction, and by utilizing the linear portion of the adsorption isotherm, a specific surface area (in m^2/g) of the adsorbent can be calculated.

A "color" for each coal stack ash fraction was assigned by the use of Munsell Soil Color Charts.[20] This collection of charts allows one to assign a Munsell notation to a particulate solid along with a color name.

C. Results and Discussion

1. Fractionation of Kaneb Ash

The weight percentage of each fraction that was obtained in the fractionation process is shown in Figure 4. The majority of the ash

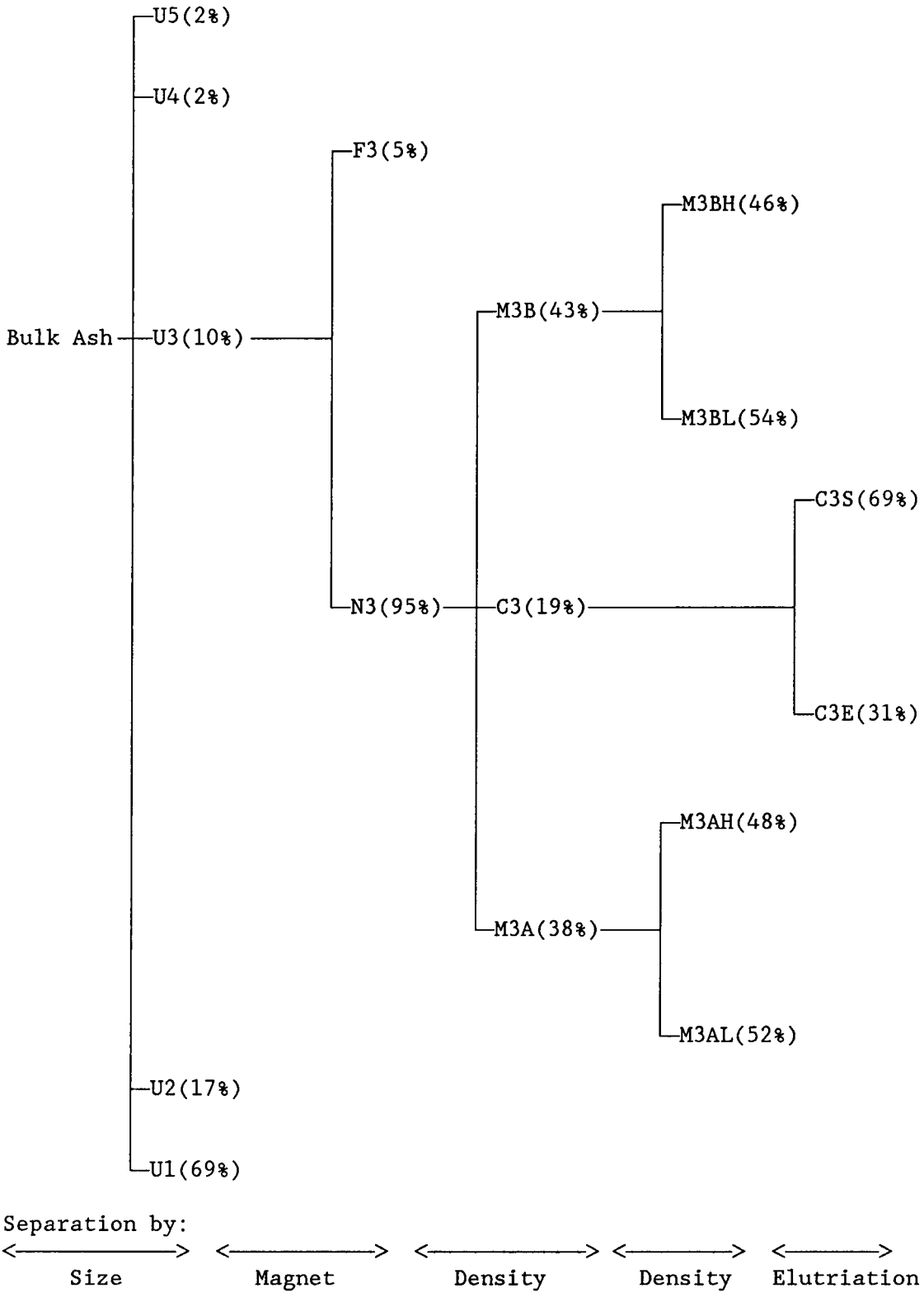

Figure 4. Fractionation Scheme including Weight Percentages of Each Fraction Relative to the Preceding Ash in the Scheme.

(69% by weight) is contained in the <45 μm size fraction U1. As the particle diameter of the fractions increases, the weight of each size fraction tends to decrease. Total carbon analyses of the size fractions U1-U5 and the ferromagnetic fractions F1-F5 are listed in Table I.

Solvent density separation of M3A and M3B with chloroform and 1,2-dibromoethane produced fractions M3AL and M3BH (Figure 2, p. 10) Weight percentages of each fraction are listed in Figure 4 (p. 16). Solvent density separation decreased the amount of carbon particles in the "mineral" fraction, as M3A contained 4.54 %C and M3AL contained only 0.25 %C. Likewise, M3B contained 5.61 %C and M3BH contained 0.87 %C. Thus, further solvent density separation decreased the amount of carbon in the "mineral" fractions.

Elutriation of the "carbonaceous" fraction C3 (35.91 %C) was carried out to increase the amount of carbon particles in the "carbonaceous" fraction. This C3 fraction was separated into an "elutriated" portion in the upper chamber of the elutriator (dubbed C3E, with E for "elutriated") and a portion that remained in the lower chamber of the elutriator (dubbed C3S, with S for sank). A %C of 67.30 was determined for the C3E fraction. The C3E fraction was used as the "carbonaceous" fraction since it contained the largest amount of bulk carbon. The weight percentages of the two fractions obtained by elutriation were 31% C3E and 69% C3S, as noted in Figure 4 (p. 16). Therefore, elutriation in a flowing stream of N_2 enabled the "carbonaceous" fraction (C3) to be treated in a manner such that a "carbonaceous" fraction (C3E) that was very high in bulk carbon content could be produced.

TABLE I

BULK CARBON COMPOSITION OF SIZE FRACTIONS AND FERROMAGNETIC FRACTIONS

Size Fraction	%C	Ferromagnetic Fraction	%C
U1	2.86	F1	0.45
U2	4.72	F2	0.56
U3	7.42	F3	0.64
U4	27.29	F4	1.41
U5	26.97	F5	1.66

2. Characterization

a. Bulk Elemental Compositions. In an effort to determine the accuracy of ICP-AES analyses of coal stack ash fractions, an ICP-AES analysis was performed on National Bureau of Standards Standard Reference Material 1633a ("coal fly ash"). Results of this analysis are presented in Table II. Excellent accuracy was observed for the major elements silicon, aluminum, and iron, with error percentages of ≤ 0.3 being observed. Elements present at 0.46-1.88 weight percentage were magnesium, potassium, calcium, and titanium; these elements were detected at <2.7% error. Trace elements (present at <0.18% by weight) sodium and sulfur were determined with percentage errors of 23.5 and 27.8, respectively. Therefore, accuracy of analyses by ICP-AES appears to be very high for major elements present in coal stack ash.

In order to evaluate the success of the fractionation process that produced a "ferromagnetic," a "carbonaceous," and two "mineral" fractions, bulk elemental compositions were obtained (by ICP-AES) for each of the four fractions. These analyses of four coal stack ash fractions (C3E, F3, M3AL, and M3BH) are presented in Table III. Each element in its most common oxidation state is represented as the corresponding oxide, with the exception of carbon. Carbon analyses were performed by Galbraith Laboratories by a combustion/gravimetric procedure whereas the remaining data in Table III are data obtained by ICP-AES. Summations of percentage by weight of constituent elements (expressed as the corresponding oxide of the element in its most common oxidation state, except carbon) are between 96 and 100% for the four fractions.

TABLE II

ELEMENTAL COMPOSITION OF COAL FLY ASH STANDARD REFERENCE MATERIAL 1633A BY ICP-AES

Element	Measured(weight %)[a]	NBS Certified(weight %)	% Error
Silicon	22.75	22.8 ± 0.8	-0.2
Aluminum	14.26	14.3 ± 1.0	-0.3
Iron	9.39	9.4 ± 0.1	-0.1
Calcium	1.09	1.11 ± 0.01	-1.8
Magnesium	0.45	0.46 ± 0.01	-2.2
Sodium	0.13	0.17 ± 0.01	-23.5
Potassium	1.83	1.88 ± 0.06	-2.7
Titanium[b]	0.78	0.80	-2.5
Sulfur[b]	0.23	0.18	+27.8

a. Analyses performed by V. B. Conrad, Consolidated Coal Company, Library, PA.

b. Values not certified by the National Bureau of Standards (NBS).

TABLE III

ELEMENTAL COMPOSITION, AS OXIDE EQUIVALENTS, OF KANEB COAL STACK ASH FRACTIONS[a,b]

Oxide	Fraction			
	Carbonaceous (C3E)	Ferromagnetic (F3)	Mineral (M3AL)	Mineral (M3BH)
SiO_2	15.28	19.28	58.32	70.42
Al_2O_3	8.66	9.57	28.25	14.48
Fe_2O_3	2.23	66.11	5.40	8.15
CaO	0.39	0.62	0.37	1.21
MgO	0.35	0.54	1.61	0.83
Na_2O	0.11	0.06	0.32	0.16
K_2O	0.77	0.87	4.04	1.90
TiO_2	0.35	0.40	1.06	0.77
SO_3	1.02	1.58	0.19	0.37
P_2O_5	0.22	0.07	0.12	0.19
C[c]	67.30	0.64	0.25	0.87
TOTAL	96.68	99.74	99.93	99.35

a. Data, for all elements except C, as weight percentage of the indicated oxide.

b. All analyses performed, except C, using ICP-AES by V. B. Conrad, Consolidated Coal Company, Library, PA.

c. Analyses performed by Galbraith Laboratories, Knoxville, TN. Data presented as weight percentage of the element.

The data in Table III (p. 21) illustrate the fact that the fractionation process was capable of producing one fraction (C3E) having a very high carbon content (67.30 %C), one strongly ferromagnetic (F3) fraction containing 66.11% Fe as Fe_2O_3, and two mineral fractions (M3AL and M3BH) that were predominantly aluminosilicate particles containing less than 1% total carbon content.

b. Surface Analyses. Parameters used for surface elemental analysis by electron spectroscopy for chemical analysis (ESCA) are listed in Table IV. The atomic orbital from which the ejected photoelectron originated is noted for each element. The binding energy of the photoelectron, which is used to determine qualitatively the presence of an element, is also listed for each element. The presence of a singlet or a doublet in the ESCA spectrum is also noted, with peak separations given in eV for cases in which doublets exist. Note that in the case of a doublet, the peak separation is added to the binding energy in order to obtain the binding energy of the accompanying peak. The sensitivity factors (relating the number of photoelectrons detected to the signal of a standard material; supplied with the instrument) that were used in the semiquantitative analysis of each element present on the surface are listed in Table IV.

Generally, carbon and oxygen were the two most abundant surface elements, as can be noted in Table V. Many of the elements in stack ash exist as oxides, carbonates, and sulfates,[15] thus contributing to the large quantities of detected surface oxygen. It has been noted that "adventitious" carbon is present on all samples analyzed by ESCA due to vacuum pump oil contaminants and atmospheric contaminants.[21] These

TABLE IV

EXPERIMENTAL PARAMETERS FOR ESCA ANALYSIS OF KANEB COAL STACK ASH FRACTIONS

Element	Photoelectron Orbital	Binding Energy[a]	Spin Multiplicity[b]	Sensitivity Factor
Carbon	1s	287	Singlet	0.250
Oxygen	1s	531	Singlet	0.660
Silicon	$2p_{3/2}$	102	Doublet (1)	0.270
Aluminum	$2p_{1/2}$	74	Singlet	0.185
Iron	$2p_{3/2}$	710	Doublet (13)	3.000
Sulfur	$2p_{3/2}$	165	Doublet (1)	0.540
Calcium	$2p_{3/2}$	347	Doublet (3)	1.580
Iodine	$3d_{5/2}$	619	Doublet (11)	6.000
Sodium	1s	1072	Singlet	2.300
Chlorine	$2p_{3/2}$	199	Doublet (2)	1.000
Fluorine	1s	686	Singlet	0.250

a. Photoelectron binding energy peak, in electron volts (eV), used for analysis upon irradiation of the sample with Mg Kα X-rays.

b. Number in parentheses notes peak separation in eV for spin doublet peaks.

TABLE V

ESCA SURFACE ANALYSES OF KANEB COAL STACK ASH FRACTIONS[a]

Fraction	C	O	Si	Al	Fe	S	Ca	I	Na	F	Total
C3E Unsp[b]	50	30	7	3	2	4	1	0	0	2	99
C3E Sp[c]	50	30	8	4	0	3	2	0	0	2	99
F3 Unsp	30	50	9	3	7	3	0	0	1	0	103
F3 Sp	20	50	10	7	20	1	0	0	1	0	109
M3AL Unsp	30	40	10	8	3	0	0	9	2	0	102
M3AL Sp	10	50	10	10	4	0	0	7	2	0	93
M3BH Unsp	30	40	10	7	3	2	0	0	2	0	94
M3BH Sp	10	50	20	10	6	2	2	0	1	0	101
M3AL Unsp[d]	40	40	10	5	4	0	0	1	0	0	100

a. Elemental compositions expressed in weight percent.

b. Unsp stands for unsputtered; surface was not sputtered with argon ions before analysis.

c. Sp stands for sputtered; surface was sputtered with argon ions before analysis.

d. This sample was degassed in a N_2 stream at 250 °C for 24 h before analysis in an effort to eliminate adsorbed ethyl iodide used in the separation process.

contaminants certainly seem to be present on the mineral fractions and the ferromagnetic fraction, since sputtering with argon ions for 1 min decreased the surface carbon content considerably. However, sputtering did not significantly decrease the amount of detected carbon on the carbonaceous ash fraction C3E.

Significant concentrations of silicon and aluminum were observed on the surfaces of all of the fractions studied, with expectedly large quantities in the mineral fractions. In all cases (except M3AL), sputtering increased concentrations of silicon and aluminum due to removal of surface contaminants and/or exposure of aluminosilicate matrices. It has been reported that silicon, aluminum, and iron concentrations increase with sampling depth, thus probably representing much of the internal matrix of fly ash.[22]

As expected, the iron surface concentration was highest on the ferromagnetic fraction. Surface concentration of Fe increased considerably from 7 to 20 percentage by weight upon sputtering, likely due to removal of hydrocarbon contamination. The iron concentration in fraction C3E decreased from 2 to 0 percent by weight upon sputtering, indicating surface enrichment of iron on the carbonaceous particles.

Fractions C3E and M3BH contained detectable amounts of sulfur, and its concentration did not change significantly upon sputtering. Fraction F3 also contained sulfur, and its concentration decreased upon sputtering. Fractions C3E and M3BH contained detectable amounts of calcium. These two fractions also contained sulfur, which could be due to the presence of $CaSO_4$, as this compound has been reported to be present on the surface of coal fly ash.[13]

The element iodine was only present in measurable quantities on fraction M3AL. It was thought that the source of this element could be residual adsorbed ethyl iodide (the solvent that was used in the solvent density separation that produced this fraction). Thus, this sample was degassed overnight at 250 °C in a stream of N_2 and again analyzed with ESCA. The surface concentration of iodine decreased from 9 to 1 percent by weight upon degassing, which indicates that degassing was capable of removing residual ethyl iodide. This is an important finding for photochemical experiments, since degassing is performed before photochemical experiments are carried out. Adsorption of PAH on the surface of each fraction is desired without the presence of other adsorbed compounds that might interfere with this adsorption process.

All fractions, except fraction C3E, contained sodium. Sputtering decreased the sodium content on M3BH and M3AL. Sputtering did not significantly alter surface concentration of sodium on F3, M3BH, and M3AL.

Fraction C3E was the only fraction that contained fluorine, and the amount of fluorine did not change significantly upon sputtering.

Figure 5 displays the 280.0-300.0 eV binding energy region for sputtered C3E, M3AL, and M3BH. Carbon, present as graphite, has a tabulated binding energy of 284 eV.[21] The observed binding energy and peak width of fraction C3E indicate a narrow distribution of chemical environments of carbon in fraction C3E near the tabulated binding energy of carbon in graphite. The binding energies and peak widths of carbon in the mineral fractions indicate a wider distribution of chemical environments of carbon, likely as a result of a mixture of graphitic

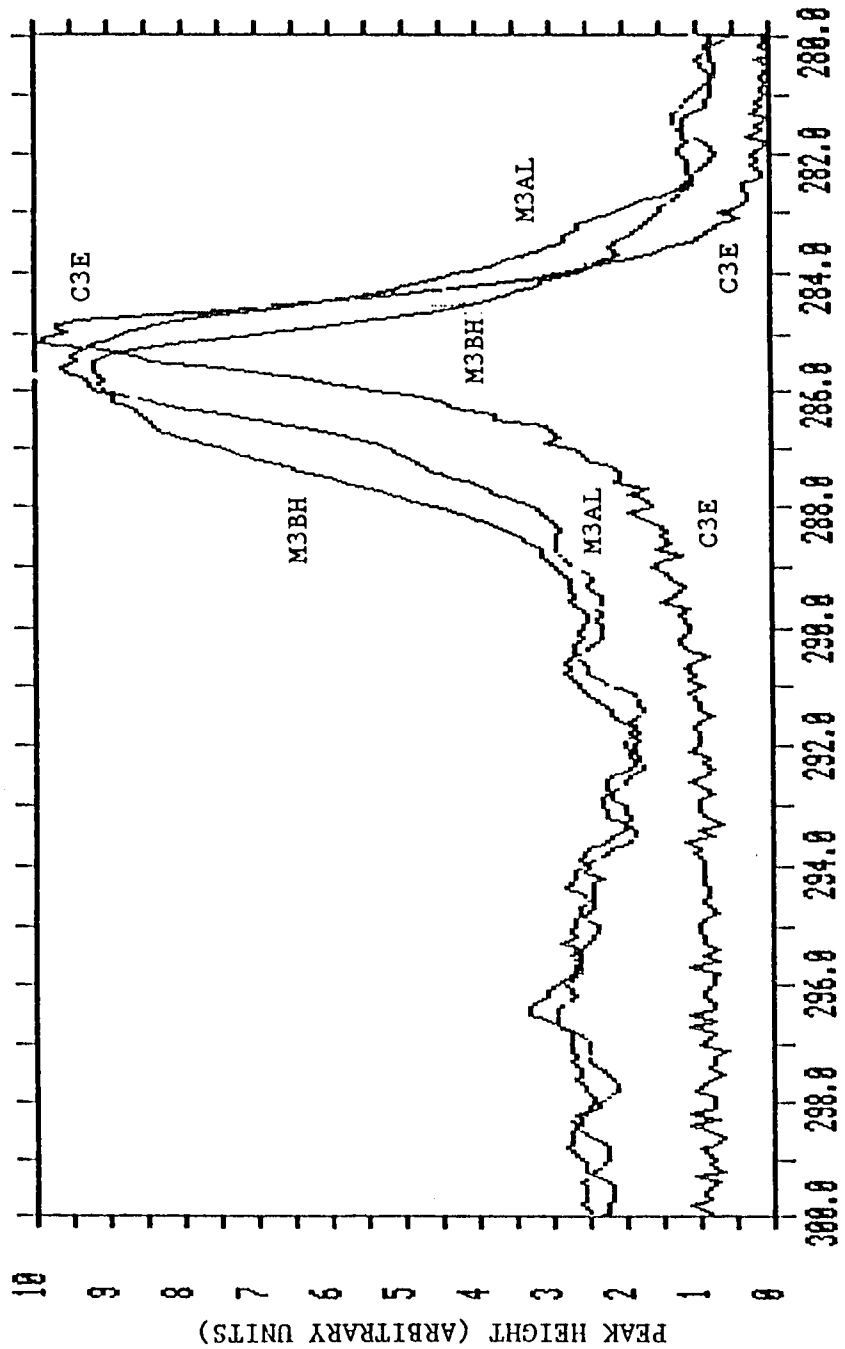

Figure 5. ESCA Analyses for Carbon in Sputtered Fractions C3E, M3AL, and M3BH.

carbon from carbonaceous particles and carbon, in the form of carbonate, from the mineral particles. Shifts in binding energies could also be due to charging effects. Graphite is a good conductor whereas mineral particles may not be as strongly conducting.[15] A nonconducting sample causes shifts to higher binding energies since a positive charge buildup occurs on the surface, due to the loss of photoelectrons. The wider peaks for carbon of the mineral fractions, however, certainly show a wider variety of chemical environments of carbon in the mineral fractions.

A peak at 171 eV for sulfur in the 158.0-178.0 eV region in Figure 6 is close to a tabulated value for sulfur as sulfate of 169 eV.[21] Elemental sulfur has a tabulated value of 164 eV,[21] and a peak emerges at 164 eV upon sputtering of C3E. Therefore, sulfate appears to extend slightly into the bulk while sulfur, in a chemical environment similar to elemental sulfur, seems not to be on the surface in detectable amounts, but rather lies just beneath the surface.

The 525.0-545.0 eV binding energy region for unsputtered and sputtered M3AL is presented in Figure 7. A peak emerges at ca. 536 eV upon sputtering, possibly due to the uncovering of oxygen in a different chemical environment than the oxygen that is responsible for the ESCA peak at 535 eV. A tabulated value of 533 eV corresponds to oxygen in SiO_2.[21]

c. Specific Surface Areas. The results of BET surface area analyses for the four Kaneb coal stack fractions are presented in Table VI. Certainly, the carbonaceous fraction C3E (67.30% bulk carbon) has the highest specific surface area (25.5 ± 0.1 m^2/g) of any of the four

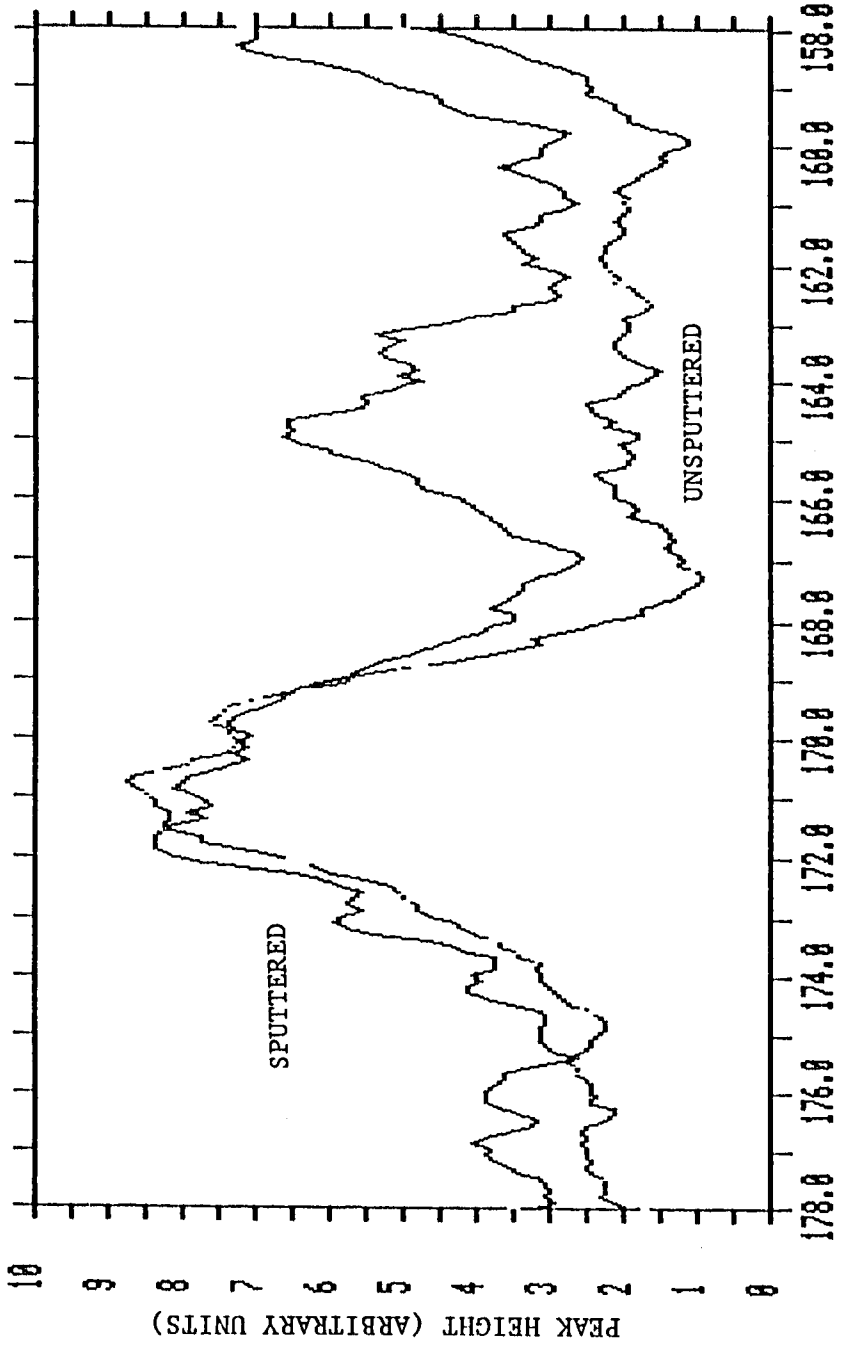

Figure 6. ESCA Analyses for Sulfur in Sputtered and Unsputtered Fraction C3E.

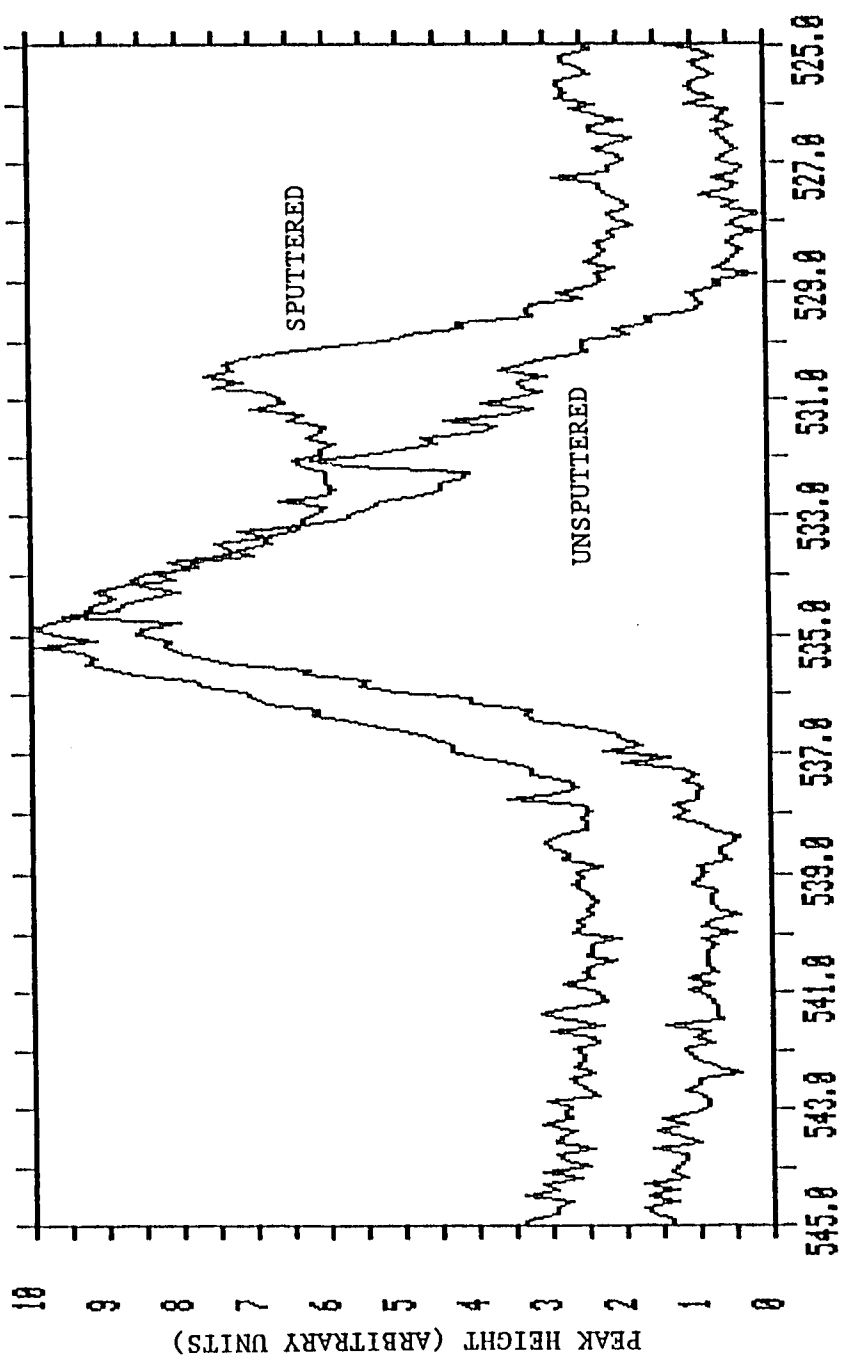

Figure 7. ESCA Analyses for Oxygen in Sputtered and Unsputtered Fraction M3AL.

TABLE VI

BET SPECIFIC SURFACE AREAS OF KANEB STACK ASH FRACTIONS[a]

Fraction	Specific Surface Area (m^2/g)[b]
Carbonaceous (C3E)	25.5 ± 0.1
Ferromagnetic (F3)	0.402 ± 0.123
Mineral (M3AL)	0.268 ± 0.002
Mineral (M3BH)	0.623 ± 0.041

a. Measured by John Sanders, University of Tennessee.

b. Expressed at the 95% confidence level.

fractions. Fraction M3AL has the lowest specific surface area of 0.268 ± 0.002 m^2/g, which is likely due to this fraction containing the smallest concentration of carbonaceous particles (0.25% bulk carbon). In fact, the surface areas of the other two fractions also increase with increasing bulk carbon content. Fraction F3 contains 0.64% bulk carbon and has a specific surface area of 0.402 ± 0.123 m^2/g; M3BH contains 0.87% bulk carbon and has a specific surface area of 0.623 ± 0.041 m^2/g.

This trend is further evidenced upon microscopic examination of the fractions. Fraction F3 contains black spherical particles having a small specific surface area, relative to that of the porous carbonaceous particles that also exist in the F3 fraction. Similarly for fraction M3AL, primarily spherical particles with low specific surface areas are mixed with carbonaceous particles of very high specific surface areas. For fraction M3BH, irregularly shaped particles similar to small pebbles are observed, also with low surface areas relative to those of the porous carbonaceous particles that are also present in fraction M3BH.

The "color" of the ash fractions was estimated with Munsell Soil Designation Soil Color Charts.[20] The results of these color assignments are listed in Table VII. Fraction C3E is black in color, as has also been noted upon microscopic examination of C3E particles. Fraction F3 is very dark gray when observed with the naked eye, yet is glossy black when observed under a microscope. The two mineral fractions M3AL and M3BH are gray and dark gray, respectively. "Hue" in the Munsell notation is described by YR and N in Table VII. The N represents no hue (achromatic) and the YR represents a hue half-way between yellow and red hue. The number to the left of the "/" mark

TABLE VII

MUNSELL SOIL COLOR DESIGNATIONS OF KANEB COAL STACK ASH FRACTIONS

Fraction	Munsell Notation	Color Name
C3E	N 2/0	black
F3	N 3/0	very dark gray
M3BH	N 4/0	dark gray
M3AL	5YR 5/1	gray

refers to the lightness of the solid with 0 for absolute black and 10 for absolute white. The number to the right of the "/" mark indicates the strength of the color (chroma) with both 0 and 1 being neutral grays.

D. Conclusions

The 75-125 μm size fraction of Kaneb coal stack was separated into 11 fractions. Methods used to separate the ash included size separation, solvent density separation, magnetic separation, and elutriation. Characterization of four fractions for bulk elemental and surface elemental compositions was carried out, indicating successful separation of a fraction enriched in carbonaceous particles, a fraction enriched in ferromagnetic particles, and two fractions containing primarily mineral particles. A carbonaceous fraction (C3E) was chosen for a study of the extractability of PAH from coal stack ash, as discussed in Chapter III (p. 35). A carbonaceous fraction (C3E), a ferromagnetic fraction (F3), and two mineral fractions (M3AL and M3BH) were chosen for a study of the photochemistry of adsorbed PAH on the surface of each fraction (Chapter IV, p. 61).

CHAPTER III

Supercritical Fluid Extraction of Vapor-deposited Pyrene from Carbonaceous Coal Stack Ash

A. Introduction

At present, identification and quantification of PAH sorbed on environmental particulate matter virtually always requires that the PAH be removed from the particulate matter prior to analysis. Techniques used for this purpose[23] include conventional Soxhlet extraction,[24] ultrasonic extraction,[25] and supercritical fluid extraction (SFE).[26] The efficiencies of such extraction procedures ultimately determine the minimum quantities of adsorbed PAH that can be detected.

Recently, the use of supercritical fluids as extraction solvents has become common.[27] The phase diagram (pressure vs. temperature) of a pure compound is presented in Figure 8.[27] A "supercritical fluid" phase exists when the pressure and temperature for a pure compound are above their critical values; hence, the term "supercritical". Densities, diffusion coefficients of solutes, and viscosities typical of gases, liquids, and supercritical fluids are listed in Table VIII.[28] A supercritical fluid exhibits a density similar to that of a liquid. Therefore, the solvent strength of a substance present as a supercritical fluid may be similar to the solvent strength of a substance present in the liquid state. However, the viscosity of a supercritical fluid is similar to the viscosity of a gas. Also, diffusion coefficients of solutes in supercritical fluids are intermediate between those observed in a gas and a liquid. Thus, the

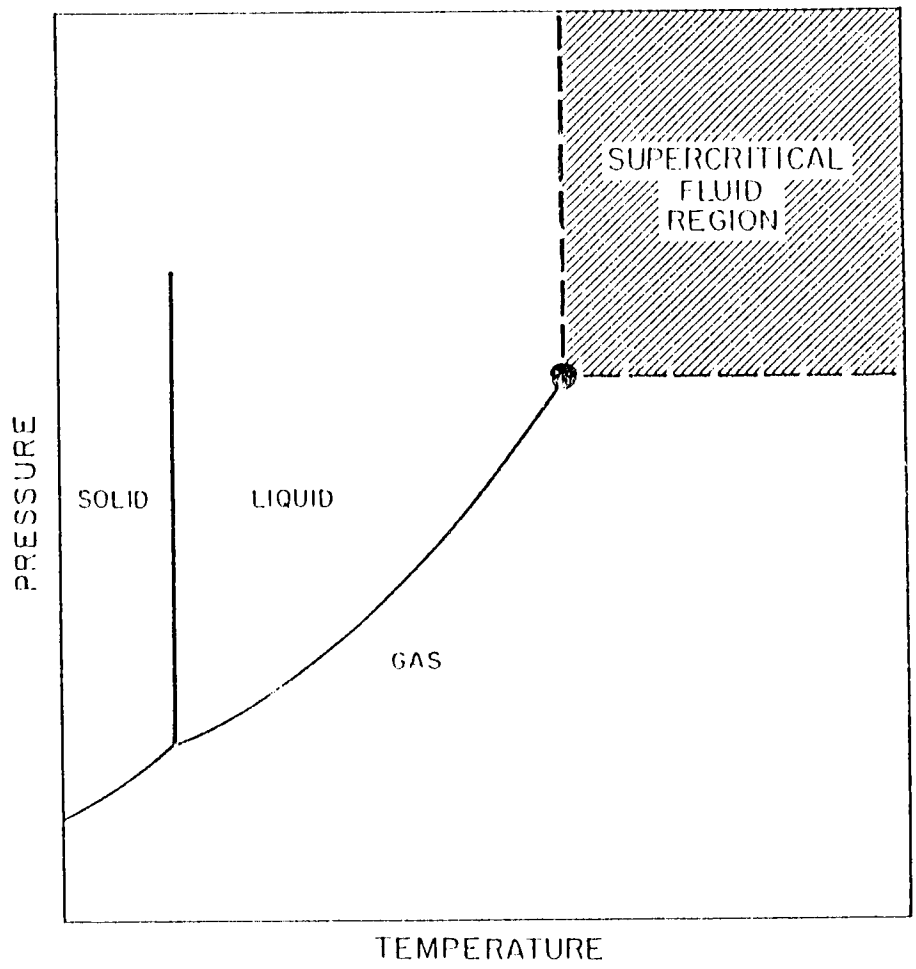

Figure 8. Phase Diagram of a Pure Compound.[27]

TABLE VIII

PROPERTIES OF GASES, LIQUIDS, AND SUPERCRITICAL FLUIDS[a]

Property (units)	Phase		
	Gas	Supercritical Fluid	Liquid
Density (g/cm^3)	$(0.6\text{-}2.0) \times 10^{-3}$	0.2-0.9	0.6-1.6
Diffusion Coefficient (cm^2/s)	0.1-0.4	$(0.2\text{-}0.7) \times 10^{-3}$	$(0.2\text{-}2.0) \times 10^{-5}$
Viscosity (cp)	$(1\text{-}3) \times 10^{-2}$	$(1\text{-}9) \times 10^{-2}$	0.2-3.0

a. From reference 28.

mass transfer properties of a supercritical fluid may allow for faster extraction rates than observed in a liquid. Higher recoveries of adsorbates from solid surfaces may also be possible when supercritical fluids are used as extractants, since the faster extraction rates make it easier to assure that the solid is "exhaustively" extracted, i.e., that the extraction recoveries of adsorbates are not limited by kinetic factors.

A widely used supercritical fluid extractant is CO_2.[27] A low critical temperature of 31 °C makes CO_2 an attractive supercritical fluid extractant, since the loss of extracted compounds by thermal degradation is unlikely. As an extractant, CO_2 is relatively nonreactive; thus, chemical reactions between the solvent and the adsorbate(s) are not probable. Also, supercritical CO_2 can be depressurized to atmospheric pressure, converting CO_2 to a gas. This depressurization occurs with a decrease in temperature; therefore, the entire extract can be collected without the presence of solvent.

It has frequently been observed that conventional extraction techniques produce substantially less than 100% recoveries of adsorbed PAH, especially for adsorbents (such as coal fly ash) that contain significant quantities of carbon.[29,30] Improved recovery of adsorbed PAH from coal stack ash with ultrasonic extraction has been reported by pretreatment of the sample with HF and/or HCl.[31] Also, several studies have indicated improved recovery of a variety of compounds from several adsorbents via supercritical fluid extraction (SFE) as compared with traditional extraction methods.[32-34] Additional advantages of SFE may include a decrease in the number of sample-handling steps and the ease

of coupling SFE to other analytical techniques, such as gas chromatography (GC).[26,35,36]

This chapter describes a comparison of the extraction efficiency of SFE and "traditional" liquid extraction methods, using pyrene (deposited in known quantity from the vapor phase) as the PAH. Coal stack ash was separated by various methods to produce a sample, named C3E, that was relatively high in carbonaceous particle content (see p. 21). This ash was used as the adsorbent for the present study because it represents an extremely challenging test of any extraction procedure, since carbonaceous particles have been shown to be primarily responsible for strong adsorption of PAH by coal stack ash.[29]

B. Experimental

1. Materials

Coal stack ash was obtained from a coal-fired power plant in Lakeland, Florida. The bulk (unseparated) coal stack ash contains 5.5% total C, since the coal-fired power plant that produced the ash was not operating efficiently at the time of collection.[37] Merck silica gel (63-200 μm particle size) was obtained from Brinkman, Inc. Pyrene and benz(a)anthracene (99+%) were purchased from Aldrich and were used as received. Methanol and toluene (Burdick and Jackson) were used as extraction solvents, supercritical fluid modifiers, and collection solvents. Carbon dioxide (SFC grade) and isobutane (instrument grade), equipped with eductor tube and helium headspace, were purchased from Scott Specialty Gases.

2. Sample Preparation

Coal stack ash was size-separated with sieves and a mechanical sieve shaker to yield 75-124 μm particles. Solvent density separation was used to produce an ash fraction (C3E) relatively high in bulk carbon content (67.30 %C), as described previously (p. 9).

Vapor deposition of pyrene onto the stack ash fraction C3E was used in conjunction with flame ionization detection (FID) to measure the quantity of pyrene sorbed by a known amount of the adsorbent, as described previously by Engelbach et al.[9,38] As illustrated in Figure 9, PAH is produced in the vapor phase in Oven 1 and subsequently swept by a stream of N_2 into Oven 2 where adsorption of the PAH onto the surface of the adsorbent occurs in the deposition cell. After the N_2/PAH stream exits the deposition cell, the vapor phase concentration is monitored with flame ionization detection (FID) as a function of deposition time. With the FID trace, the mass of the adsorbent, and mass flow rate of the PAH, the concentration of PAH on the surface of the adsorbent can be calculated, as described by Engelbach.[38]

Four revisions, however, were made to the apparatus and techniques described by Engelbach. First, a "zero" response from the FID was necessary to calculate the amount of PAH that had adsorbed on an adsorbent. In order to determine this "zero" level, previous procedure entailed removing PAH from Oven 1, setting ovens to the appropriate temperature, and subsequent determination of a FID response corresponding to only N_2 flowing into the FID. In order to improve this rather cumbersome procedure, a "shunt" line was attached with a three-way valve between the N_2 cylinder and Oven 1 (see Figure 9). With this

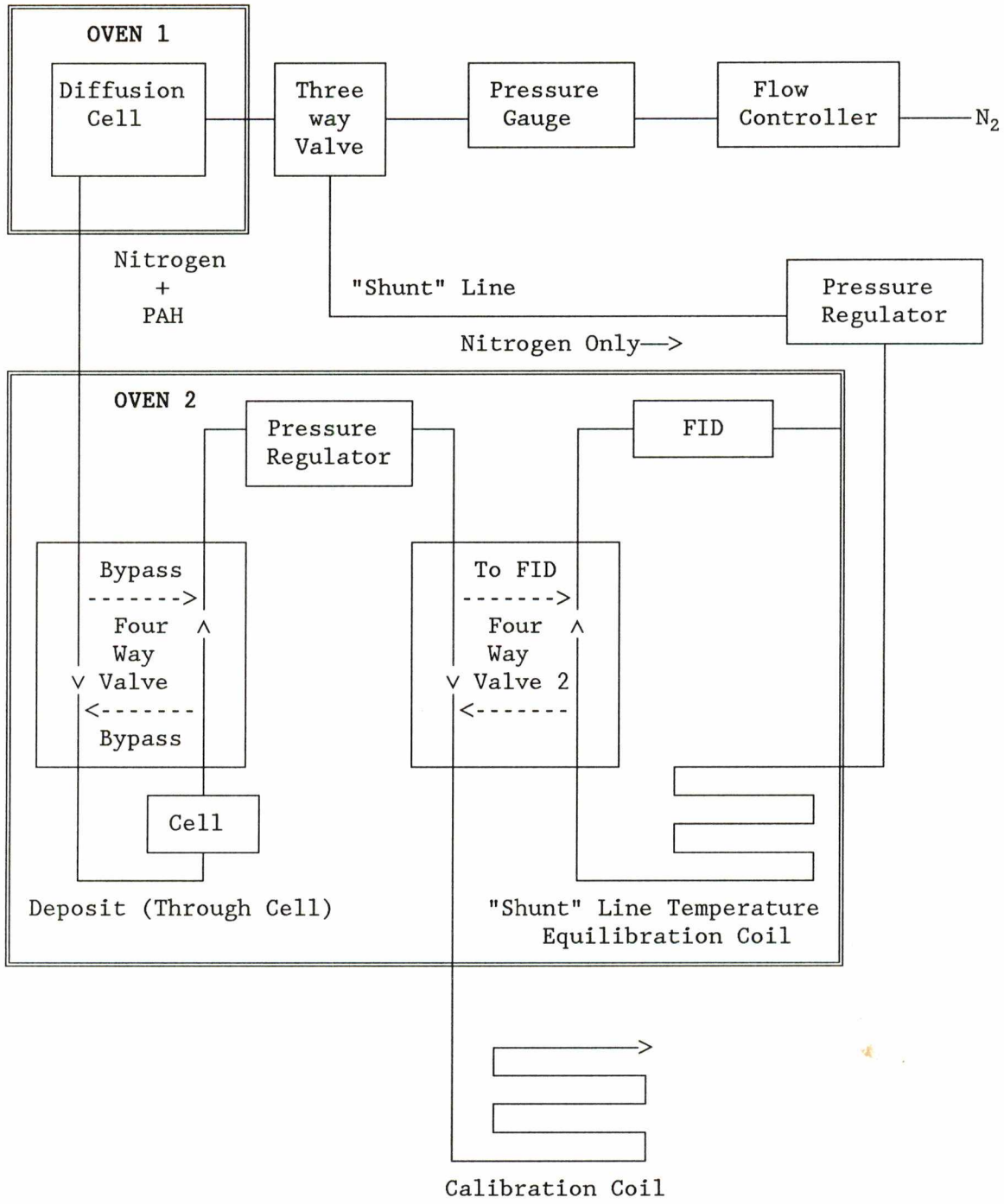

Figure 9. Schematic Diagram of Vapor Deposition Apparatus.

shunt line, pure N_2 could be diverted around Oven 1 and into Oven 2. In Oven 2, the shunt line was coiled several times in order to allow temperature equilibration of the N_2. The shunt line was then connected to the FID so that the FID response with N_2 only (not N_2 and gas phase PAH) could be determined, i.e. a "zero" response could be obtained. This revision decreased the amount of time necessary to determine a "zero" response for the FID.

In a second modification, the expanded-bed deposition cell configuration in Oven 2 was used as a diffusion cell in Oven 1 in place of the diffusion cell described by Yokley.[39] The modified deposition cell is illustrated in Figure 10. One cell, of this configuration, was employed to house the adsorbent for vapor deposition of PAH in Oven 2. Another cell, of the same configuration, was used to contain solid PAH for sublimation in Oven 1. The previous diffusion cell was configured such that N_2 would pass over the top of a bed of PAH. It has been observed that several weeks were necessary for the mass flow rate of PAH, typically expressed in μg of PAH sublimed per h, to reach a value that was reproducible from day to day. The modified diffusion cell allows for N_2 to pass through a bed of PAH resting on a glass frit. It was hoped that this configuration of the diffusion cell would allow for lower Oven 1 temperatures to be used than had previously been possible. Also, shorter periods of time should be required for the mass flow rate to become stable.

In a third modification of the vapor deposition apparatus, the calibration coil used by Engelbach[38] was modified. The calibration coil serves to collect vapor phase PAH, as a solid, upon its exit from

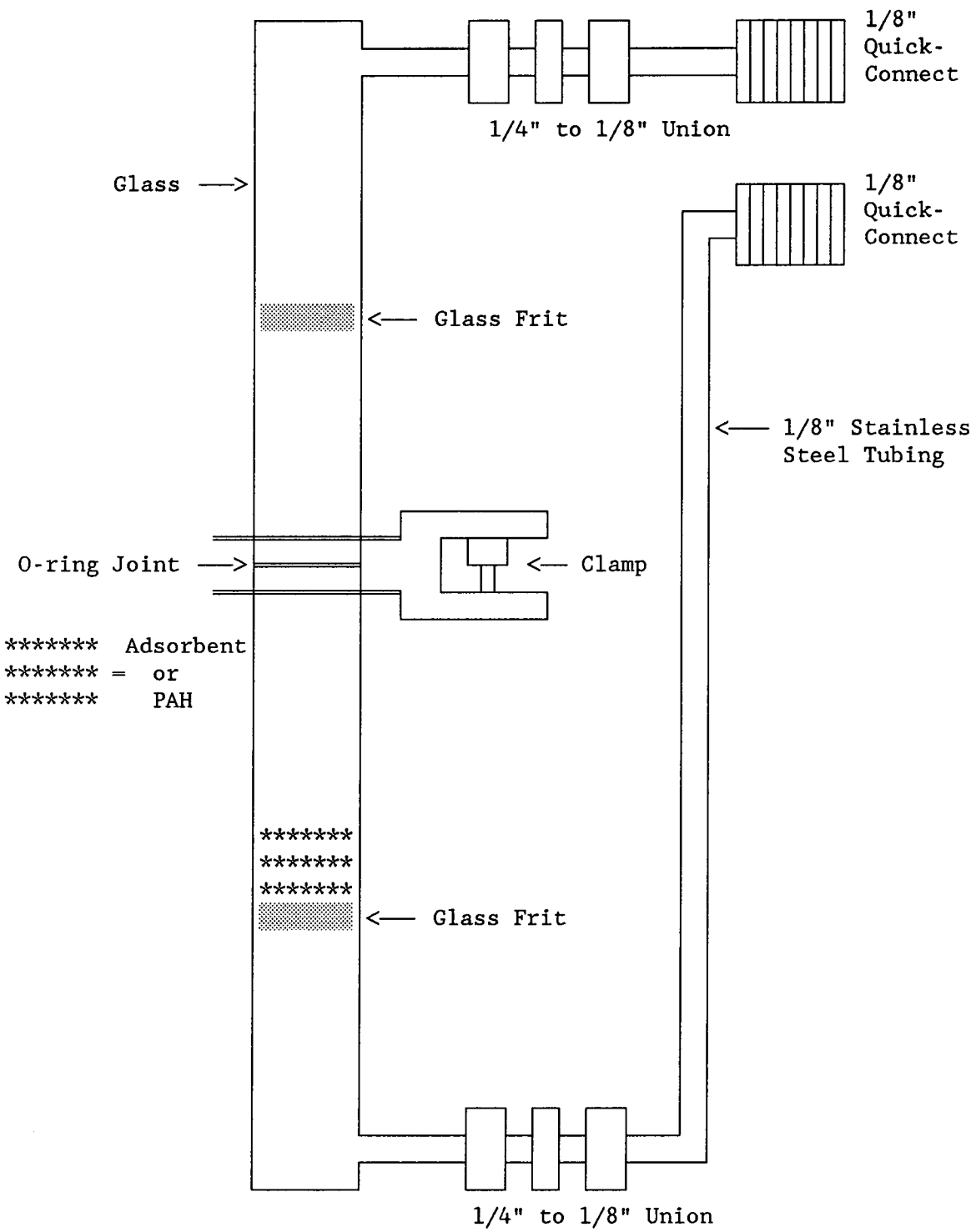

Figure 10. Schematic Diagram of Adsorption and Diffusion Cell.

Oven 2. Collection of the PAH was performed for a measured period of time (commonly 15 min) in order to calibrate the flame ionization detector response for the mass flow rate of PAH through the empty deposition cell. The modified calibration coil is shown in Figure 11. After PAH was collected in the calibration coil, the coil was rinsed with 10 mL of methanol and the PAH concentration was measured by UV-visible absorption spectrophotometry. The 1/4" o.d. Teflon tubing used by Engelbach[39] was removed from the 1/8" o.d. stainless steel tubing of the collection coil and the 1/8" o.d. stainless steel tubing was connected directly to the outlet of Oven 2 via a 1/8" stainless steel union. The calibration coil was attached to the outlet of Oven 2 via the Teflon tubing portion of the calibration coil. This alteration was performed in an effort to attain precise mass flow rates, since collection of PAH in the 1/4" Teflon tubing was thought to lead to the observed imprecise mass flow rates, due to inefficient rinsing of the interior walls of the 1/4" o.d. Teflon tubing with methanol. The 1/4" o.d. Teflon tubing was kept to serve as an "adapter" (see Figure 11) for the collection coil such that a solvent could be used to rinse the collection coil by placing solvent in the 1/4" o.d. Teflon tubing.

Finally, a change was made in the procedures used when changing from one PAH to another in the deposition apparatus. In the past, the boxes were "baked out" when changing from one PAH to another by increasing the temperatures of the ovens to ca. 200 °C, which required several days to rid the apparatus of PAH. In the modified procedure, toluene, methanol, and then water were used to rinse adsorbed PAH from the interior walls of the vapor deposition apparatus (at room

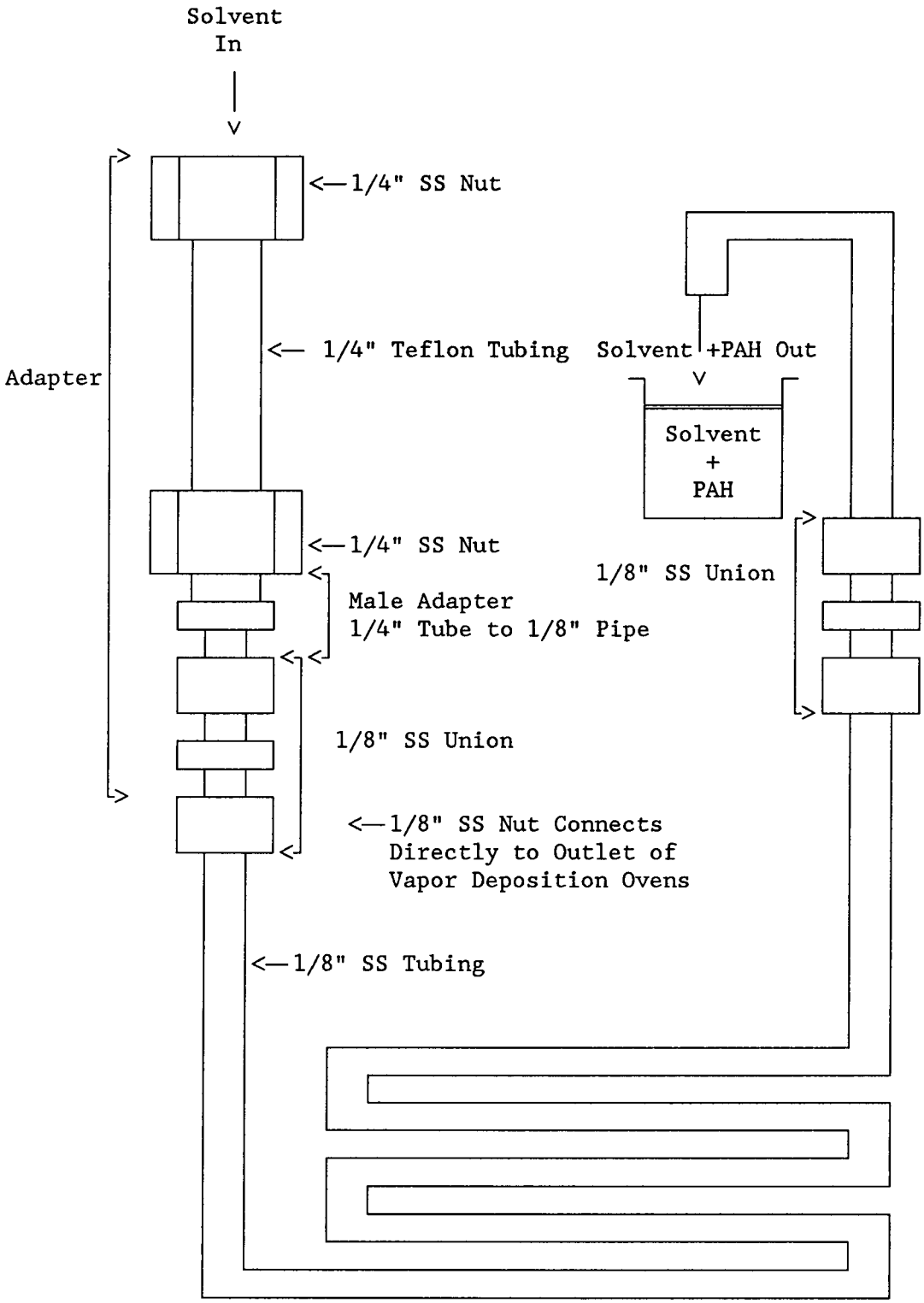

Figure 11. Schematic Diagram of Calibration Coil.

"SS" denotes stainless steel.

temperature). Each solvent was forced through the tubing of the apparatus by use of a 10 mL syringe. This method was adopted in order to decrease the amount of "down time" of the apparatus upon switching from one PAH to another.

Adsorbents were degassed for 24 h at 250 °C in a stream of nitrogen before vapor deposition of PAH. A surface pyrene concentration of 7.20 mg of pyrene per g of ash was used for extraction efficiency studies. For studies involving collection of the SFE extract on the head of a gas chromatographic column, a surface concentration of 105 μg of pyrene per g of ash was used. Silica gel was treated similarly to produce a sample containing 122 μg of pyrene per g of silica gel.

3. SFE Apparatus

All stainless steel materials were used for construction of the SFE apparatus (shown schematically in Figure 12). An Isco LC-2600 syringe pump, with a maximum operating pressure of 516 atm, was used to deliver fluids. A check valve, between the cylinder and the pump, prevented contamination of the contents of the cylinder. Pressure relief devices from High Pressure Equipment Company were installed in the cylinder-to-pump and the pump-to-cell lines for safety. A Blue M oven, with a maximum operating temperature of 260 °C, was used to maintain a constant extraction temperature. When higher extraction temperatures were needed, a Pyrex furnace was used, which was constructed by winding Nichrome ribbon around a 3" pyrex tube, and then encasing the 3" tube in a 4" Pyrex tube. The furnace temperature was monitored with an Omega Type K thermocouple.

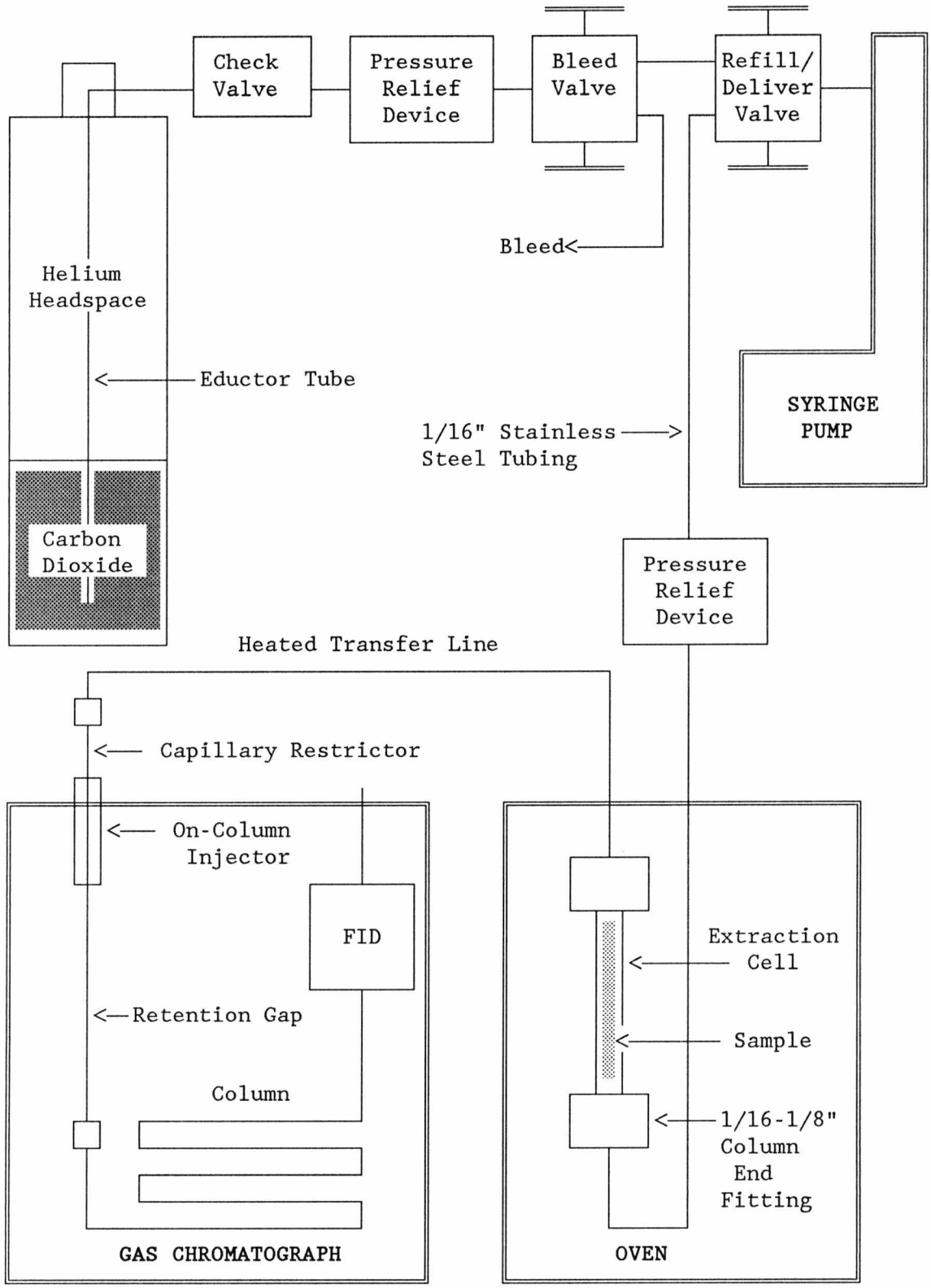

Figure 12. Schematic Diagram of Supercritical Fluid Extraction Apparatus.

The extraction cell, also illustrated in Figure 12 (p. 47), consisted of two Swagelok 1/8"-1/16" column end fittings with 2.0 μm pore diameter stainless steel frits, placed on each end of a 10 cm piece of 1/8" o.d. stainless steel tubing which housed the sample. At the end of the apparatus, the supercritical fluid (with dissolved extract) passed through 25 μm i.d. fused capillary tubing, ca. 15 cm in length, allowing the supercritical fluid to depressurize and thus be converted to a gas. This piece of fused silica capillary tubing is referred to as a "restrictor," since the pump delivers fluid through the 25 μm i.d. opening, thus "restricting" flow, and consequently maintaining high pressure thoughout the system. A heated transfer line (150 °C) carried the extract to be collected by expansion of the supercritical fluid from the capillary restrictor into a solvent or on the head of a gas chromatographic column. Polyimide-coated fused silica capillary tubing (Polymicro Technologies; 25 μm i.d. x 15 cm long) was used as the restrictor. A Supelco Supeltex M-2A 15% graphite, 85% polyimide ferrule with a 0.4 mm i.d. hole size was used to hold the capillary restrictor in place in a 1/16" Swagelok stainless steel union. A 5890A Hewlett Packard gas chromatograph equipped with an on-column injection port and a 10 m long x 0.53 mm i.d. x 2.65 μm film thickness analytical column, using 5% phenyl methyl silicone column as stationary phase, and a flame ionization detector, was used for GC analyses. A 30 cm long x 0.53 mm i.d. piece of deactivated fused silica tubing, attached between the on-column injection port and the analytical column, served as a "retention gap" (region where extract is retained).

4. SFE Methods

Liquid modifiers were added to the pump before pressurizing with CO_2 or isobutane to yield 5% by volume modified fluids. The oven temperature was increased linearly to the desired extraction temperature while the pump was pressurizing the extraction cell to 430 atm for CO_2 systems or 230 atm for isobutane systems. The extract was collected upon expansion from the restrictor capillary into 10 mL of toluene for all SFE solvent systems except methanol-modified systems, for which methanol was used as the collection solvent. Extracts were quantified by UV-visible absorption spectrophotometry. Alternatively, the extract was collected on the head of a gas chromatographic column by inserting the restrictor through an on-column injection port. The gas chromatographic oven temperature was maintained at 30 °C during collection of SFE extracts. Subsequently, extracts were quantified by matching the peak height of pyrene to peak height of an injection of a standard solution of pyrene in methanol. Gas chromatographic analyses were performed at an initial oven temperature of 30 °C, followed by a linear increase of temperature at 40 °C/min to 230 °C (the detector was kept at 325 °C) for analysis of pyrene. Each sample was repeatedly extracted until the final supercritical fluid extraction removed $\leq$ 1% of the remaining quantity of adsorbed pyrene. Each sample was then subjected to sonication with toluene in an effort to determine whether any remaining adsorbed pyrene could be extracted. A more detailed description of the supercritical fluid extraction procedure is given in the Appendix (p. 112).

5. Traditional Extraction Methods

In each of the traditional extraction procedures, sample amounts of 10-15 mg were used. For Soxhlet extractions, micro-Soxhlet extractors were used with cellulose extraction thimbles. Soxhlet extraction proceeded for 24 h, with sample exposed to fresh solvent every 15 min. For ultrasonic extractions, the sample was weighed into a 10 mL volumetric flask. Then, the flask was filled to the mark with toluene, and placed in a 125 W Branson ultrasonic cleaner for 2 h in a water bath at a temperature of 50 °C. On a few occasions, hydrofluoric and hydrochloric acid pretreatment of the ash sample was performed before sonication with toluene, as described elsewhere.[31] For exhaustive ultrasonic extraction, a sample was sonicated for 2 h at 50 °C in 50 mL of toluene. The ash was removed from the extract by filtration and then placed in 10 mL of toluene for further sonication. Batch extractions were carried out by placing the sample in a 10 ml volumetric flask, filling the flask to the mark with toluene, and allowing the sample to sit overnight in the dark.

C. Results and Discussion

1. Performance of the Modified Calibration Coil

The calibration coil serves to collect PAH vapor upon exit from Oven 2 of the vapor deposition appparatus, in order to allow measurement of the mass flow rate of PAH through the boxes (which is necessary for calculation of the quantity of PAH that adsorbed on the adsorbent); see p. 42 for further discussion. It was noticed that the major portion of PAH was collected in the calibration coil immediately upon encountering

room temperature, i.e., at the very front end of the calibration coil (see Figure 11, p. 45).

With the calibration coil configuration of Engelbach,[38] the bulk of the PAH tended to collect on the interior walls of a 1/4" o.d. piece of Teflon tubing. Frequently, PAH mass flow rates would vary considerably with this calibration coil configuration, presumably due to inefficient rinsing (with methanol) of the interior walls of the Teflon tubing, thereby resulting in imprecise measurement of mass flow rate. Therefore, the calibration coil was modified such that the PAH would collect on the interior walls of 1/8" o.d. stainless steel tubing, in the hope that the collected PAH could be efficiently rinsed from the coil. The Teflon tubing portion was then used to attach to the 1/8" o.d. stainless steel tubing in order to rinse the coil with methanol or toluene.

After the above-mentioned alteration was performed, a mass flow rate study was performed. Oven 1 was maintained at 124 °C with pyrene in the diffusion cell. Four mass flow rates were measured, for 15 min apiece. A volume of 10 mL of methanol was used to rinse the calibration coil after each collection. Mass flow rates of 109, 107, 106, and 107 μg/h were determined (107 $\pm$ 2 μg/h at the 95% confidence level). Therefore, modification of the calibration coil led to a precise determination of mass flow rates for the vapor deposition apparatus.

2. Performance of the Modified Diffusion Cell

Another modification of the vapor deposition apparatus was carried out in regard to the diffusion cell. The diffusion cell is housed in Oven 1 (Figure 9, p. 41), with N_2 flowing through the cell, in

order to provide gas-phase PAH which is subsequently swept into Oven 2 where the PAH deposits onto an adsorbent.

The diffusion cell, described by Engelbach,[38] was altered by replacing it with a deposition cell (illustrated in Figure 10, p. 43), also described by Engelbach.[38] It was hoped that, by making this change, lower Oven 1 temperatures (desired in order to avoid any thermal decomposition of the PAH) could be used and that shorter times for mass flow rate stabilization could be achieved, since N_2 would be flowing through the PAH bed rather than over the top of the bed. These objectives were indeed achieved. With the former diffusion cell configuration, a mass flow rate of 27 μg/h of benz(a)anthracene was noted at an Oven 1 temperature of 145 °C while a mass flow rate of 75 μg/h was determined at an Oven 1 temperature of only 115 °C with the new diffusion cell. Also, mass flow rate equilibration was achieved on the order of 2 days rather than weeks.

3. SFE Extract Collection Study

Losses of extracted pyrene upon collection of extract by expansion of CO_2 from the capillary restrictor must be measured in order for quantification of extracted analytes to be carried out. The extraction of vapor-deposited pyrene from silica gel has been shown to yield virtually 100% recovery of the adsorbed pyrene.[9] Therefore, silica gel containing 122 μg of pyrene per g of silica gel was used to estimate losses of extracted pyrene upon collection on a gas chromatographic column. A recovery of pyrene from silica gel of 89% was determined with CO_2 SFE at 250 °C and 430 atm with collection onto the head of a gas chromatographic column (held at 30 °C). Also, an 87%

recovery of pyrene from silica gel with CO_2/methanol SFE (250 °C and 430 atm) was observed with collection into 10 mL of methanol. Therefore, some extracted pyrene was apparently lost when CO_2 SFE was coupled directly to GC, and when CO_2 SFE extract was collected in methanol, or an error involved in the calculation of the surface concentration of pyrene gave rise to an artificially high calculated value. Neither of these problems was deemed serious.

On the other hand, liquid-modified CO_2 SFE directly coupled to GC showed complete losses of pyrene extract upon collection. Silica gel, coated with 122 μg of pyrene per g of silica gel, yielded no detectable pyrene by gas chromatographic analysis when the SFE with CO_2 and 5% methanol (45 °C, 400 atm) extract was collected on the head of a GC column held at 30 °C. In another experiment, a sample of the carbonaceous stack ash fraction C3E (105 μg of pyrene per g of ash) was extracted with CO_2/toluene at 65 °C and 400 atm. When the extract was collected into 10 mL toluene, a 51% recovery of adsorbed pyrene was observed; when the extract was collected on the head of a gas chromatographic column, no detectable pyrene was observed. For this same stack ash sample, CO_2/methanol SFE at 65 °C and 400 atm with collection into 10 mL of methanol yielded 7% of adsorbed pyrene, while collection on the head of a GC column, again, gave rise to no detectable pyrene upon gas chromatographic analysis.

It is concluded that, under these experimental conditions, pure CO_2 SFE could be directly coupled to GC without severe losses of extracted pyrene. However, collection of extracts produced by use of CO_2 modified with methanol or toluene on the head of a gas

chromatographic column led to complete loss of pyrene. Methanol and toluene are liquids at room temperature and pressure; thus, expansion of a methanol- or toluene-modified CO_2 supercritical fluid from a capillary restrictor formed liquid droplets of methanol or toluene. Subsequently, the liquid droplets that were formed presumably impeded concentration of the extract at the head of a GC column. As discussed later (Chapter IV, p. 61), SFE-GC appears to have significant promise as a technique for identification and quantification of transformation products of adsorbed PAH. Whether the inapplicability of this technique to SFE systems that employ liquid modifiers is a significant limitation of the procedure remains to be determined.

4. Efficiency of Supercritical Fluid Extraction of Pyrene

The efficiencies with which pyrene was extracted from the carbonaceous fraction C3E using CO_2, methanol-modified CO_2, toluene-modified CO_2, isobutane, methanol-modified isobutane, and toluene-modified isobutane at 250 °C are compiled in Figure 13. SFE with CO_2 was able to extract 66% of the adsorbed pyrene. Methanol-modified CO_2 yielded a 63% recovery while toluene-modified CO_2 recovered 66% of the adsorbed pyrene. Isobutane SFE extracted 64%, methanol-modified isobutane recovered 68%, and toluene-modified isobutane gave a 65% recovery of the adsorbed pyrene. The SFE systems studied exhibited remarkably similar extraction recoveries. As noted in Figure 13, isobutane SFE systems required smaller volumes of solvent (50-150 mL) than CO_2 systems (150-260 mL) to achieve equal recovery of pyrene; this observation is likely related to the higher solvating power of isobutane, as compared to CO_2, for PAH.[34] It should be noted, however,

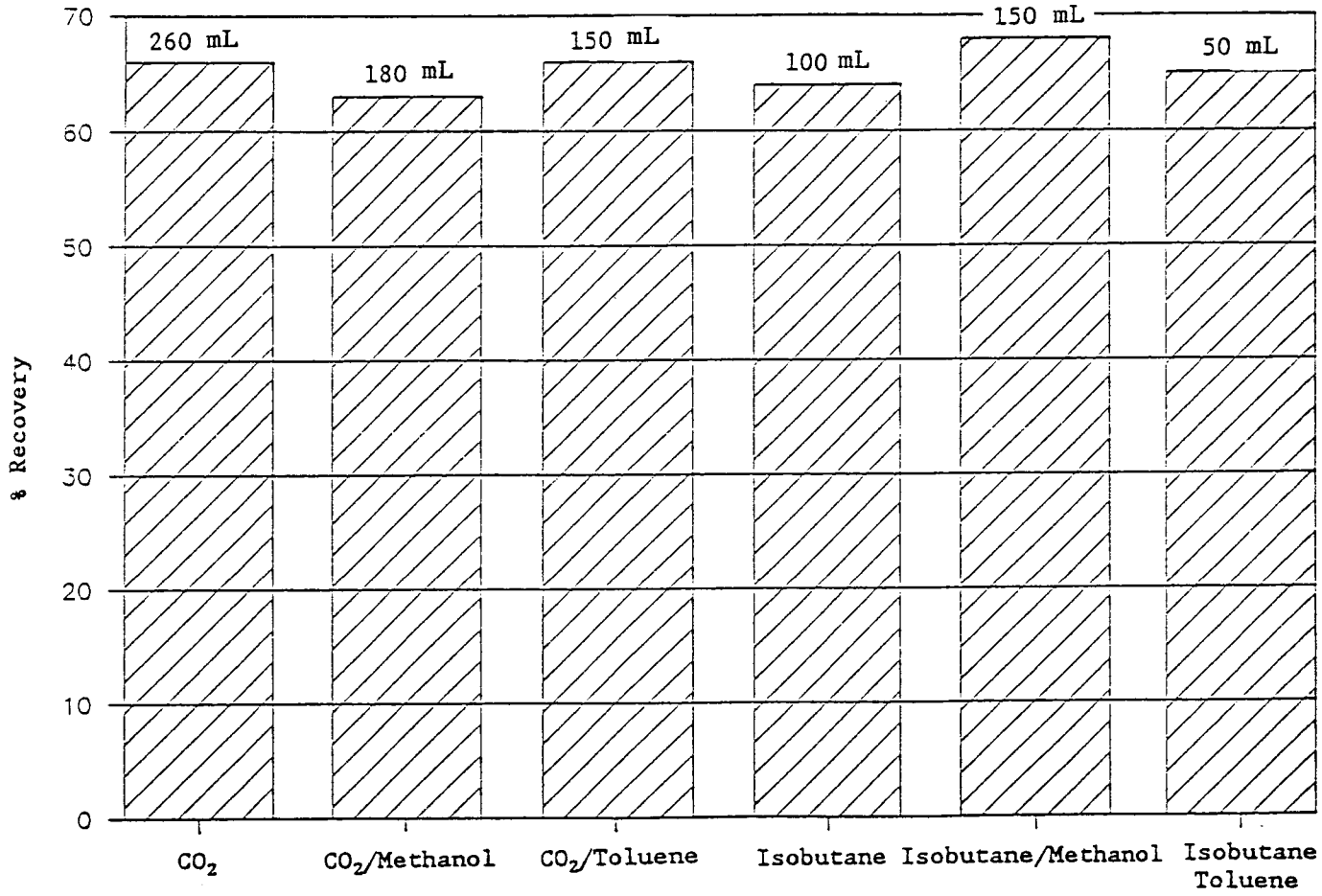

Figure 13. Efficiency of Extraction of Pyrene from Fraction C3E by Various Supercritical Fluids.

The volume required for exhaustive extraction for each solvent system is noted above each bar. Each sample was extracted until the final extraction removed ≤ 1% of the remaining quantity of adsorbed pyrene.

that essentially the same limiting recovery of adsorbed pyrene was obtained with CO_2 and isobutane. Also, the addition of a polar (methanol) and a nonpolar (toluene) modifier did not significantly increase the extraction efficiency of adsorbed pyrene for either CO_2 or isobutane.

Using CO_2 SFE at 250 °C, the recovery of pyrene decreased from 66% to 51% as the CO_2 pressure was decreased from 430 to 210 atm. Clearly, therefore, use of the higher pressure is essential.

The use of temperatures greater than 250 °C (to a maximum of 440 °C) was studied with toluene-modified CO_2 SFE. The use of toluene-modified CO_2 at 250 °C gave rise to the same extraction efficiency (66%) of adsorbed pyrene as did toluene-modified CO_2 SFE at 440 °C. Therefore, increasing the extraction temperature of toluene-modified CO_2 from 250 °C to 440 °C did not improve recovery of pyrene from the coal stack ash.

Each sample subjected to SFE was subsequently extracted by ultrasonic extraction with toluene. No detectable pyrene was removed in this manner from any of the samples mentioned above except that which had been extracted by CO_2 at 210 atm and 250 °C (51% recovery of pyrene) for which 3% of the initial quantity of pyrene was extracted by sonication with toluene after SFE.

5. Efficiency of Extraction of Pyrene by Traditional Liquid Extraction Methods

Recoveries of pyrene from carbonaceous stack ash particles with liquid extraction methods and supercritical fluid extraction methods are

listed in Table IX. Soxhlet extraction with 10 mL of methanol yielded 62% recovery of adsorbed pyrene. Similarly, ultrasonic extraction with toluene yielded 63% recovery of adsorbed pyrene. Exhaustive ultrasonic extraction with toluene, using a total of 60 mL toluene, yielded 65% of pyrene from the stack ash fraction. Therefore, ultrasonic extraction with 10 mL toluene is virtually an "exhaustive" extraction of the pyrene from this adsorbent.

Batch extraction with toluene was capable of removing 54% of pyrene from the stack ash fraction. Hence, the ultrasonic extraction process increased the recovery of adsorbed pyrene from 54% to 63%. Acid pretreatment prior to ultrasonic extraction with toluene gave rise to 54% recovery of adsorbed from the stack ash. Thus, in contrast to previous observations,[31] acid pretreatment did not improve recovery of pyrene from coal stack ash by ultrasonic extraction with toluene.

D. Conclusions

For pyrene adsorbed on carbonaceous coal ash, supercritical fluid extraction, conventional Soxhlet extraction with methanol, and ultrasonic extraction with toluene yielded very similar recoveries. The use of modifiers (methanol, toluene) did not improve recovery of pyrene from the carbon-rich stack ash for CO_2 and isobutane systems at 250 °C. Isobutane systems required smaller volumes of solvent than CO_2 systems in order to achieve equal recoveries of adsorbed pyrene. Acid pretreatment prior to ultrasonic extraction with toluene did not improve recovery of adsorbed pyrene from carbonaceous coal stack ash. Ultrasonic extraction was shown to produce a higher recovery (63%) than

TABLE IX

RECOVERIES OF ADSORBED PYRENE FROM FRACTION C3E OBSERVED WITH SFE AND TRADITIONAL EXTRACTION METHODS

Extraction Method	Solvent	Recovery
Soxhlet	Methanol	62%
Ultrasonic	Toluene	63%
Batch	Toluene	54%
Exhaustive Ultrasonic	Toluene	65%
Acid Pretreatment to Ultrasonic	Toluene	54%
SFE	CO_2	66%
SFE	CO_2/Methanol	63%
SFE	CO_2/Toluene	66%
SFE	Isobutane	64%
SFE	Isobutane/Methanol	68%
SFE	Isobutane/Toluene	65%

batch extraction with toluene (54%). Ultrasonic extraction of pyrene from the carbonaceous stack ash was shown to proceed as completely as possible using only 10 mL of toluene.

For collection of an SFE extract on a gas chromatographic column at an oven temperature of 30 °C, methanol- and toluene-modified SFE systems were shown to cause complete losses of extracted pyrene upon collection. Pure CO_2 SFE, however, could be successfully coupled to GC without significant losses of extracted pyrene.

Approximately 35% of the pyrene on this stack ash appears "irreversibly" adsorbed. None of the commonly-used extraction methods was capable of removing greater than ca. 65% of the initially adsorbed quantity of pyrene. SFE did not improve recovery of pyrene from this coal stack ash fraction, though SFE has been reported to provide improved recoveries of adsorbed PAH from other coal stack ashes.[33] Also, acid pretreatment to ultrasonic extraction has been reported to improve recoveries of PAH from coal stack ashes,[31] yet was not capable of producing improved recovery of adsorbed pyrene from this coal stack ash fraction.

A possible reason for increased recoveries of PAH from coal stack ash, as presumably observed with SFE and acid pretreatment,[31,33] is that the coal stack used by other investigators likely contained $\leq$ 5% C. Thus, improved recoveries of PAH may have been observed for PAH (deposited from solution) on mineral or iron-enriched particles. In this study, however, a stack ash consisting almost solely of carbonaceous particles was used. Carbonaceous particles are presumed to be responsible for irreversible adsorption of PAH on coal stack ash,[29]

and an increase in molecular weight of the PAH leads to a decrease in extraction efficiency of PAH from coal stack ash.[23] Hence, it is likely that PAH with higher molecular weight than pyrene are likely to irreversibly adsorb to an even greater extent than pyrene on coal ashes that contain large proportions of carbonaceous particles.

Another difference in this work from that previously described by other investigators[31,33] is that deposition of pyrene onto the coal stack ash particles was performed from the vapor phase, rather than from a liquid solution. Competition between solvent molecules and PAH for strong adsorption sites might cause PAH to be adsorbed on weak adsorption sites, thus enabling higher recoveries of adsorbed PAH when PAH is deposited from a liquid solution. Deposition of the PAH from the vapor phase, however, eliminates such competition; thus, PAH are more likely to adsorb on the strongest adsorption sites which could account for lower recoveries of adsorbed PAH.

CHAPTER IV

Photochemistry of PAH Adsorbed on Coal Stack Ash

A. Introduction

Polycyclic aromatic hydrocarbons (PAH), that are produced during the combustion of fossil fuels, may be capable of undergoing chemical and/or photochemical transformations upon release into the environment.[40,41] The formation of oxygenated products has been noted as a primary environmental fate of PAH.[42] Some oxygenated derivatives of PAH have been observed to be even more mutagenic than nitro-PAH (which are notorious mutagens[43]) in the Ames mutagenicity test.[44] A fraction of diesel exhaust extract, containing polycyclic aromatic ketones, was found to contain direct-acting Ames mutagens (i.e., it required no activation by mammalian enzymes).[45] Also, a diesel engine exhaust soot extract fraction, containing ketone and quinone derivatives of PAH, was shown to be a highly mutagenic extract fraction.[46] Hence, the environmental fate of PAH and derivatives of PAH must be determined in assessing the impact of pollution caused by the combustion of fossil fuels.

Numerous reports in the literature document the photochemical reactivity of PAH. When dissolved in organic solvents, PAH have been determined to be photosensitive.[47] Likewise, the disappearance rate of PAH as adsorbates on atmospheric soot particles has been shown to increase upon exposure to sunlight.[48] Oxidation of PAH adsorbed on atmospheric soot particles by O_3 has been shown to be catalyzed by exposure to ultraviolet light.[41,49] A mixture of diones was found to

arise as photoproducts after ultraviolet irradiation of benzo(a)pyrene in a solution of benzene.[50] Also, benzo(a)pyrene adsorbed on glass fiber filters reacts with O_3 to yield a mixture of dione products.[51] Extracts of particulate matter collected from ambient air has been shown to contain 27 identified quinone and ketone derivatives of PAH (possibly formed from photochemical oxidation of adsorbed PAH).[52] Also, pyrene has been shown to yield a mixture of dione products after ultraviolet irradiation of pyrene adsorbed on thin-layer chromatographic silica gel plates.[53]

The photochemical behavior of PAH existing as adsorbates on the surface of environmental solids has been noted to depend strongly on the nature of the substrate.[54] Coal stack ashes with high C and/or Fe content have been claimed to be primarily responsible for the suppression of photodegradation of PAH on coal stack ash in a study of pyrene and benz(a)pyrene on 8 coal stack ashes,[55] although the role of particles consisting primarily of iron oxide, present in the fly ash, is somewhat controversial.[56] As noted previously, coal stack ash is a mixture of several particle types. Any study of photochemistry of PAH adsorbed on the surface of coal stack ash is actually likely to be a study of photochemical reactions on a variety of surfaces. In Chapter II, it was noted that various subfractions, having different compositions and physical properties, can be produced from coal ash. To identify the particle type(s) on which the degradation of PAH proceeds most efficiently, the photochemical decay of PAH on each fraction must be studied.

In the literature, only one mention of production of a PAH

photoproduct from PAH adsorbed on the surface of coal stack ash exists.[58] Behymer and Hites have reported detection of anthracene-9,10-dione and benz(a)anthracene-7,12-dione as photoproducts of anthracene and benz(a)anthracene, respectively, by the use of gas chromatography-mass spectrometry (Figure 13).[58] Benz(a)anthracene-7,12-dione has also been identified as a photoproduct of benz(a)anthracene adsorbed on Al_2O_3, a model adsorbent.[59] Therefore, the photochemical fate of PAH, and oxygenated derivatives of PAH, requires more attention in the case in which PAH are present as adsorbates on the surface of coal stack ash.

Past attempts by this research group have led to inconclusive evidence of PAH photoproduct identification on coal stack ash. Identification of photoproducts of PAH is difficult since photoproducts could be produced in amounts too small to be detectable. Photoproducts that are produced on the surface of coal ash could also be highly photosensitive, thus decaying after formation from PAH yet before analysis. Interferences, brought about by concentration of extracts and contact with contaminated glassware, could prevent detection of photoproducts of PAH.

In an attempt to identify photochemical tranformation products of benzo(a)pyrene adsorbed on coal ash, Yokley employed micro-Soxhlet extraction of illuminated benzo(a)pyrene that had been vapor-deposited on several stack ashes, followed by concentration of the extract.[39] Analysis of the resulting extracts was attempted by a variety of methods, including direct probe mass spectrometry, gas chromatography-mass spectrometry, Fourier transform infrared spectroscopy, UV-visible

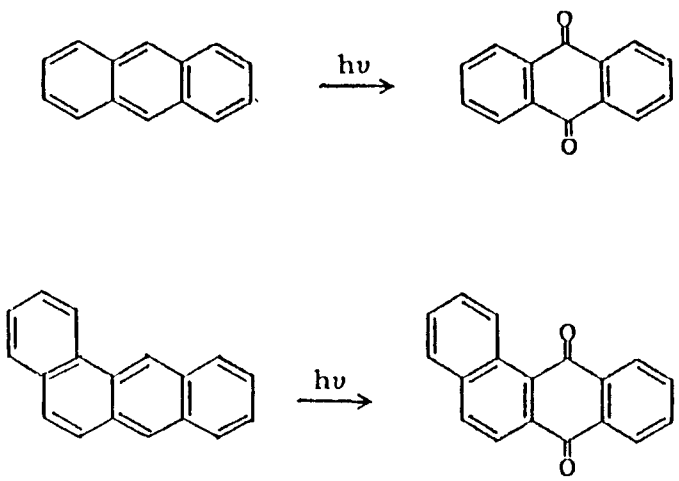

Figure 14. Photochemical Reactions of Anthracene and BaA on Coal Stack Ash.[58]

absorption spectroscopy, and liquid chromatography. Even though concentration of the extract was performed, the limits of detection were not sufficiently low in each method of analysis to provide conclusive evidence for the formation of any benzo(a)pyrene photoproducts.

Many analytical methods have failed to detect small amounts of photoproducts of PAH. An analytical approach that has not previously been applied to this problem is supercritical fluid extraction (see Chapter 3) directly coupled to gas chromatography with flame ionization detection (SFE-GC-FID) or with mass spectrometric detection (SFE-GC-MS).[59,60] In SFE-GC, no dilution of the extract occurs, since the supercritical fluid is converted to a gas upon expansion from a capillary restrictor, thereby depositing the entire extract at the head of a gas chromatographic column. By comparison with conventional liquid extraction-concentration sample preparation procedures, lower levels of contamination tend to be observed in SFE-GC, since no concentration step is necessary. Also, a decrease in the number of sample-handling steps compared to conventional liquid extraction-concentration procedures may lead to greater experimental precision.

One goal of this chapter is to examine the influence of particle type on the photoreactivity of BaA adsorbed on coal ash. Pyrene is utilized as an adsorbate in these studies in an effort to monitor the influence of particle type on the photoreactivity of a PAH other than BaA. The trends observed for each PAH will then be compared in order determine whether a particular trend is unique to only one of the PAH or the same trends are observed for both PAH. Another objective of this chapter is to evaluate the utility of supercritical fluid

extraction directly coupled to gas chromatography (with flame ionization detection or mass spectrometric detection) for the identification of a reported photoproduct of benz(a)anthracene, benz(a)anthracene-7,12-dione.

B. Experimental Goals

1. Photochemical Depletion of Vapor-deposited BaA and Pyrene on Four Stack Ash Fractions

It is desired to study the extent of photochemical decay of BaA and pyrene adsorbed on carbonaceous, iron-enriched, and nonmagnetic mineral fractions of a coal stack ash in order to compare the photoreactivity of these PAH adsorbed on different coal stack ash particles.

2. Photoproduct Identification by SFE-GC-MS

A primary objective is to determine if analyses, by SFE-GC-FID, of illuminated samples of BaA adsorbed on a mineral fraction coal stack ash indicate the presence of detectable quantities of photodecomposition product(s) of BaA. If so, initial studies will entail comparing GC retention times of suspected photoproduct(s) with those of authentic samples of possible benz(a)anthracene (BaA) transformation products (e.g., benz(a)anthracene-7,12-dione (BaAD)). If such preliminary identifications are positive, confirmatory evidence for the identity of photoproduct(s) will be sought by SFE-GC-MS.

3. SFE Extraction Efficiency Study of BaAD

One possible reason for lack of detection of a photoproduct of PAH on the surface of coal stack ash is that the photoproduct(s) could

be irreversibly adsorbed to the surface. In an effort to quantify the amount of BaAD produced on the surface for reaction yield calculations, an estimation of the extractability of photoproduct(s) of BaA with CO_2 SFE and with Soxhlet or ultrasonic extraction with methanol from silica gel and two mineral fractions of Kaneb stack ash must be obtained.

4. SFE-GC-FID Photochemical Kinetic Study

The third experimental goal is to study the photochemical decay of benz(a)anthracene (BaA) and coinciding appearance of identified photoproduct(s) with SFE-GC-FID. A decrease in the amount of BaA and an increase in the amount of photoproduct(s), with increasing illumination time, will give added evidence to identification of the photochemical product(s).

5. Study of the Relative Photoreactivities of BaA and BaAD

Another important objective is to determine the relative photoreactivity of BaA and its photoproduct(s), using the method of ultrasonic or Soxhlet extraction with methanol and subsequent quantification with UV-visible absorption spectrophotometry (which is experimentally more straightforward than SFE). Such an experiment could add confirmatory evidence to photoproduct identification, since photoproduct identification would be difficult to explain if the photoproduct were photolyzed more rapidly than the reactant!

Deposition of the PAH onto the surface of the ash must be carried out in such an experiment. In order to ascertain the relevance of such a deposition procedure, the determination of a half-life for the photoproduct (as initially deposited) is desired for comparison to a half-life of photoproduct actually formed on the surface from a surface-

bound reactant.

6. Collection Efficiency and Precision Experiments

The efficiency with which the supercritical fluid extracts can be collected at the head of a GC column must be evaluated. Losses of compound(s) upon expansion of CO_2 from the capillary restrictor (Figure 12, p. 47) could be a significant source of error in quantitative photoproduct analysis. Also, the reproducibility of SFE-GC-FID measurements must be estimated.

C. Experimental Materials and Apparatus

Benz(a)anthracene, benz(a)anthracene-7,12-dione, and pyrene were purchased from Aldrich and were used as received. Flaked graphite was purchased from Southwestern Graphite Co. Merck silica gel (63-200 μm particle size) was obtained from Brinkman, Inc. Kaneb coal stack ash fractions M3AL, M3BH, C3E, and F3 (see p. 15, Chapter II), and a heavy mineral fraction of Texas lignite coal stack ash (TX M3BH, see reference 37 for a description) were used. Supercritical fluid chromatography grade carbon dioxide, obtained from Scott Specialty Gases, was used as the supercritical fluid extractant. Burdick and Jackson high purity toluene was used as a solvent for the supercritical fluid extract in SFE-GC-MS studies. Burdick and Jackson high purity methanol was used as an extractant for the extraction of BaA and BaAD using Soxhlet and ultrasonic extraction methods.

The SFE apparatus is described in Chapter III (p. 46). In this work, one modification of the apparatus described in Chapter III was made, namely, that the SFE apparatus was directly coupled to a gas

chromatograph (with flame ionization detection). The capillary restrictor in the SFE apparatus was inserted into an on-column injection port of a Hewlett-Packard 5890A gas chromatograph (GC) equipped with a 10 m long x 0.53 mm i.d. x 2.65 μm film thickness 5% phenyl methyl silicone column. For SFE-GC-MS studies, a Hewlett-Packard 5890A GC, equipped with a 0.25 mm i.d. x 30 m long Hewlett-Packard HP-1 crosslinked methyl silicone gum column, and coupled to a 5970B quadrupole mass spectrometer, was used. A Hamilton type 1701-RN syringe was used to collect the extract from the SFE for transport to the GC-MS.

The apparatus used for vapor deposition of BaA and BaAD is described in Chapter III (p. 40). Engelbach's configuration of the diffusion cell[38] was used for BaAD and pyrene studies while a modified diffusion cell (Figure 10, p. 43) was used for vapor deposition of BaA.

D. Experimental Methods

1. Deposition and Photochemical Techniques

Vapor deposition was used for deposition of BaAD on Kaneb coal ash fractions M3AL (see Chapter II, p. 15, for a description), Texas lignite fraction M3BH (p. 64), and silica gel for extraction efficiency studies. Vapor deposition was also used for deposition of BaA on Kaneb fractions M3AL and M3BH (see Chapter II for a description) for reaction yield experiments. The temperatures of Ovens 1 and 2 in the vapor deposition apparatus were 145 °C and 160 °C, respectively, for vapor deposition of BaAD. The temperatures of Ovens 1 and 2 were 115 °C and 175 °C, respectively, for vapor deposition of BaA. For vapor depositions of pyrene, the temperatures of Ovens 1 and 2 were 145 °C and

180 °C, respectively. The flow rate of N_2 through the vapor-deposition apparatus was 40 mL/min in all cases. Both the transfer line between the two ovens and the transfer line leading to the calibration coil (see Figure 11, p. 45) were maintained at 200 °C, as measured by an Omega Type K thermocouple and Beckman Tech 330 digital voltmeter (22 MΩ input impedance). Photodegradation studies of pyrene and BaA adsorbed on the four stack ash fractions of Kaneb stack ash were performed with vapor-deposited samples.

Deposition of PAH onto the surface of coal stack ash can also be achieved by making a slurry of coal stack ash and a solution of the PAH to be adsorbed in a suitable organic solvent. This procedure is termed "solution deposition." Solution deposition, which is much more rapid than vapor deposition, was used to deposit BaA and BaAD on samples of TX M3BH and silica gel in order to determine their relative photoreactivities. Solution deposition was also used for SFE-GC-FID studies of consumption of BaA and subsequent formation of a photoproduct of BaA on TX M3BH and silica gel. For solution deposition, an ash sample was weighed into a 50 mL beaker and then a solution of PAH in methanol was pipetted onto the ash in order to just cover the ash (e.g., 0.146 mL of 636 ppm BaA in methanol was contacted with 0.5000 g of silica gel). The methanol was allowed to evaporate until the mass of the beaker and ash was the same as before the solution was added, in order to assure complete removal of methanol from the surface of the adsorbent. Usually, it was necessary to place the beaker in an oven at 70 °C for approximately 1-2 h in order to complete the evaporation process. The ash was then removed from the beaker, and the beaker was

rinsed with 10 mL of methanol. The amount of BaA that adhered to the beaker (collected in the 10 mL of methanol used to rinse the beaker) was quantified by UV absorption spectroscopy. The amount of BaA that adhered to the beaker was then subtracted from the total amount of BaA that was added to the sample for calculation of the amount of BaA adsorbed on the adsorbent.

Photochemical experiments were performed by placing sample in a 1 cm i.d. quartz cell having a 5 cm piece of 2 mm o.d. quartz rod mounted on the inside. The cell, positioned 39 cm from the Xe lamp light source, was attached to a rotary evaporator motor for rotation of the cell (around its longitudinal axis) during illumination, in an effort to expose all particulate surfaces to similar amounts of light, as described by Yokley.[39] The temperature of an adsorbent in the illumination cell rose by less than 15 °C over a 24 h illumination period.[37] The output of the Xe light source was passed through a 20 cm water filter in order to eliminate infrared radiation from the lamp. The illumination source was a Cermax LX 300 UV xenon illumator, with the power supply current set at 11 A. This source was chosen since the output spectrum of the source is similar to the solar spectrum, particularly in the 200-300 nm region (where PAH strongly absorb). Hipps measured the filtered amount of intensity for this lamp of 137 ± 16 W/m^2, at a power supply setting of 11 A, by use of an aqueous chemical actinometer of p-nitroanisole and pyridine.[61]

2. Techniques Used in Supercritical Fluid Extraction Studies

For SFE-GC-FID analyses, the gas chromatographic He flow, flame ionization detector (FID), and FID gases were turned off while the GC

oven temperature was set at 30 °C. The capillary restrictor (p. 44, 15 cm long) was inserted into the on-column injection port of the GC. After loading the extraction cell with sample and filling the pump with solvent (see Appendix, p. 112, for further details), pumping of solvent to the extraction cell was initiated. A pressure of 400 atm and temperature of 150 °C were used upon delivery of 20 mL CO_2 to the extraction cell for each extraction. A bubble flowmeter was used at the end of the GC column in order to estimate the CO_2 flow rate (which was usually 50-100 mL/min at 400 atm). The absence of flow indicated either a leak or a blockage of CO_2 somewhere in the system. A leak caused the pump to cycle at a much higher rate than normal (ca. 1 cycle per 2 s) to maintain the set pressure of 400 atm, while a blockage caused the pump to cycle at a lower rate than normal in order to maintain the set pressure. Also, the formation of ice on the outside of the GC column indicated expansion of the CO_2 from the restrictor and, thus, no leakage of CO_2 prior to the restrictor. The system was checked for leaks by touch (a cold sensation indicated a leak), since CO_2 cools upon expansion, thereby allowing for easy leak detection!

When an extraction was completed, the capillary restrictor was removed from the on-column injection port of the GC, the He flow was turned on (15 mL/min), the N_2 makeup flow to the FID was set at 11 mL/min (the FID requires ca. 30 mL/min total flow (He + N_2)), the FID electrometer and FID gases (H_2 and air) were turned on, the detector temperature was set to 325 °C, and the column temperature was increased linearly at 40 °C/min from 30 °C to 230 °C. Identification of chromatographic peaks was performed by matching the retention time of an

unknown compound with that of a known amount of authentic samples of suspected compounds. Once eluting compounds were tentatively identified, they were quantified by matching the peak height for an injection of a known amount of an authentic sample of the compound to the peak height of the observed compound.

After a compound was tentatively identified on the basis of a match in retention time with the retention time of a standard, confirmatory identification of the compound was performed by GC-MS. Gas chromatographic conditions for GC-MS studies were as follows. The injector temperature was 250 °C and the detector temperature was 280 °C. The initial oven temperature was held at 150 °C for 2 min, then was increased linearly at a rate of 10 °C/min to a final value of 230°C. The voltage of the ionization source (electron impact) in the Hewlett-Packard 5970B quadrupole mass spectrometer was 70 eV. SFE was carried out with 20 ml CO_2 at 400 atm and 150 °C. Since the SFE was located in a separate room from the GC-MS, collection of the SFE extracted compounds was performed into a gas chromatographic syringe, with plunger removed, by inserting the restrictor into the syringe. This operation was followed by drawing 2 μL of toluene into the syringe in order to dissolve extracted compounds for injection into the GC-MS.

A solution-deposited sample of BaAD on silica gel was used to determine the collection efficiency and reproducibility of the SFE-GC-FID method. Portions of this sample (ca. 20 mg) were extracted and analyzed by SFE-GC-FID in quadruplicate.

E. Results and Discussion

1. Disappearance Studies of Pyrene and BaA on Kaneb Coal Stack Fractions

In an effort to ascertain the influence of the type of particle surface on the efficiency of photolysis of adsorbed PAH, BaA and pyrene were adsorbed on each of four Kaneb (KA) coal stack ash fractions (described in Chapter II). Each sample was illuminated for 24 h and extracted before and after illumination. The results of this study are tabulated in Tables X and XI. BaA and pyrene showed essentially no photoconversion on KA C3E, the carbonaceous stack ash fraction. This observation is in agreement with earlier results[48,49] in which it is noted that ashes high in carbon content are most likely to stabilize adsorbed PAH to photolysis. BaA and pyrene adsorbed on KA F3, the iron-enriched fraction, exhibited intermediate photoreactivity when compared with that observed for the same compounds adsorbed on the two nonmagnetic mineral fractions. Hence, iron-enriched particles may play some role in stabilization of adsorbed PAH to photoconversion, in contrast to conclusions of Behymer and Hites[49] and Miller et al.[62] However, carbonaceous particles are primarily responsible for stabilization of PAH adsorbed on coal fly ash. A model adsorbent, flaked graphite, also stabilized adsorbed BaA to photolysis (Table X). This observation is similar to that of Saucy and co-workers, who found that carbon black particles stabilized anthracene and pyrene to photoconversion.[63] In contrast, pyrene on silica gel was completely consumed after 24 h irradiation. Thus, pyrene is stabilized by adsorption on the surface of coal stack ash (even on the mineral

TABLE X

APPARENT PHOTOCHEMICAL CONSUMPTION OF BaA ADSORBED ON KANEB COAL STACK ASH FRACTIONS

Adsorbent	BaA Before Illumination[a]	BaA After Illumination[a]	%Conversion
KA C3E "Carbonaceous"	3640 ± 135	3536 ± 126	-3%
KA F3 "Iron-enriched"	52 ± 9	45 ± 9	-13%
KA M3AL "Light Mineral"	41 ± 4	32 ± 5	-22%
KA M3BH "Heavy Mineral"	62 ± 9	50 ± 3	-19%
Flaked Graphite	859 ± 2	944 ± 110	0%

a. Amount of BaA extracted (in μg BaA/g adsorbent) before and after 24 h illumination.

TABLE XI

APPARENT PHOTOCHEMICAL CONSUMPTION OF PYRENE ADSORBED ON KANEB COAL STACK ASH FRACTIONS

Adsorbent	Pyrene Before Illumination[a]	Pyrene After Illumination[a]	%Conversion
KA C3E "Carbonaceous"	4406 ± 127	4650 ± 132	0%
KA F3 "Iron-enriched"	26 ± 3	24 ± 4	-8%
KA M3AL "Light Mineral"	41 ± 4	32 ± 3	-22%
KA M3BH "Heavy Mineral"	65 ± 4	44 ± 8	-32%
Silica Gel	122 ± 9	0	-100%

a. Amount of pyrene extracted (in μg pyrene/g adsorbent) before and after 24 h illumination.

particles) in comparison to pyrene adsorbed on silica gel. Pyrene and BaA behaved similarly on the four fractions of Kaneb stack ash. This point is illustrated in Figure 15. Thus, the type of coal stack ash particle appears to determine surface photoreactivity of adsorbed pyrene and BaA more than the chemical structure of pyrene or BaA.

2. Confirmation of BaAD as a Photoproduct of BaA

Behymer and Hites[57] reported the observation of BaAD as a photoproduct of BaA adsorbed on the surface of coal fly ash by GC-MS. The present work was initiated in an effort to further confirm the identification of BaAD as a photoproduct of BaA and to ascertain the feasibility of SFE-GC-MS for the analysis of PAH photoproducts on the surface of coal stack ash.

Figure 16 shows a GC-MS total ion chromatogram of an extract of 202 mg BaA solution-deposited on TX M3BH that had been illuminated for 22 h. The retention time of BaA was determined (by injection of an authentic sample of BaA) to be 11.9 min; an authentic sample of BaAD eluted at 13.8 min under the column conditions used in this work. The retention times of the extracted compounds matched the retention times of the authentic samples of BaA and BaAD. Figure 17 shows the mass spectrum of photochemically-produced BaAD on TX M3BH. Figure 18 displays the mass spectrum of an authentic sample of BaAD. A reasonable match of mass spectra indicated that the identity of the chromatographic peak at 13.8 min was indeed very likely to be BaAD. Therefore, the use of SFE-GC-MS enabled the confirmation of BaAD as a photoproduct of BaA adsorbed on the surface of a mineral fraction of stack ash.

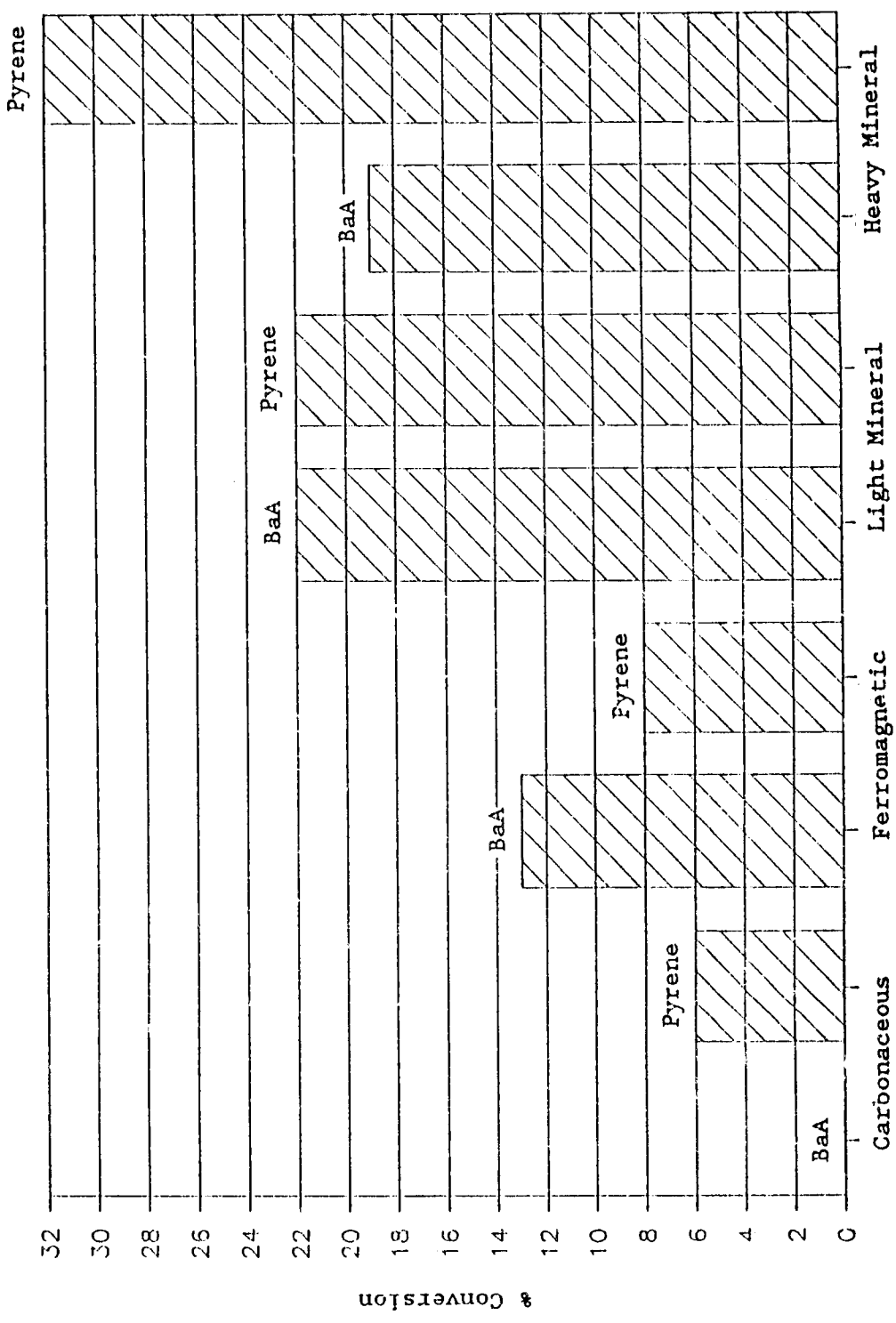

Figure 15. Photoreactivity Comparison of BaA and Pyrene on Kaneb Coal Stack Ash Fractions.

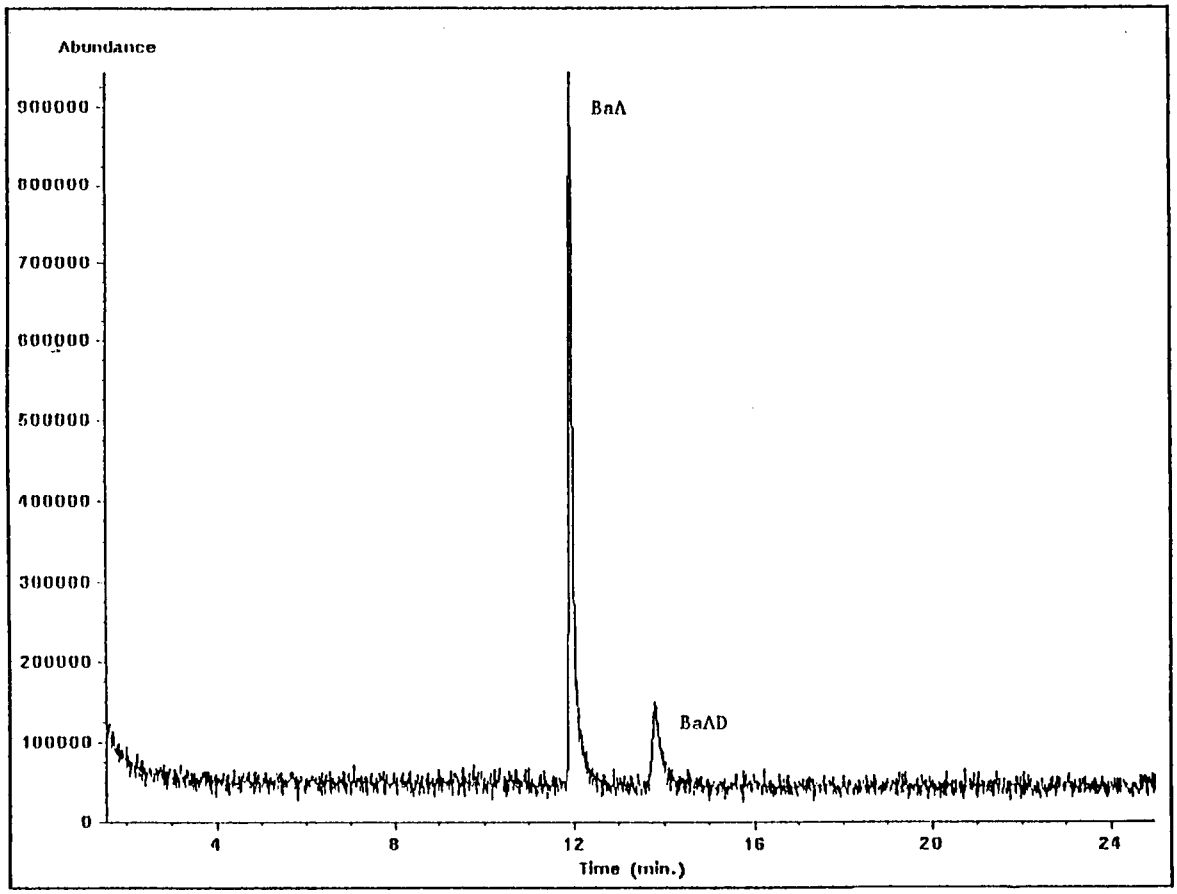

Figure 16. GC-MS Total Ion Chromatogram of Illuminated BaA Adsorbed on TX M3BH.

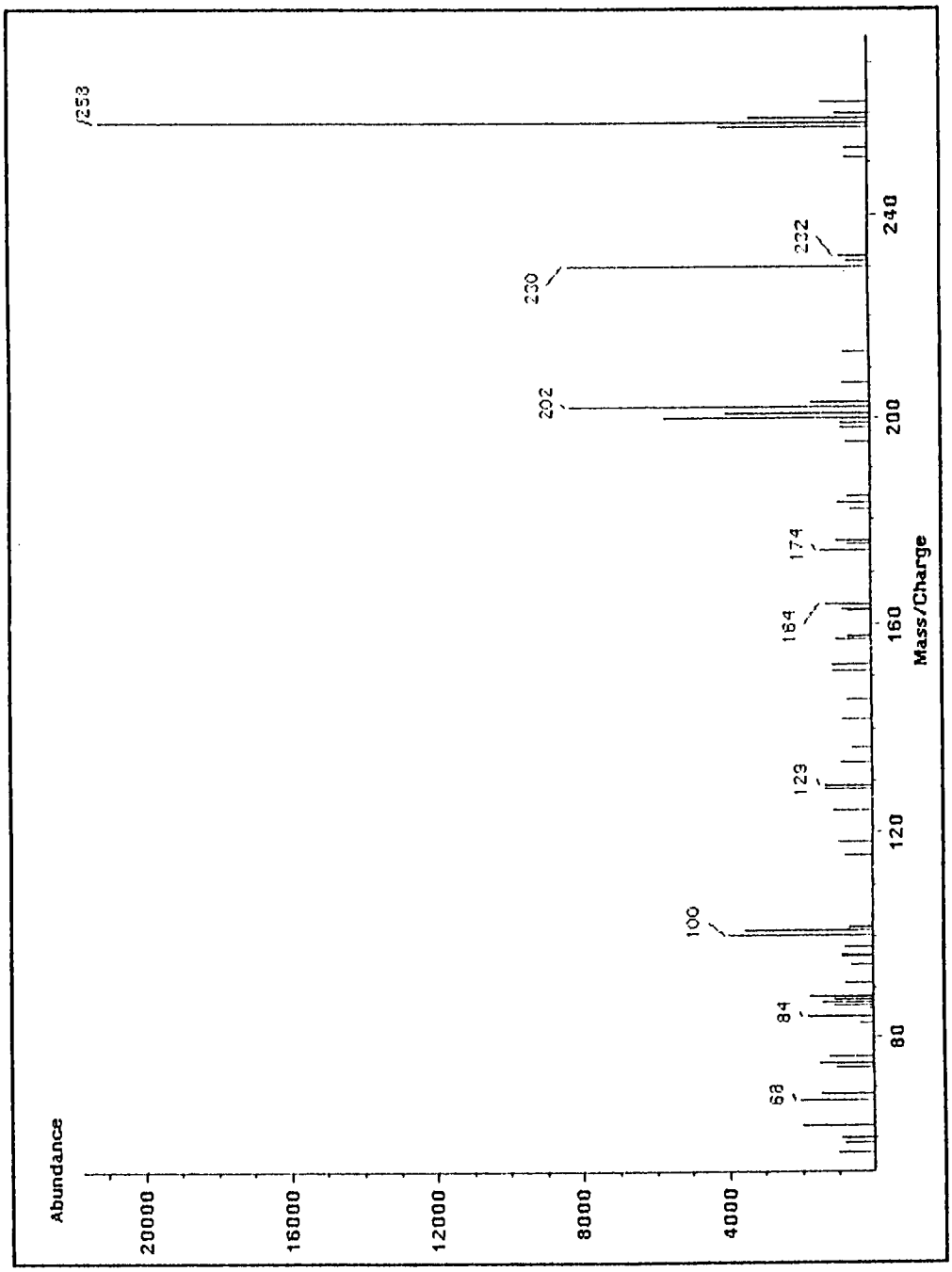

Figure 17. Mass Spectrum of Photochemically-Produced BaAD on TX M3BH.

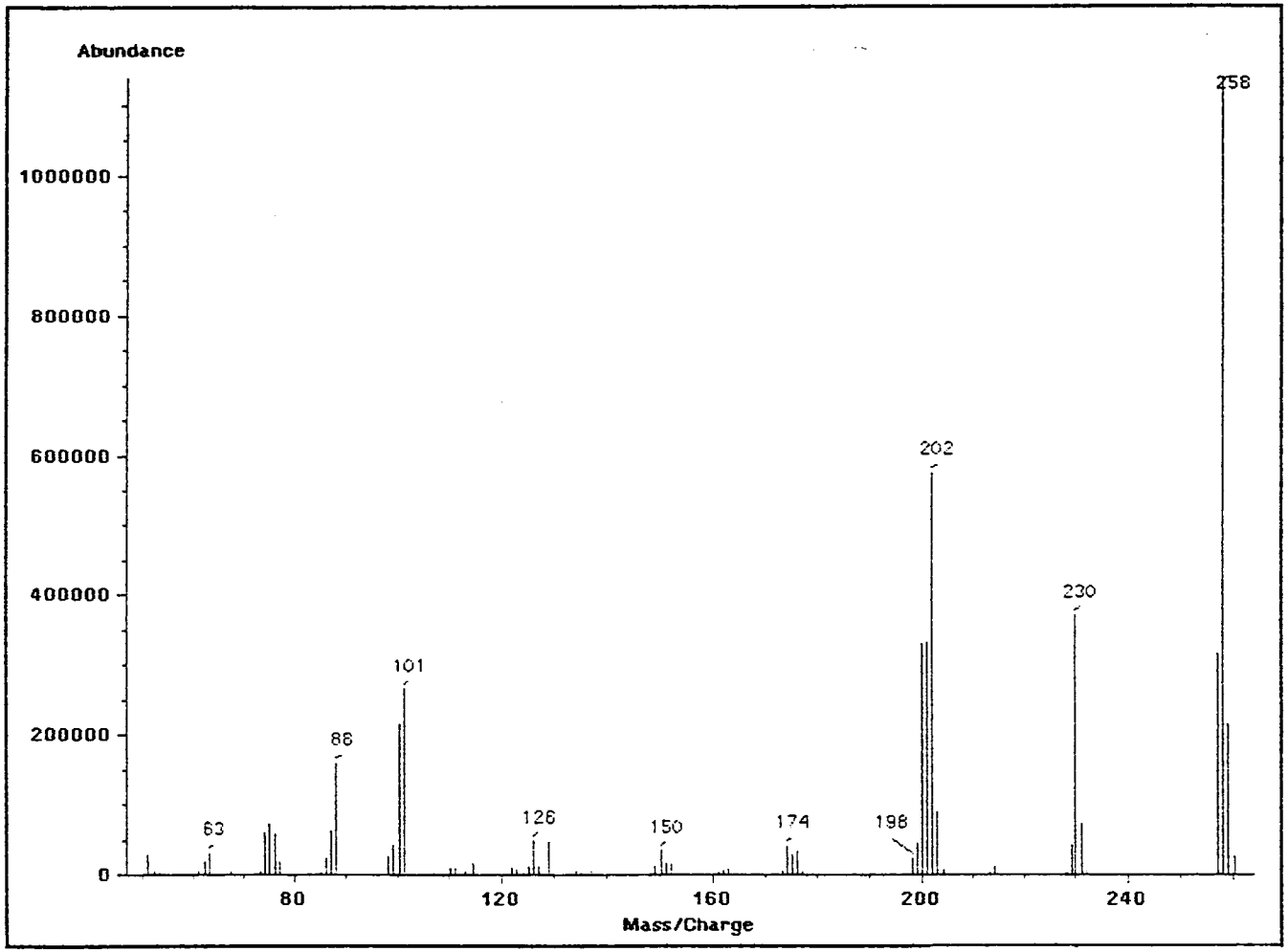

Figure 18. Mass Spectrum of Authentic Sample of BaAD.

3. BaAD Extraction Efficiency Study

The efficiency with which BaAD can be extracted from the surface of silica gel and mineral fractions of coal stack ash must be known in order to quantify a yield of BaAD from photolysis of BaA. Beer's law plots for UV absorption spectroscopy of BaA and BaAD in methanol are shown in Figures 19 and 20. A slope of 0.283 absorbance units/ppm, with a correlation coefficient (R) of 0.9988, was determined for BaA by linear regression. For BaAD, a linear regression slope of 0.09321 absorbance units/ppm was calculated, with an R value of 0.99964. These calibration plots were used for quantification of SFE extracts collected into methanol for this extraction efficiency experiment and the photoreactivity study.

Nearly quantitative recovery ($\geq$80%) of the photoproduct BaAD was found after vapor- and solution-deposition of BaAD on silica gel and the coal ash fractions KA M3AL and TX M3BH as tabulated in Table XII. Thus, when BaAD is formed by photochemical oxidation of BaA on the surfaces of these adsorbents, a large fraction of BaAD is presumably recovered by SFE with 20 mL CO_2 at 400 atm and 150 °C. From these data, it seems likely that incomplete extraction recovery of BaAD from silica gel and TX M3BH is not the major cause of significantly lower than 100% apparent yield of this photoproduct.

4. Study of Rate of Photodecomposition of Adsorbed BaA and Yield for Production of BaAD

The rate of disappearance of BaA solution-deposited on silica gel and on Texas lignite coal ash fraction M3BH (see reference 37 for a

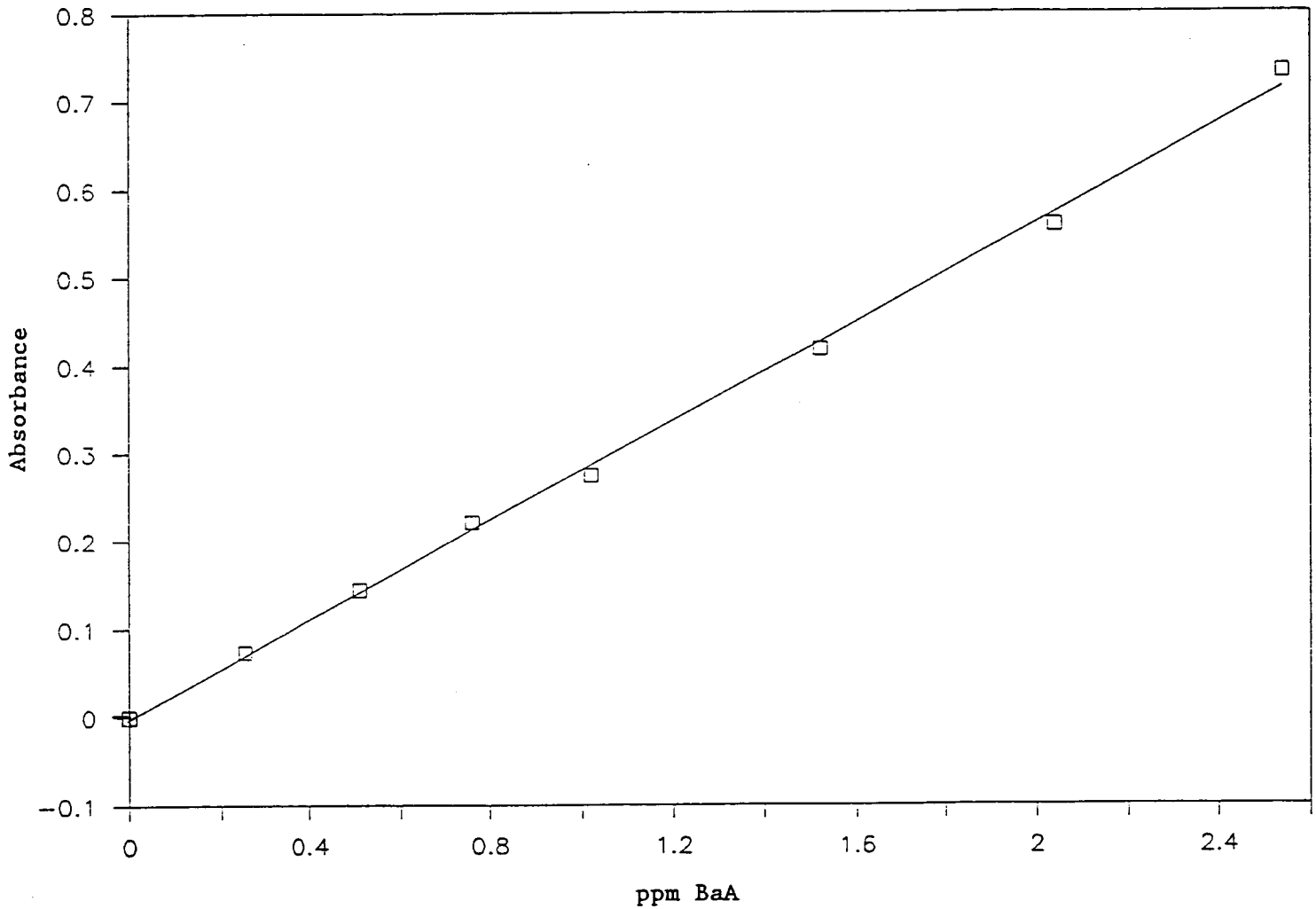

Figure 19. UV Absorption Calibration Curve for BaA.

Solvent was methanol; peak height monitored at 288 nm; 1 cm pathlength.

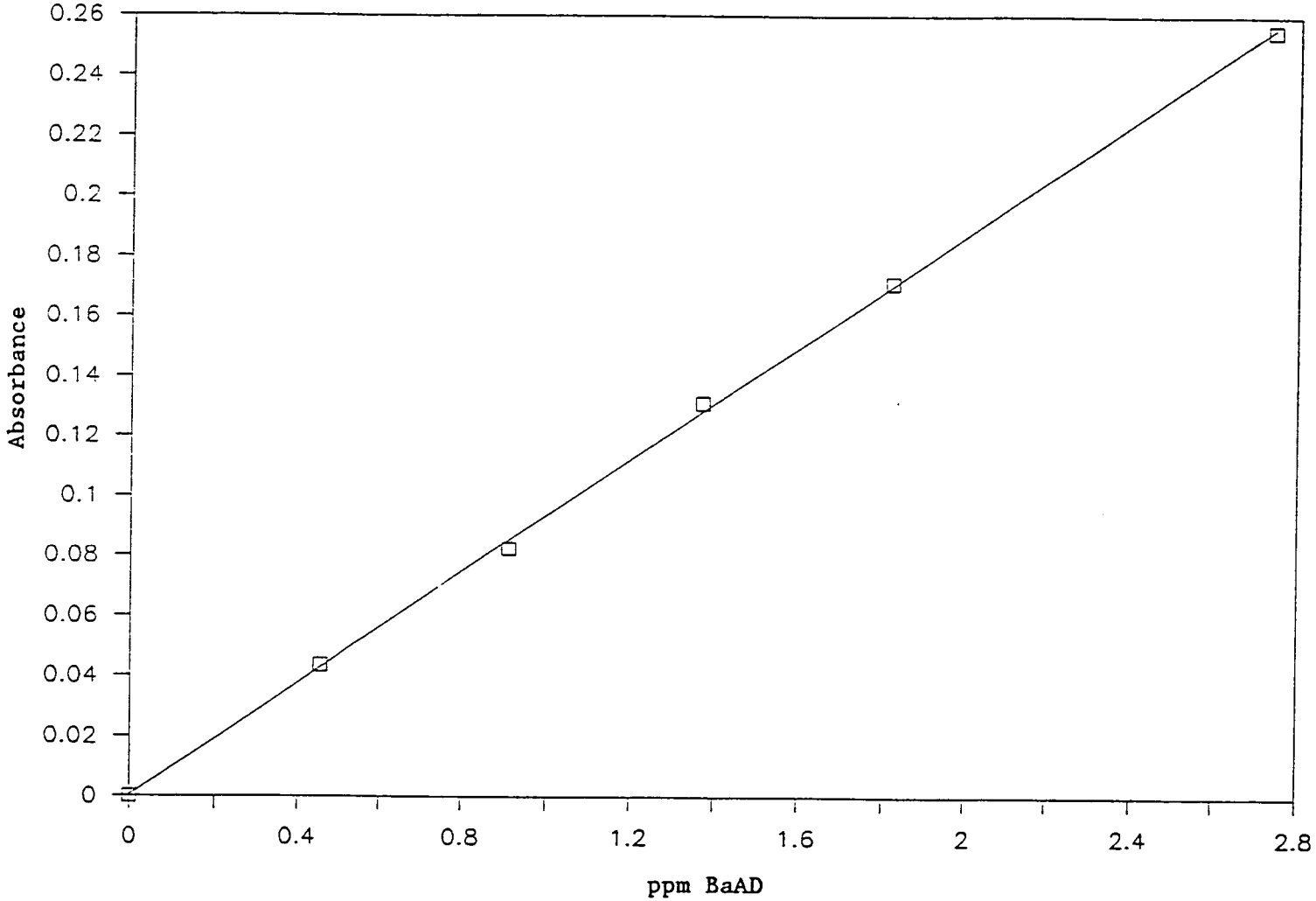

Figure 20. UV Absorption Calibration Curve for BaAD.

Solvent was methanol; peak height monitored at 282 nm; 1cm pathlength.

TABLE XII

EXTRACTION EFFICIENCY OF BaAD FROM COAL STACK ASH FRACTIONS AND SILICA GEL

Adsorbent	Coverage (μg/g)	MeOH Recovery[a]	SFE Recovery[b]
KA M3AL "light mineral"[c]	24	72%	84%
TX M3BH "heavy mineral"[c]	181	96%	87%
Silica Gel[c]	338	96%	95%
KA M3AL "light mineral"[d]	41	85%	100%
TX M3BH "heavy mineral"[d]	597	95%	81%
Silica Gel[d]	1250	108%	104%

a. Soxhlet extraction with methanol was performed for KA M3AL; ultrasonic extraction was performed for silica gel and TX M3BH samples.

b. SFE with CO_2 at 400 atm and 150 °C, collection into methanol.

c. Sample prepared by deposition of BaAD from solution.

d. Sample prepared by deposition of BaAD from the vapor phase.

description) was monitored with SFE-GC-FID. The chromatographic retention time of BaA was 6.30 min and the retention time of BaAD was 7.08 min with chromatographic conditions as described on p. 72; thus, the reactant and product could be analyzed simultaneously. Disappearance of BaA occurred concomitantly with the formation of BaAD as shown in Figures 21 and 22. A plot of quantity extracted vs. illumination time was constructed for BaA and BaAD. At the data point of the kinetic study of BaA on TX M3BH (Figure 21) at 80.65 h of irradiation, at which time 20.5 nmole of BaAD per g of ash remained, 0.27 nmole BaAD was detected. Due to a contaminant present in the CO_2 that eluted at the same time as the BaAD, the limit of detection for BaAD under these experimental conditions was determined to be 0.21 nmole of BaAD. Therefore, monitoring of formation (and subsequent photolysis) of BaAD adsorbed on TX M3BH could not be achieved in excess of 80.65 h. A decrease in the level of impurities in the CO_2, an increase in the amount of sample extracted, and/or a higher surface coverage of BaA could lead to an improved limit of detection for BaAD.

From the information contained in Figures 21 and 22, one can calculate the percentage yield of BaAD by assuming 1 mole of BaA produces 1 mole of BaAD. Table XIII lists the quantities of BaA and BaAD that were detected for illumination times of 0, 5, 10, 15, and 25 min, using silica gel as the adsorbent. A percentage yield for BaAD of $20 \pm 2\%$ was determined for the 5, 10, 15, and 25 min irradiation times.

A similar data analysis was performed for BaA on TX M3BH in an effort to quantify the yield of BaAD. The results are presented in Table XIV. For a 13.15 h irradiation, a 19% yield was calculated,

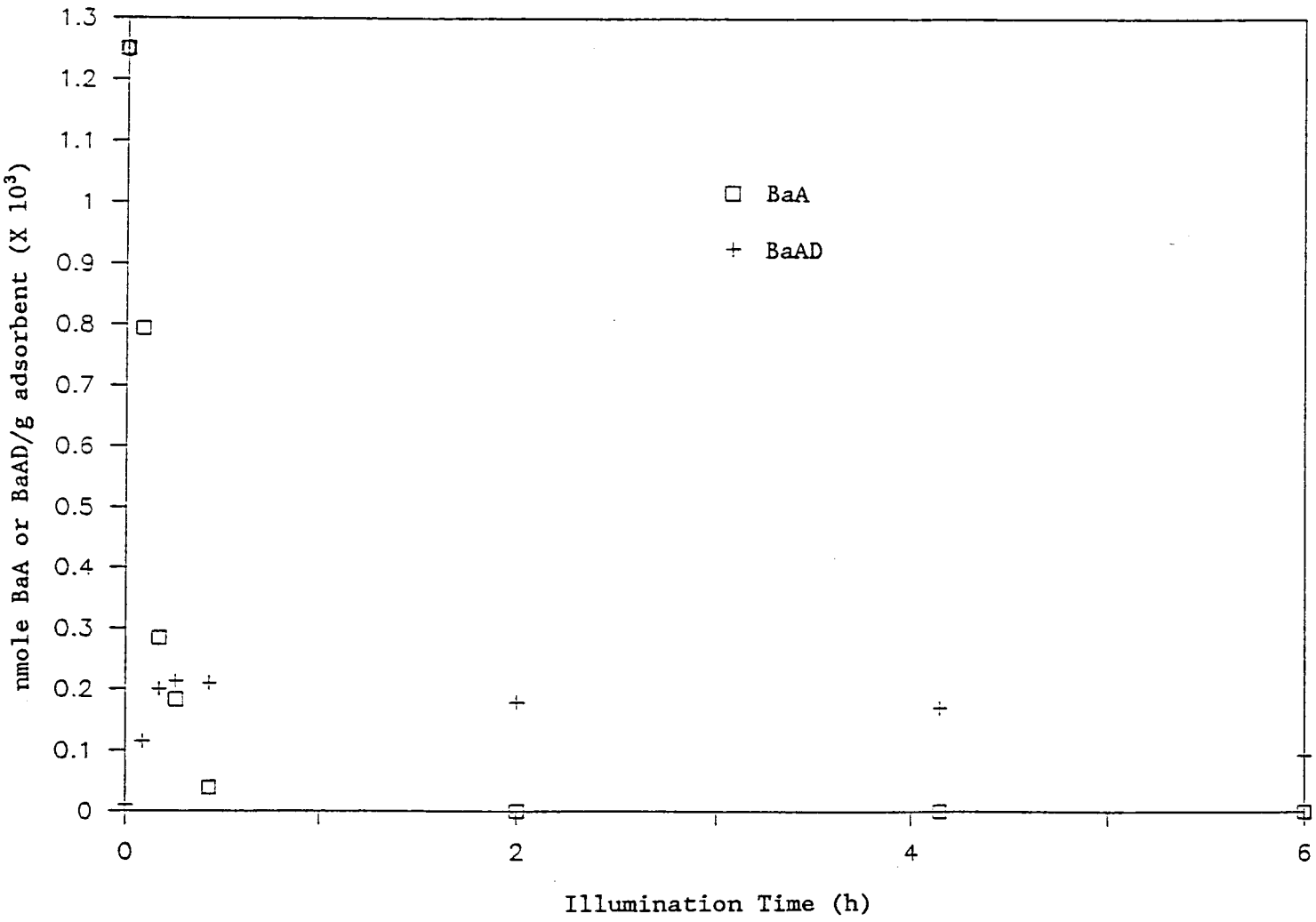

Figure 21. Formation of BaAD from Photolysis of BaA Adsorbed on Silica Gel.

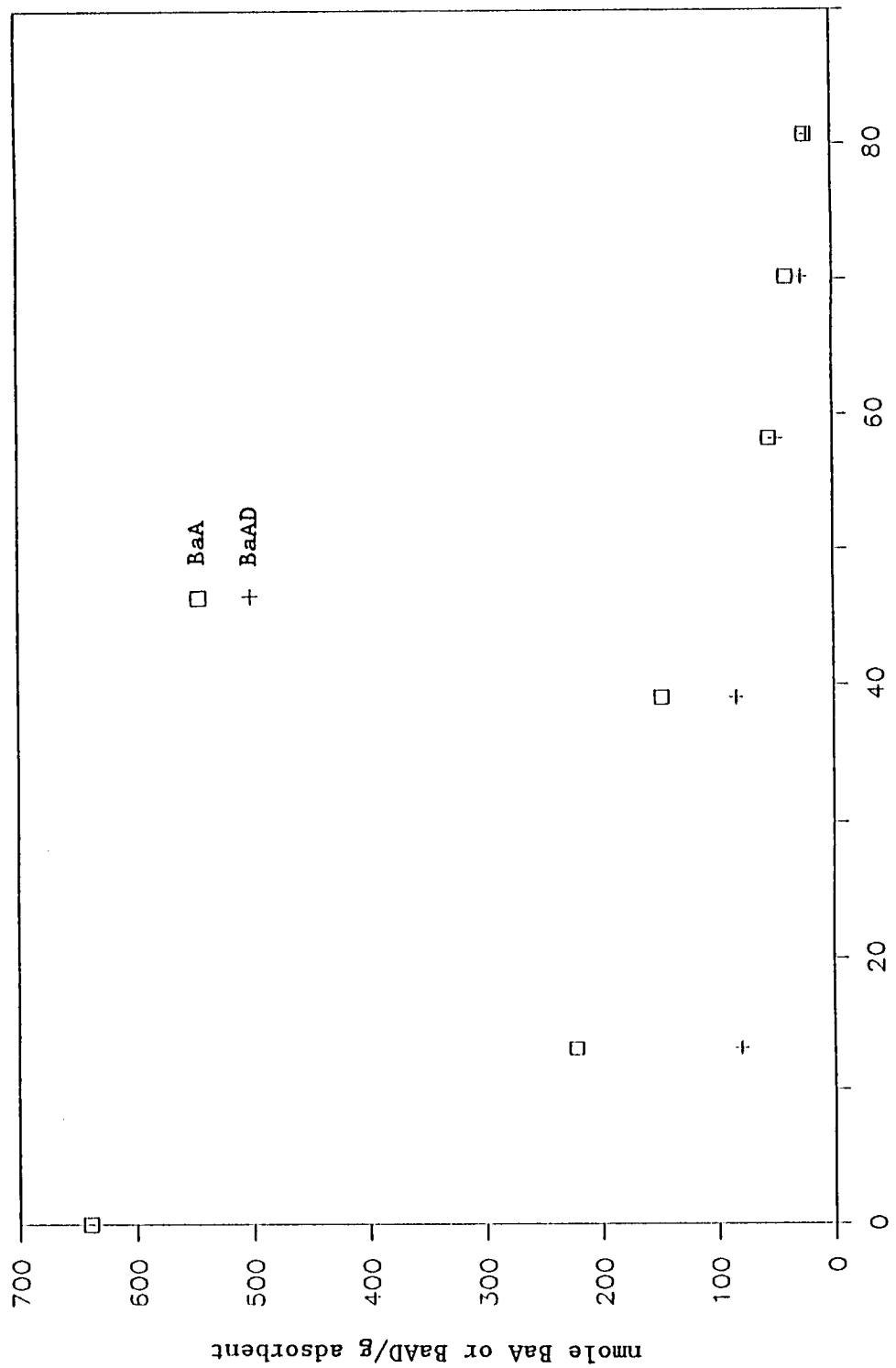

Figure 22. Formation of BaAD from Photolysis of BaA Adsorbed on TX M3BH.

TABLE XIII

YIELD OF BaAD FROM PHOTOLYSIS OF BaA ADSORBED ON SILICA GEL

Illumination Time (min)	Amount BaA Extracted[a]	Amount BaAD Extracted[a]	Amount BaA Consumed[a]	Amount BaAD Detected[a]	Apparent Yield[b]
0	1250	9.7	-	-	-
5	794	115	456	105	23%
10	284	200	966	190	20%
15	183	213	1067	203	19%
25	84	210	1166	200	17%

a. Amount of BaA or BaAD in nmole BaA or BaAD per g adsorbent.

b. Yield of BaAD assuming that consumption of 1 mole BaA produces 1 mole BaAD.

TABLE XIV

YIELD OF BaAD FROM PHOTOLYSIS OF BaA ADSORBED ON TX M3BH

Illumination Time (h)	Amount BaA Extracted[a]	Amount BaAD Extracted[a]	Amount BaA Consumed[a]	Amount BaAD Detected[a]	Apparent Yield[b]
0	640	0	-	-	-
13.15	222	80.2	418	80.2	19%
39.05	148	83.7	492	83.7	17%
58.15	54.8	49.2	585	49.2	8.4%
70.15	39.9	26.9	600	26.9	4.5%
80.65	22.8	20.5	617	20.5	3.3%

a. Amount of BaA or BaAD in nmole BaA per g adsorbent.

b. Yield of BaAD assuming that consumption of 1 mole BaA produces 1 mole BaAD.

similar to the yield determined on silica gel of 21 ± 2%. However, as the illumination time was increased, the apparent yield of BaAD decreased, eventually reaching 3.3% for 80.65 h illumination. Only data obtained at relatively short illumination times can be realistically used to estimate the reaction yield (19%) since, as the illumination time increases, the extent of photolysis of BaAD increases (as discussed in the next section, p. 92), leading to artificially low calculated yields.

In a separate set of experiments, yields were determined for vapor-deposited samples of BaA on Kaneb mineral fractions KA M3AL and KA M3BH. Samples were analyzed before and after 24 h illumination by SFE-GC-FID. BaA vapor-deposited on KA M3AL (40.8 μg BaA/g ash) exhibited a 6.1% yield of BaAD while a 7.3% yield of BaAD was noted with BaA vapor-deposited on KA M3BH (62.0 μg BaA/g ash). These yields of BaAD on mineral fractions KA M3AL and KA M3BH (vapor-deposited with BaA) are smaller than yields noted on the mineral fraction TX M3BH of Texas (solution-deposited with BaA) at ca. 24 h illumination time. This difference could be due to the different surfaces encountered by BaA (different ash fractions), the mode of deposition, and/or the surface concentration of BaA in each instance (640 μg BaA/g TX M3BH vs. 40.8 and 62.0 μg BaA/g ash for KA M3AL and KA M3BH, respectively). Regardless, the yield of BaAD from photolysis of BaA adsorbed on the surface of mineral particles of coal stack ash was observed to fall between 3.3 and 19%, i.e., to be in all cases substantially smaller than 100%.

A study by Konig et al. revealed a similar percentage yield of BaAD (20%) observed upon irradiation of BaA adsorbed on Al_2O_3.[45] These

investigators also noted a competing photochemical reaction occurring in which BaA was converted to 3-(2-carboxophenyl)-2-naphthaldehyde (illustrated below), with an apparent yield of <1%.[45] The minute

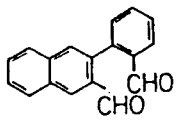

quantity of the second reaction product observed by Konig et al.[45] is consistent with the observation in the present work that no detectable peaks, other than those attributed to BaA and BaAD, were noted in the chromatograms after illumination of BaA adsorbed on silica gel. Konig and co-workers did not mention the detection of other reaction products that would account for the other 80% of the BaA that was depleted.[45] Likewise, a study by Fox and Olive demonstrated a 12-19% photochemical yield of anthracene-9,10-dione from anthracene (a compound similar to BaA) adsorbed on atmospheric particulate matter.[42] Clearly, BaAD is a significant product of the photochemical oxidation of BaA adsorbed on silica gel, but other (as yet unidentified products) presumably are also formed. If another compound was formed from the photolysis of BaA in these studies, its detection may have been hindered by subsequent photolysis of that compound to other products.

5. Relative Photoreactivities of BaAD and BaA

The rate of photolysis of reactant and product (BaA and BaAD) needs to be measured so that realistic estimates of yield of BaAD can be obtained. The relative photoreactivities of BaA and BaAD were estimated by solution-depositing BaA on silica gel and TX M3BH and also by solution-depositing BaAD on different samples of these adsorbents. For each adsorbent, BaA and BaAD were deposited at similar surface

coverages. On silica gel, BaA was deposited at 243 μg BaA per g of silica gel. On a separate portion of silica gel, BaAD was deposited at 338 μg BaAD per g of silica gel. Surface coverages of 117 μg BaA per g of ash and 173 μg BaAD per g of ash were used on samples of TX M3BH. Then, a kinetic study was performed on each of the four samples by illuminating for a given time and monitoring the decrease in reactant concentration by ultrasonic extraction with methanol and subsequent quantification with UV absorption spectroscopy.

On silica gel, assuming first order kinetic behavior of the adsorbates (as observed by Alebic et al.),[64] a dramatic difference in photoreactivity of the two compounds was noted (Figures 23 and 24). The half-life for adsorbed BaA was found to be 0.0491 h with a first order rate constant (k) of 14.1 h^{-1}. The half-life of BaAD, deposited on silica gel, was 5.11 h with a k value of 0.136 h^{-1}. Thus, on silica gel, the relative first-order rate constants for BaA and BaAD are 14.1/0.136 = 104.

A sample of BaA adsorbed on silica gel was analyzed for BaA and BaAD content with increasing illumination time (Figure 21, p. 87). After 25 min of illumination, virtually all of the BaA was depleted, leaving only BaAD on the surface. The BaAD on the surface, at this point, was produced from surface-bound BaA. Three more illuminations were carried out on this sample in order to obtain enough data so that a half-life of BaAD could be determined from a first-order plot, where the BaAD was formed on the surface from photodecomposition of adsorbed BaA, rather than deposited on the surface from a solution of BaAD in methanol. A half-life of 4.76 h (k = 0.146 h^{-1}) was determined for BaAD

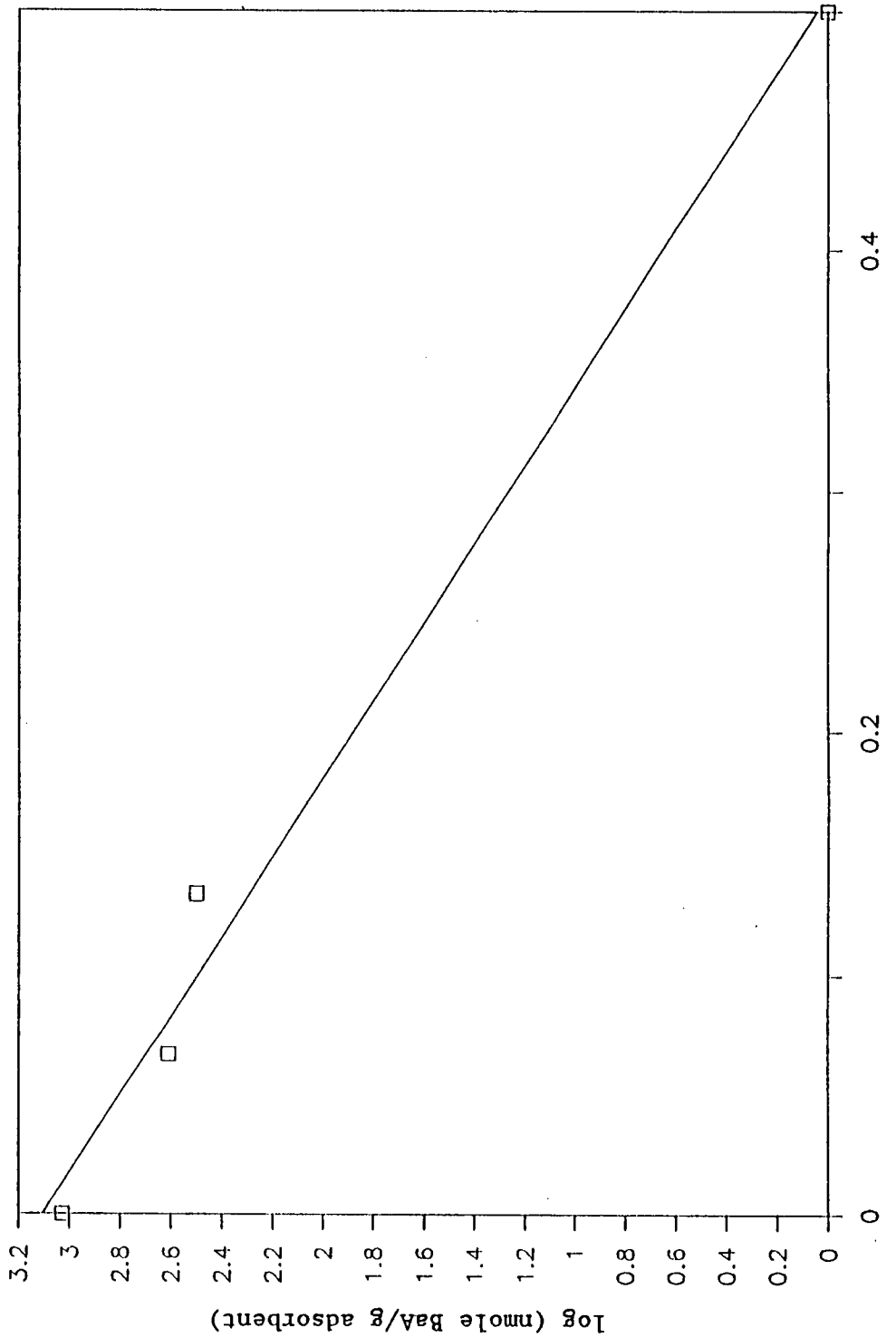

Figure 23. First-Order Photochemical Decay of BaA Adsorbed on Silica Gel.

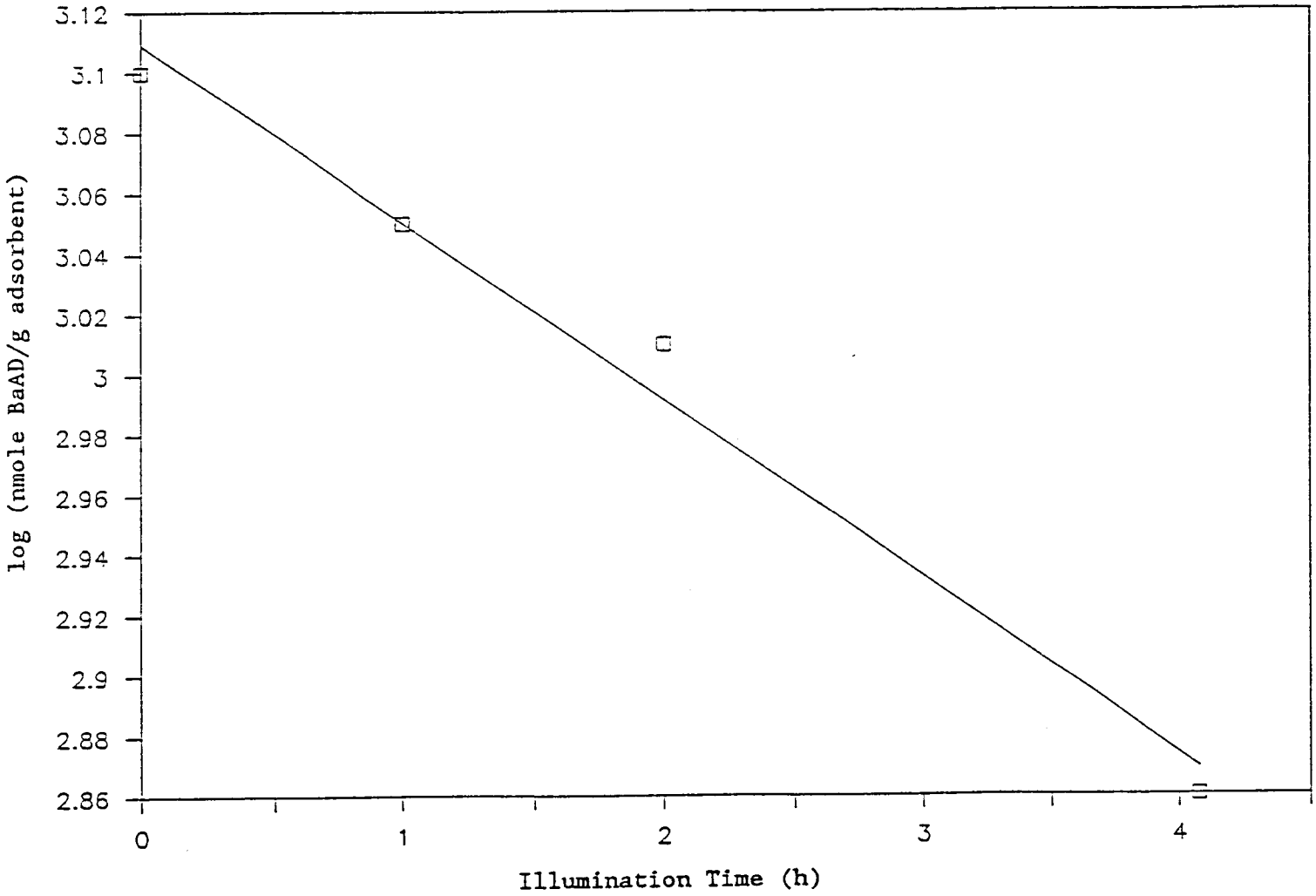

Figure 24. First-Order Photochemical Decay of BaAD Adsorbed on Silica Gel.

formed on the surface of silica gel by photodecomposition of adsorbed BaA (Figure 25). A half-life of 5.11 h ($k = 0.136\ h^{-1}$) was determined for BaAD that was deposited on the surface. Solution-deposited BaAD exhibits similar photoreactivity to BaAD that is actually formed on the surface of silica gel by photolysis of its precursor, BaA. Therefore, the rate constant obtained from adsorbing BaAD on the surface of silica gel from a solution of BaAD in methanol is representative of the kinetic behavior of photolysis of BaAD produced on the surface from the photolysis of BaA. It follows that BaAD is much less photoreactive than its precursor, BaA, on the surface of silica gel (Figures 23 and 24, pp. 94, 95), indicating that the ca. 20% yield (significantly <100%) of BaAD from photolysis of BaA is not due to loss of BaAD due to further photodecomposition within the relatively short irradiation time of 25 min (Table XIII, p. 89).

On TX M3BH, a much less dramatic difference in photoreactivities of BaA and BaAD was observed, as shown in Figures 26 and 27. The half-life of deposited BaA was found to be 13.5 h with a first-order rate constant value of $0.0513\ h^{-1}$. The half-life of adsorbed BaAD was 23.8 h with a first-order constant value of $0.02912\ h^{-1}$. Hence, the rate of photodecomposition of BaAD is about half that of BaA. The kinetic data are summarized in Table XV. This behavior is in agreement with results noted earlier with SFE-GC-FID studies, where BaAD was found to decay at a significant rate compared to BaA on TX M3BH, thus producing lower apparent BaAD yields with increasing illumination time (Table XIV, p. 90). Thus, a comparison of the photoreactivity of deposited BaAD that of BaAD produced on the

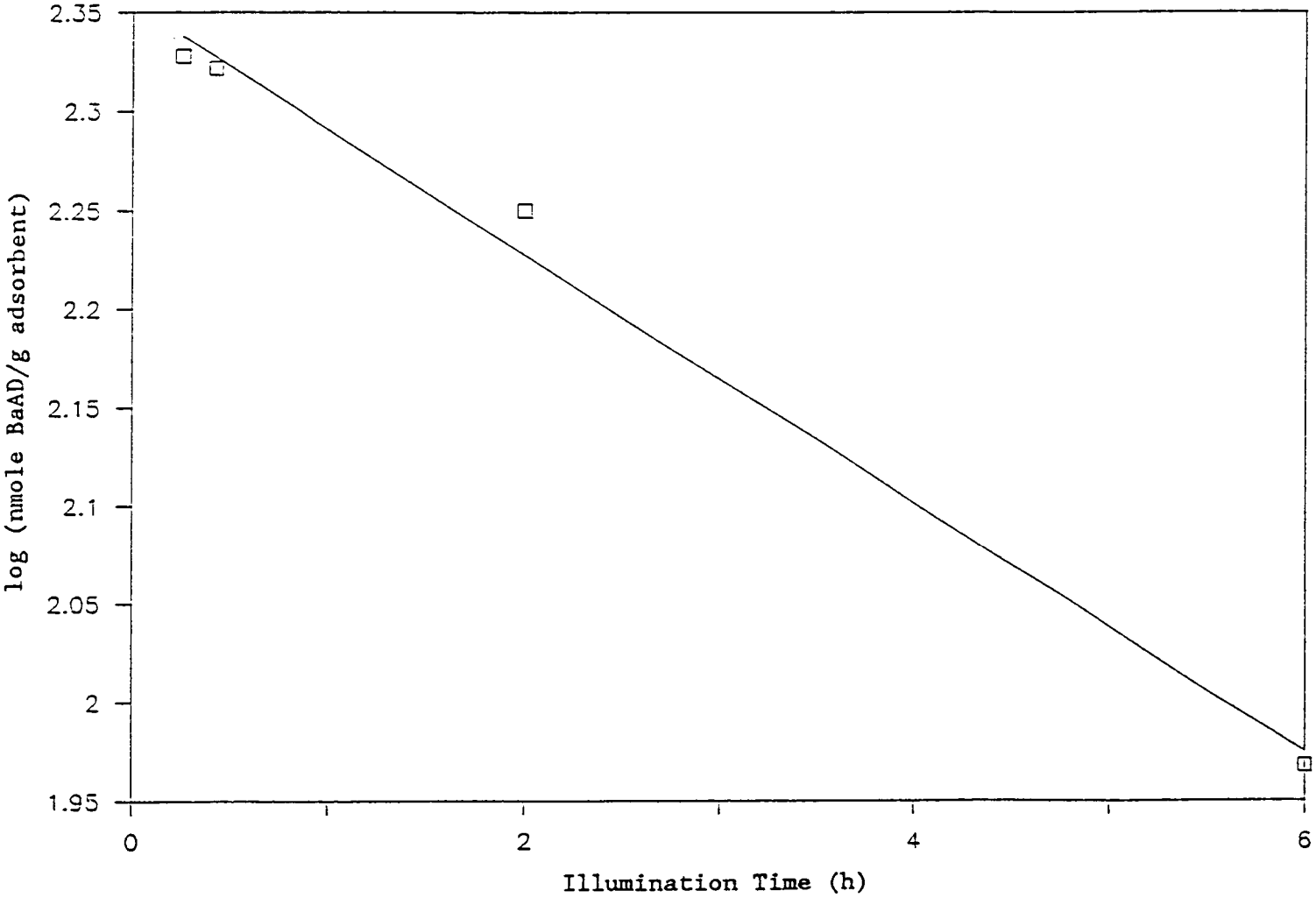

Figure 25. First-Order Photochemical Decay of Photochemically-Produced BaAD Adsorbed on Silica Gel.

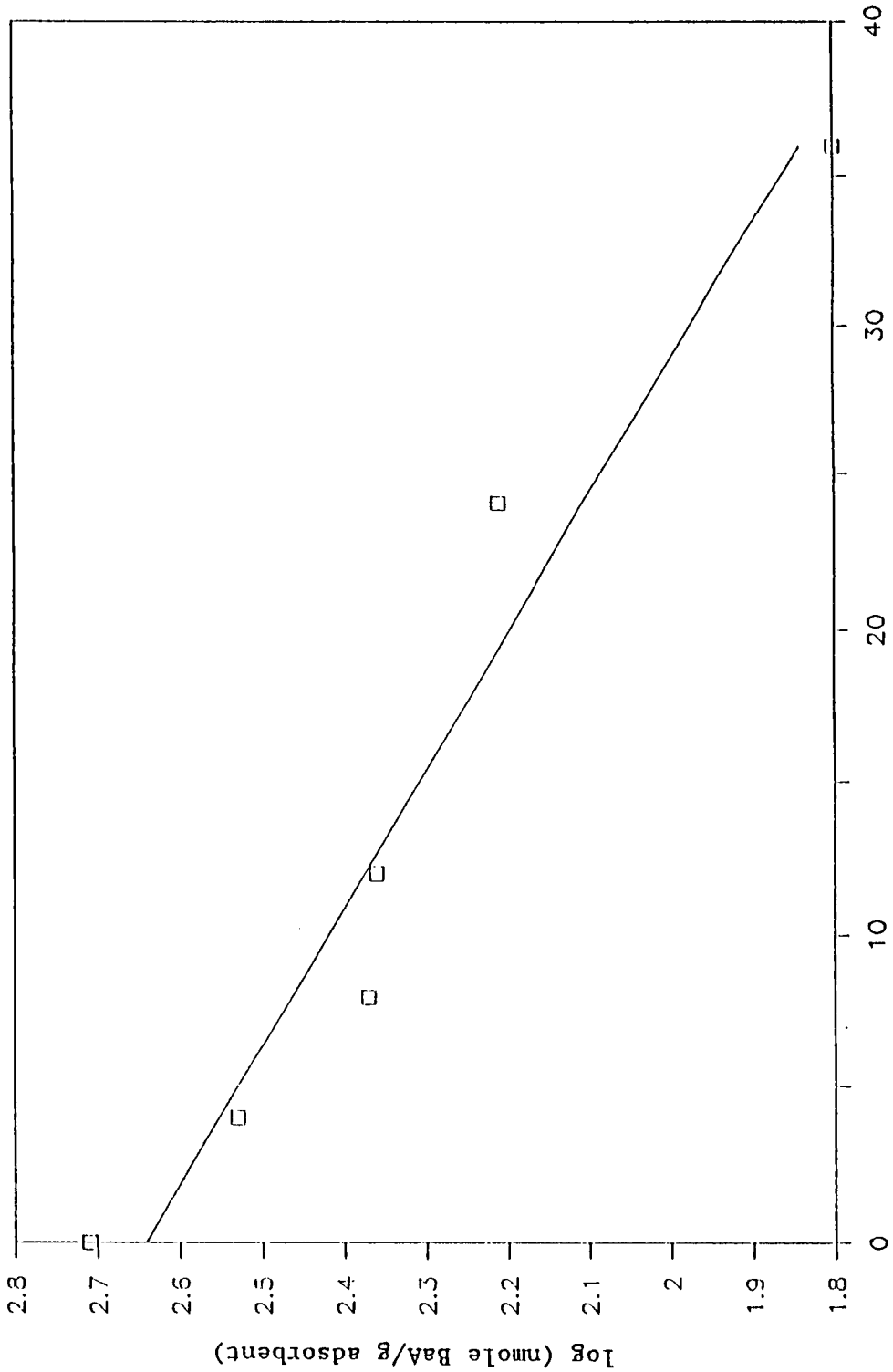

Figure 26. First-Order Photochemical Decay ot BaA Adsorbed on TX M3BH.

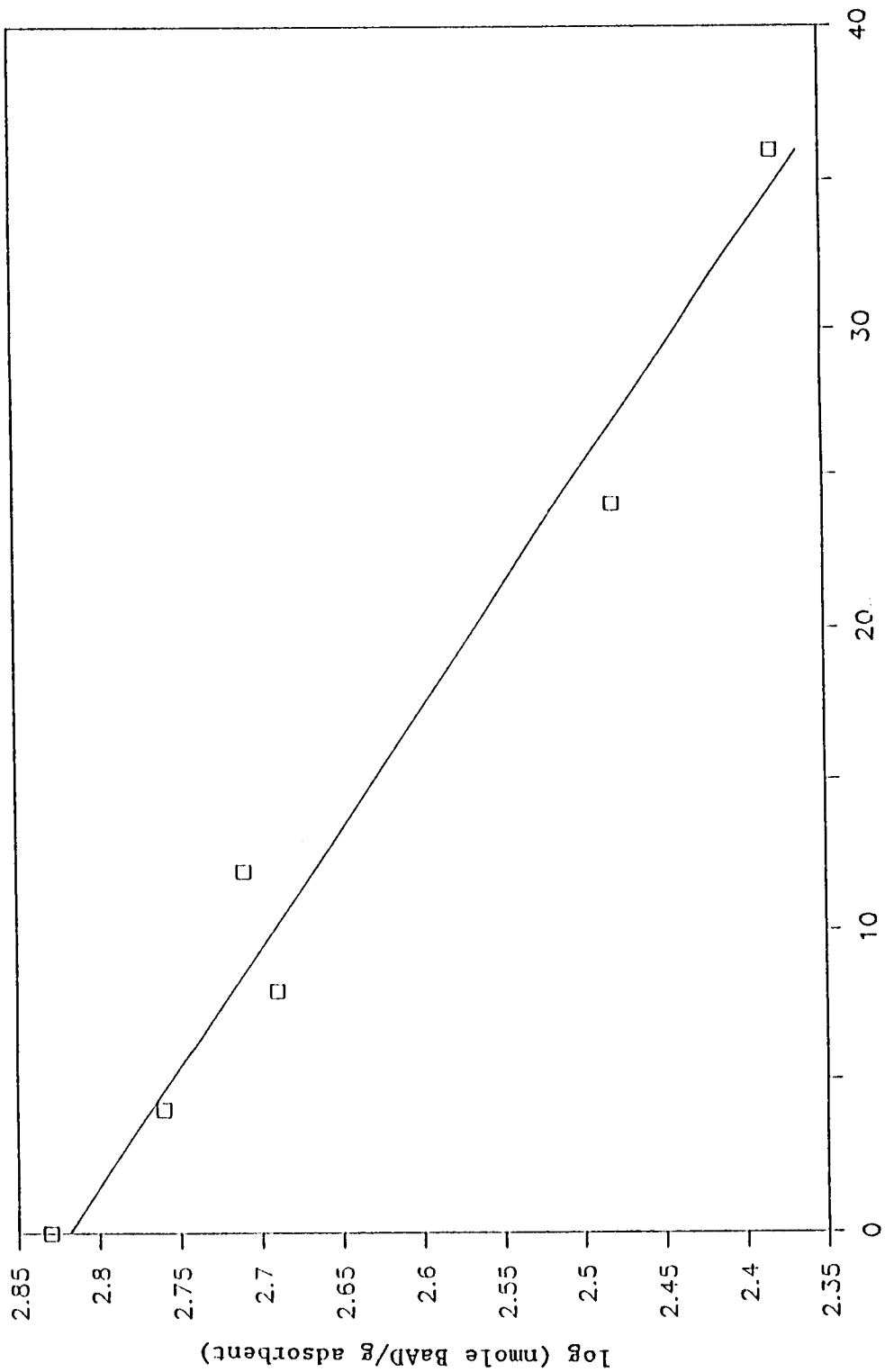

Figure 27. First-Order Photochemical Decay of BaAD Adsorbed on TX M3BH.

TABLE XV

KINETIC DATA FOR PHOTOLYSIS OF BaA AND BaAD ON SILICA GEL AND TX M3BH

Adsorbate	Adsorbent	N[a]	$k(h^{-1})$[b]	$t_{1/2}(h)$[c]	R[d]
BaA	TX M3BH	6	0.0513	13.5	0.9723
BaAD	TX M3BH	6	0.0291	23.8	0.9856
BaA	Silica Gel	4	14.1	0.0491	0.9948
BaAD	Silica Gel	4	0.136	5.11	0.9920
BaAD	Silica Gel[e]	4	0.146	4.76	0.9960

a. Number of data points for linear regression analysis.

b. First-order rate constant in h^{-1}.

c. Half-life in h.

d. Correlation coefficient from linear regression.

e. Decay of BaAD photochemically-produced from BaA on the surface; other samples were prepared by depositing the adsorbate on the surface.

surface of TX M3BH by photolysis of BaA was not attempted. On both silica gel and TX M3BH, BaAD was found to be more stable to photoconversion than BaA. This finding is similar to observations of Kamens et al,[65] who observed oxygenated PAH adsorbed on wood soot particles to be more stable to photoconversion than the parent PAH.

6. SFE-GC-FID Collection Efficiency and Precision Study

The loss of extracted BaAD upon collection of the supercritical fluid extract at the head of a gas chromatographic column would lead to low calculated yields of BaAD from BaA. Thus, a sample of BaAD solution-deposited on silica gel at 348 μg BaAD per g of silica gel was extracted by SFE (20 mL of CO_2 at 150 °C and 400 atm) in quadruplicate. The sample was extracted in quadruplicate in an effort to quantify the precision of the SFE-GC-FID procedure. Silica gel was selected as the adsorbent since past studies have generally shown virtually quantitative recoveries of adsorbed PAH from silica gel.[9] The extractions yielded 334 $\pm$ 14 μg (N=4) BaAD per g of silica gel. The average recovery for four extractions was 96% of the deposited BaAD. A relative standard deviation of 4% was observed for the SFE-GC-FID procedure.

Therefore, there is no reason to suspect that significant quantities of BaAD are lost in collection of the SFE extract on the head of the GC column. The fact that the yield of BaAD produced by photolysis of adsorbed BaA is much less than 100% cannot be attributed to losses of BaAD during the collection process. Results also indicated that BaAD could be extracted at nearly quantitative levels ($\geq$80%) from silica gel and two mineral stack ash fractions.

All of the evidence summarized above indicates that the ca. 20%

yield of BaAD for photolysis of BaA adsorbed on silica gel was due to the formation of one or more additional photoproducts that were not detected in these experiments. Yields of BaAD of less than 21% on coal stack ashes were shown to be due in part to photolysis of BaAD subsequent to formation, but were also likely due to the formation of other products that were not detected in this work.

F. Conclusions

The carbonaceous fraction, KA C3E, of Kaneb coal stack ash was shown to be primarily responsible for stabilizing adsorbed PAH to photoconversion. PAH adsorbed on nonmagnetic mineral fractions, KA M3AL and KA M3BH, displayed the greatest photoreactivity, while adsorption of PAH on the ferromagnetic mineral fraction (KA F3) gave rise to intermediate photoreactivity. A model adsorbent, flaked graphite, stabilized adsorbed BaA to photolysis, while extensive photolysis was noted for pyrene adsorbed on silica gel. Therefore, PAH are most likely to undergo appreciable atmospheric phototransformations when adsorbed on coal stack ash that contains small amounts of carbon particles, i.e., from coal combusted with very high efficiency.

The photochemical decomposition of benz(a)anthracene (BaA) adsorbed on silica gel and three mineral fractions of coal stack ash (TX M3BH, KA M3AL, and KA M3BH) was monitored with coinciding appearance of a photoproduct, benz(a)anthracene-7,12-dione (BaAD), by the use of SFE-GC-FID. Yields of BaA ranging from 3.3 to 21% were noted. SFE-GC-MS was used to confirm the identification of BaAD as a photoproduct of BaA. BaAD was shown to be extractable ($\geq$80%) from silica gel and mineral

fraction surfaces, indicating the capability of SFE with 20 mL CO_2 at 400 atm and 150 °C to remove surface-bound BaAD. BaAD is slightly less photoreactive than BaA on mineral fraction TX M3BH, while BaA on silica gel is much more photoreactive than BaAD. A collection efficiency experiment showed that sizable quantities of BaAD were not lost upon collection of the SFE extract at the head of the GC column. These data indicate that one or more other products are formed upon photolysis of BaA that were not detected in this work. The formation of BaAD from the photolysis of adsorbed BaA has been shown to occur on the surfaces of silica gel and mineral particles of coal stack ash, thus demonstrating the applicability of SFE-GC-FID and SFE-GC-MS for the analysis of PAH phototransformation products.

CHAPTER V

Summary

Coal stack ash, an inhomogeneous mixture of nonmagnetic mineral, ferromagnetic mineral, and carbonaceous particles, was separated into one carbonaceous, one ferromagnetic, and two nonmagnetic mineral fractions. The ferromagnetic fraction contained 66.11% Fe as Fe_2O_3 and low carbon content (0.64% bulk carbon). Elutriation and solvent density separation were not capable of eliminating all of the carbonaceous particles from the noncarbonaceous fractions, since the mineral fractions M3AL and M3BH contained 0.25 and 0.87 %C, respectively. Silicon and aluminum were found to be present on the surface (and in the bulk) of the mineral fractions, likely in the form of oxides. The specific surface area was found to be highest on the carbonaceous fraction, which had a specific surface area of 25.5 ± 0.1 m^2/g. The remaining fractions had <1 m^2/g surface area, primarily due to the small amounts of carbonaceous particles that remained in the noncarbonaceous fractions. Future research should focus on methods which would rid the carbonaceous particles from the mineral and ferromagnetic fractions.

The efficiency of photolysis of pyrene and benz(a)anthracene (BaA) was measured on each ash fraction in an effort to identify particles responsible for the stabilization of these compounds adsorbed on the surface of coal stack ash. The carbonaceous particles were found to be primarily responsible for stabilizing these compounds to photolysis, with the ferromagnetic fraction giving rise to intermediate

stabilization of the compounds to photolysis. The highest rate of photolysis of pyrene and BaA was observed on the two mineral fractions. It is likely that the minute amounts of carbon left in the mineral fractions (0.25 and 0.87% bulk carbon for KA M3AL and KA M3BH) were responsible for incomplete photolysis of adsorbed PAH.

Supercritical fluid extraction (SFE) was used in an effort to increase extraction efficiency of pyrene from the carbonaceous stack ash fraction. Pure isobutane, pure CO_2, and methanol- and toluene-modified solvent systems were not capable of increasing extraction recoveries of pyrene compared to traditional extraction methods of Soxhlet and ultrasonic extraction with methanol or toluene. Approximately 1/3 of the adsorbed pyrene seems to be irreversibly adsorbed to the carbonaceous particles. Future research should attempt to determine the fate of this portion of the adsorbed pyrene.

Supercritical fluid extraction directly coupled to gas chromatography (with flame ionization detection or mass spectrometric detection) was shown to be applicable to the identification of a photochemical reaction product of BaA adsorbed on stack ash. A product of the photochemical reaction of BaA adsorbed on silica gel and three mineral fractions was BaA-7,12-dione (BaAD). The formation of BaAD from photolysis of adsorbed BaA was monitored with yields of BaAD ranging from 3.3 to 21% on stack ash samples and silica gel. Higher yields (ca. 20%) were noted on silica gel due to the greater stability of BaAD to photolysis than BaA (by a factor of 104). On stack ash, yields of BaAD similar to those observed on silica gel from adsorbed BaA were noted at short illumination times, yet increasing the illumination times caused

BaAD yields to decrease, because BaAD was found to be only twice as stable as BaA to photolysis when adsorbed on coal stack ash. The extraction efficiency of BaAD using SFE was shown to be $\geq$80%; thus, incomplete extraction of photochemically-produced BaAD was determined not to be a significant factor in the ca. 20% yield of BaAD from adsorbed BaA. No other photochemically-produced compounds were detected from the photolysis of adsorbed BaA. Therefore, the formation of BaAD from adsorbed BaA is certainly an important photochemical pathway of BaA present on the surface of coal stack ash. Oxidative photochemical reactions of polycyclic aromatic hydrocarbons other than BaA should be studied further by the use of SFE directly coupled to gas chromatography.

LIST OF REFERENCES

LIST OF REFERENCES

1. H. H. Schobert, J. Chem. Ed., 66, 242 (1989).

2. C. E. Chrisp, G. L. Fisher, and J. E. Lammert, Science, 199, 73 (1978).

3. L. D. Hulett, Jr., A. J. Weinberger, K. J. Northcutt, and M. Ferguson, Science, 210, 1356 (1980).

4. M. Katz and C. Chan, Environ. Sci. Technol., 14, 838 (1980).

5. J. M. Daisey, M. J. D. Low, and J. M. D. Tascon, in "Polycyclic Aromatic Hydrocarbons: Mechanisms, Methods, and Metabolism," M. Cooke and A. J. Dennis, Eds., Battelle Press, Columbus, 1985, p. 307.

6. K. A. Van Cauwenberghe, in "Handbook of Polycyclic Aromatic Hydrocarbons," A. Bjorseth and T. Ramdahl, Eds., Marcel Dekker, New York, 1985, Chap. 10.

7. J. N. Pitts, Jr., Environ. Health Perspect., 47, 115 (1983).

8. W. A. Korfmacher, D. F. S. Natusch, D. R. Taylor, G. Mamantov, and E. L. Wehry, Science, 207, 763 (1980).

9. R. J. Engelbach, A. A. Garrison, E. L. Wehry, and G. Mamantov, Anal. Chem., 59, 2541 (1987).

10. L. D. Hulett and A. J. Weinberger, Environ. Sci. Technol., 14, 965 (1980).

11. T. R. Keyser, D. F. S. Natusch, C. A. Evans, Jr., and R. W. Linton, Environ. Sci. Technol., 12, 768 (1978).

12. R. J. Lauf, L. A. Harris, and S. S. Rawlston, Environ. Sci. Technol., 16, 218 (1982).

13. W. H. Griest and L. A. Harris, Fuel, 64, 821 (1985).

14. G. L. Fisher, B. A. Prentice, D. Silberman, J. M. Ondov, A. H. Biermann, R. C. Ragaini, and A. R. McFarland, Environ. Sci. Technol., 12, 447 (1978).

15. G. E. Cabannis and R. W. Linton, Environ. Sci. Technol., 18, 271 (1984).

16. S. V. Mattigod and J. O. Ervin, Fuel, 62, 927 (1983).

17. J. K. Sanders, University of Tennessee, personal communication, March 2, 1990.

18. R. F. Farrell, S. A. Mathes, and A. J. Mackie, "A Simple Low-Cost Method for Dissolution of Metal and Mineral Samples in Plastic Pressure Vessels," U. S. Bureau of Mines Report No. 8480 (1980).

19. S. Brunauer, P. H. Emmett, and E. Teller, Science, 60, 309 (1938).

20. "Munsell Soil Color Charts," Munsell Color, Baltimore, 1975.

21. C. D. Wagner, W. M. Riggs, L. E. Davis, and J. F. Moulder, in "Handbook of X-Ray Photoelectron Spectroscopy," G. E. Muilenburg, Ed., Perkin-Elmer Corporation, Eden Prairie, Minnesota, 1979, pp. 1-31.

22. J. A. Campbell, R. D. Smith, and L. E. Davis, Appl. Spectrosc., 32, 316 (1978).

23. W. H. Griest and J. E. Caton, in "Handbook of Polycyclic Aromatic Hydrocarbons," A. Bjorseth, Ed., Marcel Dekker, New York, 1983, Chap. 3.

24. G. A. Junk and J. J. Richard, Anal. Chem., 58, 962 (1986).

25. W. H. Griest, B. A. Tomkins, and J. R. Caffrey, Anal. Chem., 60, 2169 (1988).

26. S. B. Hawthorne and D. J. Miller, J. Chromatogr., 24, 258 (1986).

27. M. McHugh and V. Krukonis, in "Supercritical Fluid Extraction, Principles and Practice," Butterworths, Boston, 1986, p. 4.

28. G. G. Hoyer, Chemtech, 7, 440 (1985).

29. W. H. Griest and B. A. Tomkins, Environ. Sci. Technol., 20, 291 (1986).

30. P. A. Soltys, T. Mauney, D. F. S. Natusch, and M. R. Schure, Environ. Sci. Technol., 20, 175 (1986).

31. C. D. Chriswell, I. Ogawa, M. J. Tschetter, and R. Markuszewski, Environ. Sci. Technol., 22, 1506 (1988).

32. M. M. Schantz and S. N. Chesler, J. Chromatogr., 363, 397 (1986).

33. S. B. Hawthorne and D. J. Miller, Anal. Chem., 59, 1705 (1987).

34. B. W. Wright, C. W. Wright, R. W. Gale, and R. D. Smith, Anal. Chem., 59, 38 (1987).

35. B. W. Wright, S. R. Frye, D. G. McMinn, and R. D. Smith, Anal. Chem., 59, 640 (1987).

36. I. L. Davies, M. W. Raynor, J. P. Kithinji, K. D. Bartle, P. T. Williams, and G. E. Andrews, Anal. Chem., 60, 683A (1988).

37. T. D. J. Dunstan, R. F. Mauldin, Z. Jinxian, A. D. Hipps, E. L. Wehry, and G. Mamantov, Environ. Sci. Technol., 23, 303 (1989).

38. R. J. Engelbach, "Photochemical Investigation of Polycylic Aromatic Hydrocarbons Vapor-adsorbed on Coal Fly Ash", Ph. D. Dissertation, The University of Tennessee, Knoxville (1986).

39. R. A. Yokley, "The Photochemistry of Polycyclic Aromatic Hydrocarbons Adsorbed on the Surface of Coal Fly Ash", Ph. D. Dissertation, The University of Tennessee, Knoxville (1985).

40. V. W. Cope and D. R. Kalkwarf, Environ. Sci. Technol., 21, 643 (1987).

41. J. F. Thomas, M. Mukai, and B. D. Tebbens, Environ. Sci. Technol., 2, 33 (1968).

42. M. A. Fox and S. Olive, Science, 202, 582 (1979).

43. T. Nielsen, Environ. Sci. Technol., 18, 157 (1984).

44. T. L. Gibson and G. Tironi, in "Polynuclear Aromatic Hydrocarbons: Mechanisms, Methods, and Metabolism," M. Cooke and A. J. Dennis, Eds., Battelle Press, Columbus, Ohio, 1985, pp 463-475.

45. J. Konig, E. Balfanz, W. Funcke, and T. Romanowski, Anal. Chem., 55, 599 (1983).

46. M. Yu and R. A. Hites, Environ. Sci. Technol., 53, 951 (1981).

47. W. A. Korfmacher, E. L. Wehry, G. Mamantov, and D. F. S. Natusch, Environ. Sci. Technol., 14, 1094 (1980).

48. R. A. Yokley, A. A. Garrison, E. L. Wehry, and G. Mamantov, Environ. Sci. Technol., 20, 86 (1986).

49. T. D. Behymer and R. A. Hites, Environ. Sci. Technol., 22, 1311 (1988).

50. G. K. C. Low, G. E. Batley, and C. I. Brockbank, J. Chromatogr., 392, 199 (1987).

51. R. M. Kamens, Z. Guo, J. N. Fulcher, and D. A. Bell, Environ. Sci. Technol., 22, 103 (1988).

52. D. A. Lane and M. Katz, in "Fate of Pollutants in the Air and Water Environments," I. H. Suffet, Ed., Wiley-Interscience, New York, N. Y., 1977, pp 137-154.

53. Y. Masuda and M. Kuratsune, Air Wat. Int. J., 10, 805 (1966).

54. J. N. Pitts, Jr., D. M. Lokensgard, P. S. Ripley, K. A. Van Cauwerberghe, L. Van Vaeck, S. D. Shaffer, A. J. Thill, and W. L. Besler, Jr., Science, 210, 1347 (1980).

55. J. Konig, E. Balfanz, W. Funcke, and T. Romanowski, in "Polynuclear Aromatic Hydrocarbons: Formation, Metabolism, and Measurement," M. Cooke and A. J. Dennis, Eds., Battelle Press, Columbus, Ohio, 1983, pp 711-720.

56. M. N. Inscoe, Anal. Chem., 36, 2505 (1964).

57. T. D. Behymer and R. A. Hites, in "Polynuclear Aromatic Hydrocarbons: Chemistry, Characterization, and Carcinogenisis," M. Cooke and A. J. Dennis, Eds., Battelle Press, Columbus, Ohio, 1986, pp 65-75.

58. J. Konig, E. Balfanz, W. Funcke, and T. Romanowski, in "Polycyclic Aromatic Hydrocarbons: Mechanisms, Methods, and Metabolism," M. Cooke and A. J. Dennis, Eds., Battelle Press, Columbus, Ohio, 1985, pp 739-748.

59. S. B. Hawthorne, M. S. Krieger, and D. J. Miller, Anal. Chem., 60, 472 (1988).

60. B. W. Wright, J. L. Fulton, A. J. Kopriva, and R. D. Smith, in "Supercritical Fluid Extraction and Chromatography," B. A. Charpentier and M. R. Sevenants, Eds., American Chemical Society, Washington, D. C., 1988, pp 44-61.

61. A. D. Hipps, "Photochemical Investigations of Surface Adsorbed Polycyclic Aromatic Hydrocarbons," M. S. Thesis, The University of Tennessee, Knoxville (1989).

62. V. R. Miller, E. L. Wehry, and G. Mamantov, Environ. Toxicol. Chem., in press.

63. D. A. Saucy, R. M. Kamens and R. W. Linton, in "Polynuclear Aromatic Hydrocarbons: Chemistry, Characterization, and Carcinogenisis," M. Cooke and A. J. Dennis, Eds., Battelle Press, Columbus, Ohio, 1986, pp 811-825.

64. A. Alebic, T. Cvitas, and L. Klasinc, Environ. Sci. Technol., 28, 62 (1990).

65. R. M. Kamens, H. Karam, J. Guo, J. M. Perry, and L. Stockburger, Environ. Sci. Technol., 23, 801 (1989).

APPENDIX

APPENDIX

Supercritical Fluid Extraction Procedure

1. Construction and Assembly of Extraction Cell

The extraction cell (illustrated in Figure 12, p. 47) consists of two 1/8-1/16" stainless steel (SS) unions with 2.0 μm pore size frits with a piece of 1/8" o.d. SS tubing between the two unions. The extraction cell should be constructed with care in order to assure that the ends of the piece of SS tubing rest firmly on the SS frits. Also, the tubing ends should be smooth such that this connection can be made so that none of the material to be extracted escapes from within the 1/8" o.d. SS tubing once the extraction cell is assembled.

An aspirator line with a rubber stopper can be used to draw methanol through the 1/8" side of each union. This process expels any particles and/or extract that may have been deposited inside the SS frits. The 1/8" o.d. SS tubing portion of the extraction cell can be cleaned by rinsing the tube with methanol. All portions of the cell should be rinsed sequentially with toluene, methanol, and then acetone before the cell is used for the first time in order to remove adsorbed contaminants from manufacturing processes. After cleaning, the three cell parts should be placed in an oven at ca. 70 °C for 30 min for evaporation of any remaining methanol or acetone.

2. Loading the Extraction Cell

Remove the extraction cell and allow the cell to cool to room temperature. Assemble the cell with one union loosely fitted on the tubing and the other union securely tightened to the tubing. Weigh the

extraction cell.

A plastic pipette tip can be cut so that the smaller end of the tip can slide over the 1/8" piece of SS tubing. The material to be extracted can then be transferred into the cell through the pipette tip. Finally, the cell can be completely assembled and reweighed, allowing the mass of the added material to be calculated by difference.

3. Filling the Pump with Pure CO_2

Turn on the pump by switching the toggle valve from "Standby" to "Operate." Be sure that the pump pressure is <110 atm, since a pressure above this will cause the safety relief device in the pump-to-cylinder line to rupture (the pressure of CO_2 in the cylinder is 80 atm).

Close the bleed valve and the refill/deliver valve. Open the valve on the cylinder. Open the bleed valve in order to pressurize the line up to the last valve before the pump (the refill/deliver valve). At this point, BE SURE that the "Do Not Pressurize" indicator is NOT on. If it is on, the pump must run in the "Pump" mode until the "Do Not Pressurize" indicator goes off. Otherwise, damage to the pump will occur upon refilling. Also, be sure that the pump is in the "Refill" mode before the pump is pressurized since switching from "Deliver" to "Refill" with 80 atm of CO_2 on the piston will send the piston crashing down to the bottom of the cylinder, thus breaking a shear pin which protects gears from being damaged. The reason for this taking place is the fact that the pump must change gears when switching from "Deliver" to "Refill", catching the pump between gears when the pressure is applied.

Open the refill/deliver valve to the incoming CO_2. With three of the four switches on the pump set to "Refill," "Operate," and "Pump," switch the fourth switch from "Stop" to "Run" in order to begin refilling. Once the desired amount of CO_2 is obtained (volume of CO_2 in pump is displayed by a volume indicator located on the side of the piston tube), turn the switch from "Run" to "Stop." Close the two valves to the CO_2 cylinder.

4. Filling the Pump with CO_2 and a Modifier

A liquid modifier can be added to the CO_2. To do so, first close the valve on the cylinder and open the bleed valve slowly in order to depressurize the cylinder-to-pump line. Release any remaining pressure in the pump by leaving the pump in the "Deliver" mode after an extraction; this procedure takes ca. 30 min. Alternatively, a quicker way to release pump pressure is to again leave the pump in the "Deliver" mode, yet also slowly disassemble the extraction cell. Then, there is a union on the cylinder-to-pump line that can be disassembled. Through this disassembled union, the liquid modifier can be drawn into the pump with the same pump settings as the refill procedure (see p. 113). The union is then reassembled. CAUTION: After the liquid modifier is drawn into the pump, the "Do Not Pressurize" indicator will be on. Therefore, the pump must be run in the "Pump" mode until the "Do Not Pressurize" indicator is off. The pump is then filled with pressurized liquid CO_2 as per above instructions (p. 113).

5. Setting the Extraction Pressure

Set the "Display Set Point Pressure" to the desired value, taking into consideration that the pump will pressurize to within 5% of

this set value.

6. Installation of Restrictor

With a glass cleaving tool, score 25 μm i.d., 150 μm o.d. fused silica capillary tubing in order to give a 15 cm length. Install this restrictor by assembling the 1/16" union (downstream from the extraction cell) with a 0.4 mm hole size 85% polyimide, 15% graphite ferrule and tighten the union until the restrictor is held firmly in place. If collection of the extract on the head of a gas chromatographic (GC) column is preferred, turn off He carrier gas flow, turn off the flame ionization detector and associated gases, set the GC oven at 30 °C, and insert the capillary restrictor through the on-column injection port into a 0.53 mm i.d. column. If collection of the extract by expansion of the supercritical fluid into a liquid solvent is preferred, insert the capillary restrictor into an appropriate volume of liquid solvent.

7. Turn on Oven

Turn on the oven that houses the extraction cell and set the oven to the desired temperature. It takes approximately 30 minutes for the oven to equilibrate. One can allow the oven to equilibrate before pumping begins. Alternatively, one can turn the oven on after pumping begins and allow the oven to equilibrate during the pumping process.

8. Turn on Variac

Turn on the Variac that controls the heating of the transfer line. Set the Variac to 75 in order to achieve a transfer line temperature of 150 °C.

9. Perform Extraction

Open the refill/deliver valve (see Figure 12, p. 47) so that

the CO_2 can exit the pump and flow into the extraction system. Check to be sure that the refill/deliver valve is not open to the cylinder-to-pump line, but rather that CO_2 in the pump flows to the extraction cell through the refill/deliver valve. On the front panel of the pump, switch toggle valve from "Refill" to "Deliver," and depress the "Rapid Pressurization Cycle" button in order to begin pumping. As the system is pressurizing, a leak can be detected by touch at the extraction cell or the 1/16" union that holds the capillary restrictor, since CO_2 cools upon expansion. Noting flow from the capillary restrictor indicates that there is not a leak in the system. If collection is being performed by expansion of the supercritical fluid into a liquid solvent, flow of CO_2 is readily noticed. If collection is being performed by expansion of the supercritical fluid at the head of a GC column, ice formation on the outside surface of the column at the point where CO_2 expansion is occurring inside of the column implies that a leak is not present. Also, a bubble flow meter attached to the end of the gas chromatographic column can detect sufficient flow of CO_2 gas at 50-100 ml/min.

When the pump has emptied, switch the pump from "Run" to "Stop" in order to stop the extraction.

10. Perform Analysis

If collection on the head of a GC column is desired, calculate the maximum amount of analyte that can be extracted and be sure that the attenuation of the FID on the GC is set to accommodate the anticipated signal. Attenuation of the FID on the GC is controlled via "range" and "attenuation" settings. A general rule of thumb is that 4 μg of pyrene

gives a full scale response at a chart recorder attenuation of 1 mV and a GC attenuation of 2^{0} and range of 2^{12}. Then, after pumping has ceased and the pump pressure has gone down to 80 atm (due to depressurization of CO_2 through the restrictor), the restrictor can be removed from the on-column injection port, the He carrier gas flow can be turned on (and the He flow rate measured), the detector and associated gases can be turned on, and the chart recorder can be turned on. Wait until the GC signal reaches the "zero" level, be sure that the temperature ramp conditions are satisfactory, and begin the GC analysis.

VITA

Robert Frank Mauldin was born on May 18, 1962, in Fort Worth Texas. He graduated from Westview High School in Martin, Tennessee in May, 1980. He earned a B.S. with a major in Chemistry and a minor in Philosophy from the University of Tennessee, Martin, in May, 1985. Robert entered graduate school in September, 1985, at the University of Tennessee, Knoxville. He served for two years as a teaching assistant at the University of Tennessee, Martin, and for five years as a teaching assistant at the University of Tennessee, Knoxville.

Robert's primary career interest is to be an effective educator in Chemistry (and related disciplines such as the Philosophy of Science and Environmental Ethics) at the undergraduate level. He has accepted a tenure-track Assistant Professor of Chemistry position at Georgia Southern University in Statesboro, Georgia, to begin in September, 1990. His concern for the preservation of the environment, and his love of teaching (teaching is in his blood, as both of his parents are teachers), led him to pursue a Ph.D. in Chemistry. His hobbies include fishing, bicycling, softball, hiking, and goofing around with his dog. Robert values his family highly, and spends considerable time with his wife, his parents, his sister, and his wife's parents.